



Discovery of Ketone-Based Covalent Inhibitors of Coronavirus 3CL Proteases for the Potential Therapeutic Treatment of COVID-19

Robert L. Hoffman,* Robert S. Kania, Mary A. Brothers, Jay F. Davies, Rose A. Ferre, Ketan S. Gajiwala, Mingying He, Robert J. Hogan, Kirk Kozminski, Lilian Y. Li, Jonathan W. Lockner, Jihong Lou, Michelle T. Marra, Lennert J. Mitchell, Jr., Brion W. Murray, James A. Nieman, Stephen Noell, Simon P. Planken, Thomas Rowe, Kevin Ryan, George J. Smith, III, James E. Solowiej, Claire M. Steppan, and Barbara Taggart

Cite This: *J. Med. Chem.* 2020, 63, 12725–12747

Read Online

ACCESS |



Metrics & More

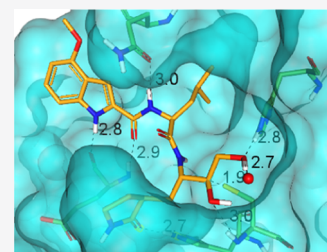


Article Recommendations



Supporting Information

ABSTRACT: The novel coronavirus disease COVID-19 that emerged in 2019 is caused by the virus SARS CoV-2 and named for its close genetic similarity to SARS CoV-1 that caused severe acute respiratory syndrome (SARS) in 2002. Both SARS coronavirus genomes encode two overlapping large polyproteins, which are cleaved at specific sites by a 3C-like cysteine protease (3CL^{pro}) in a post-translational processing step that is critical for coronavirus replication. The 3CL^{pro} sequences for CoV-1 and CoV-2 viruses are 100% identical in the catalytic domain that carries out protein cleavage. A research effort that focused on the discovery of reversible and irreversible ketone-based inhibitors of SARS CoV-1 3CL^{pro} employing ligand-protease structures solved by X-ray crystallography led to the identification of 3 and 4. Preclinical experiments reveal 4 (PF-00835231) as a potent inhibitor of CoV-2 3CL^{pro} with suitable pharmaceutical properties to warrant further development as an intravenous treatment for COVID-19.



INTRODUCTION

In late 2019, cases of an unknown respiratory tract infection were first reported in Wuhan, China. By February 2020, the novel coronavirus SARS CoV-2 was identified as the causative agent for COVID-19.^{1,2} Genome analysis of this virus revealed a high similarity to SARS CoV-1, the coronavirus that caused severe acute respiratory syndrome (SARS) in 2002–2003.^{2–4} Like SARS CoV-1, which resulted in 799 deaths among the 8464 probable cases,⁵ SARS CoV-2 can induce fever, coughing, and difficulty breathing that rapidly becomes more serious in some cases. The spread of SARS CoV-2 has been more extensive than that of SARS CoV-1, causing a global pandemic with the current number of worldwide infections surpassing eight million and deaths surpassing 400,000.⁶ The SARS CoV-1 genome encodes for two large polyproteins pp1a (~450 kDa) and pp1ab (~750 kDa) that contain overlapping sequences and include a 3C-like cysteine protease (3CL^{pro}). The function of this internally encoded 3CL^{pro} is integral to the processing of these proteins and critical for viral replication.⁷ The SARS CoV-1 3CL^{pro} shares a high degree of structural homology and similar substrate specificity with the coronavirus 3C-like cysteine proteases of hCoV 229E and TGEV⁸ but is most similar to the SARS CoV-2 3CL^{pro}. Specifically, the SARS CoV-1 and SARS CoV-2 share 96% identity between their respective 3CL^{pro} sequences and 100% identity in the active site.⁸ A recent report by Dai et al. demonstrates that crystallographic information and structure–

activity relationships obtained with the SARS CoV-1 3CL^{pro} could facilitate the design of potent SARS CoV-2 3CL^{pro} inhibitors with antiviral potency.⁹

There are numerous reports of reversible cysteine protease inhibitors, which include aldehydes,^{10–13} thio- or oxymethylketones,¹⁴ cyclic ketones,¹⁵ amidomethylketones,¹⁶ nitriles,^{17,18} or various 1,2-dicarbonyl motifs.^{19,20} The electrophilic carbon of these chemotypes reacts reversibly with the sulfur atom of an active-site cysteine forming a covalently bound tetrahedral complex. Stabilization of this charged protein–ligand transition state by an “oxyanion hole” present in the active site has been observed with certain inhibitor classes by X-ray crystallography and NMR.^{21,22} A recent report describes the optimization of a series of peptidomimetics designed with an α -ketoamide warhead, which achieves broad-spectrum inhibition against the M^{pro} for several coronaviruses and enteroviruses. Importantly, the reported protease potencies correlate to antiviral potencies, and the authors suggest that the reported SARS CoV-1 3CL^{pro} activity of their lead could be predictive of the SARS CoV-2 3CL^{pro} activity.²³

Received: June 19, 2020

Published: October 15, 2020



Alternative modes of enzyme inhibition are **covalently bound irreversible inhibitors**. While chemically reactive affinity labels such as **chloromethylketones (CMKs)** have demonstrated potent protease inhibition and in certain instances *in vivo* activity, their inherent chemical reactivity precludes development as clinical agents due to safety concerns.²⁴ However, **acyloxymethylketones** first reported by Krantz as “quiescent affinity labels” for cathepsin B have demonstrated potent levels of enzyme inhibition with relatively low chemical reactivity.^{25,26} Mechanistic studies of this class of inhibitors with the cysteine protease caspase-1 support the intermediacy of a thiohemiketal arising from the initial 1,2-carbonyl attack. Orientation and stabilization of the acyloxy leaving group within the S_1' domain (Figure 1) of the protease can facilitate **S_N2 displacement via sulfur migration**, resulting in irreversible or bimodal (reversible inhibition followed by slow inactivation) inhibition.²⁷

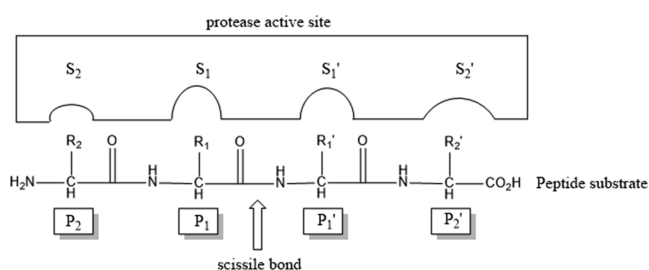


Figure 1. Subsite nomenclature for proteolytic enzymes is shown. Amino acid residues to the left of the polypeptide scissile amide bond are numbered sequentially, beginning with P_1 and increasing toward the N-terminus. Amino acid residues to the right of the scissile bond are numbered sequentially, beginning with P_1' and increasing toward the C-terminus. Complimentary regions of the protease active site employ the corresponding S numbering.

Following the SARS outbreak, a CoV-1 3CL^{pro} homology model was published in 2003 with comparisons made to the human rhinovirus (HRV) 3C^{pro}.²⁸ Although these two proteases share very little sequence conservation, the substrate consensus sequences have **a Gln residue in common at P_1** . Analysis of the HRV 3C^{pro} crystal structure with **1 (rupintrivir; Figure 2)** revealed binding interactions that are like those observed for **1** bound to TGEV 3CL^{pro}, which was used in the construction of their homology model. The authors concluded

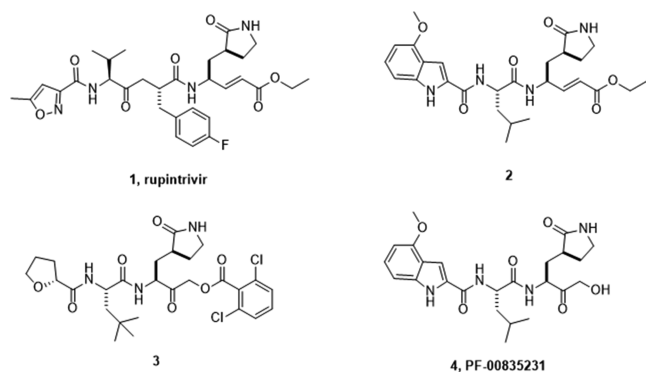


Figure 2. HRV clinical candidate **rupintrivir** and SARS CoV-1 3CL^{pro} inhibitor **2** employing Michael acceptor-based warheads along with optimized SARS CoV-1 3CL^{pro} inhibitors **3** and **4** containing a carbonyl designed for attack by the catalytic cysteine residue.

that Michael acceptor **1** would serve as a starting point to expedite the identification of a potent SARS CoV-1 3CL^{pro} inhibitor.

Performing a similar analysis, we tested **1** and additional HRV 3C^{pro} inhibitors that displayed very weak to unmeasurable SARS CoV-1 3CL^{pro} inhibition. Concurrently, new Michael acceptor derivatives were designed that tested P_1/P_2 alterations and truncation of the P_3/P_4 binding motif to optimize SARS CoV-1 3CL^{pro} inhibition. Compound **2**, a derivative that contains an indole capping group at P_2 , displayed modest levels of irreversible inhibition ($k_{obs}/I = 586 \pm 11 \text{ M}^{-1} \text{ s}^{-1}$) that enabled cocrystallization in complex with SARS CoV-1 3CL^{pro} (PDB code 6XHO).²⁹ Comparison of this structure with the complex of **1** in HRV 3C^{pro} helped to rationalize the poor performance of the warhead, which had been successful in HRV. The structure of the SARS CoV-1 3CL^{pro} complex revealed an eclipsed torsion about the resulting sp^3 α,β -carbons from the Michael acceptor (Figure 3). Furthermore, the carbonyl oxygen sp^2 lone pair electrons are not aligned well with either 3CL^{pro} hydrogen bond donor of the oxyanion hole. Specifically, the hydrogen bond between the carbonyl oxygen and the Gly143 NH in the SARS CoV-1 3CL^{pro} complex is 3.4 Å, while the corresponding hydrogen bond distance is a much more favorable 2.8 Å in the complex of **1** with HRV 3C^{pro}. In contrast to these unfavorable interactions, the constrained lactam³⁰ at the P_1 site, which was designed to be isosteric with the highly conserved P_1 glutamine present in all SARS CoV substrates, is well positioned in the S_1 pocket making a favorable hydrogen bond to His163. The NH of the lactam is within the hydrogen bond distance to Glu166 and the backbone oxygen of Phe140 in the 3CL^{pro}. Additionally, the NH of the indole P_2 capping moiety makes a hydrogen bond with the protein backbone while it extends across an otherwise lipophilic surface over the P_3 pocket.

Although the structure of **2** in complex with SARS CoV-1 3CL^{pro} is the final product, the above analysis is expected to apply similarly to the more relevant and structurally close transition state. Accordingly, a focused design strategy aimed at replacing the warhead while retaining the P_1 lactam and utilizing the methoxy indole capping group in the early rounds of optimization was initiated. Specifically, an ideal electrophilic warhead would be bioisosteric, with the scissile amide carbonyl of peptidyl substrates ensuring proper alignment within the oxyanion hole of the protease. To better mimic the tetrahedral intermediate generated in the amide bond cleavage, we designed **ketone-based covalent reversible and irreversible inhibitors** of SARS CoV-1 3CL^{pro}, as illustrated by **3** and **4**. Compound **4** was selected as a development candidate for SARS CoV-1 but with the successful public health response that ended the 2003 pandemic, the clinical advancement of **4** was suspended. Following the COVID-19 outbreak, testing has demonstrated that **4** is a potent inhibitor of the SARS CoV-2 3CL^{pro} ($K_i = 0.27 \pm 0.1 \text{ nM}$) and a cocrystal structure with **4** bound in the active site has been solved. In addition to the potent inhibition of the 3CL^{pro} and viral replication of several coronaviruses, **4** possesses solubility as well as metabolic and chemical stability characteristics, which are consistent with a continuous infusion IV therapeutic treatment for COVID-19. We report the research focused on the discovery of reversible and irreversible ketone-based inhibitors of SARS CoV-1 3CL^{pro} employing ligand-protease structures solved by X-ray crystallography, which led to the identification of **4** as a molecule

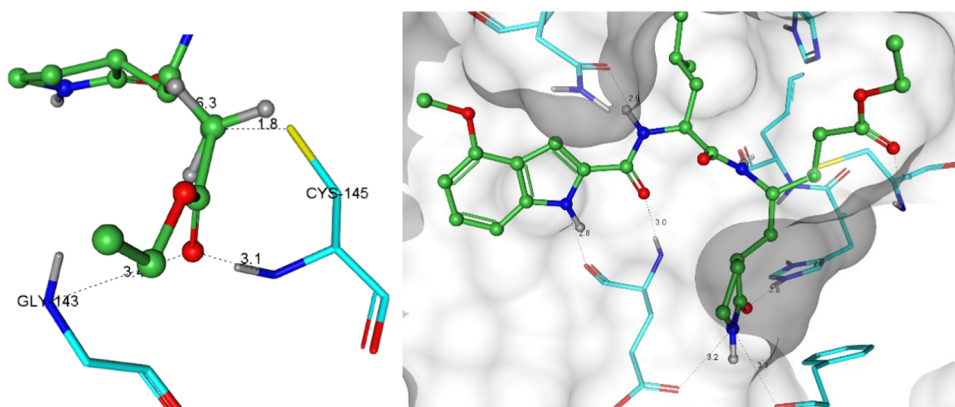
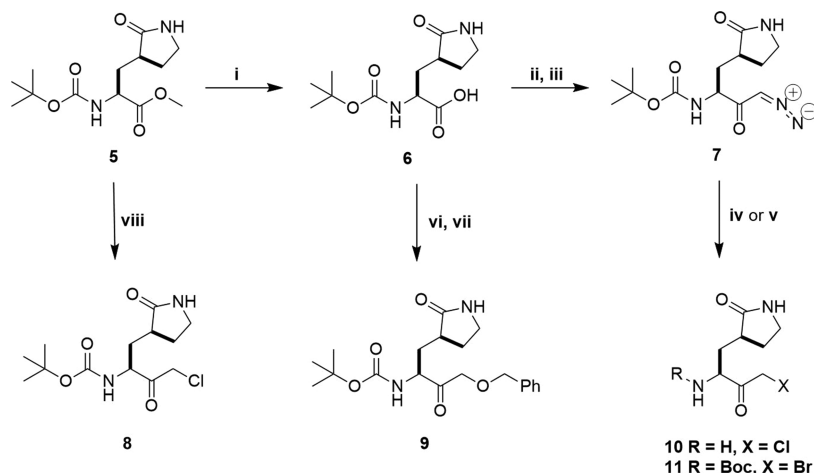


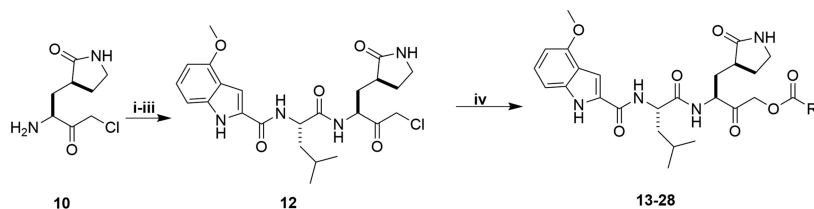
Figure 3. Cocystal structure of the covalent adduct of **2** bound to SARS CoV-1 3CL^{pro} (PDB code 6XHO). The Connolly surface for the inhibitor binding pocket is shown in gray. The bonds are represented as the dashed lines, with the bond length measured between heavy atoms. The views are centered on warhead with active-site interactions and of complete inhibitor–protein interactions depicted.

Scheme 1. Preparation of P₁ Synthetic Intermediates



^a(i) 3 M NaOH, MeOH (95%), (ii) isobutylchloroformate (IBCF), triethylamine (TEA), tetrahydrofuran (THF), (iii) CH₂N₂/ether (92%), (iv) 4 M HCl/dioxane (83%), (v) 1.0 equiv 48% HBr (83%), (vi) HNCH₃(OCH₃), EDC, HOBT, NMM, dichloromethane (DCM) (79%), (vii) Mg, HgCl₂, BOM-Cl, THF, −78 °C (50%), and (viii) lithium diisopropylamide (LDA), ClCH₂I, THF (54%).

Scheme 2. Preparation of Substituted Acyloxymethylketones and Aminomethylketones



^a(i) Boc-Leu-OH, HATU, NMM, *N,N*-dimethylformamide (DMF), 0 °C (64%), (ii) 4 M HCl/dioxane, (iii) HATU, 4-MeO-2-indolecarboxylic acid, NMM, DMF, 0 °C (61%), and (iv) CsF, DMF, carboxylic acid, 60 °C (43–91%).

warranting further evaluation for its potential to treat coronaviruses, including COVID-19.

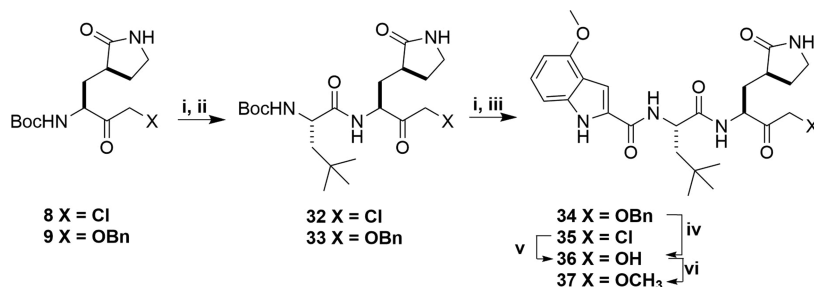
RESULTS AND DISCUSSION

Chemistry. Central to our strategy of examining ketone-based thiophiles was the preparation of an array of intermediates containing diverse methylketone moieties and protecting groups. The preparation of halomethylketone intermediates was accomplished in a two-step procedure by the generation of a diazoketone intermediate³¹ or directly by a

modified Kowalski–Haque reaction,³² as depicted in Scheme 1.

Saponification of amino ester **5**³³ afforded the corresponding amino acid **6** in nearly quantitative yield. Acid **6** was treated with isobutylchloroformate and triethylamine, and the resulting mixed anhydride was reacted with diazomethane³⁴ to provide high isolated yields of **7**. Diazoketone **7** was treated with hydrochloric acid for simultaneous nitrogen deprotection and conversion to the chloromethylketone (CMK) intermediate **10**. Alternatively, the *N*-Boc-protected bromomethylketone was prepared by treatment of **7** with stoichiometric

Scheme 3. Preparation of Hydroxymethylketone Derivatives



^a(i) 4 M HCl/dioxane, (ii) Boc-Leu-OH, HATU, NMM, DMF, 0 °C, (iii) HATU, 4-MeO-2-indolecarboxylic acid, NMM, 0 °C, (iv) Pd/C, H₂, EtOH (77%), (v) CsF, DMF, benzoylformic acid, 60 °C, and then MeOH, cat. K₂CO₃ (53%), and (vi) CH₃I, Ag₂O, DCE (9%).

quantities of 48% HBr in dichloromethane to provide **11**. Another preparation of CMK intermediates that avoids the use of diazomethane was accomplished by the reaction of **5** with excess LDA and chloriodomethane to afford **8** in moderate yields. A direct approach to oxymethylketone intermediate **9** was achieved by conversion of acid **6** to the corresponding Weinreb amide followed by treatment with the Grignard generated from benzyl chloromethyl ether.³⁵

A key element for rapid access to substituted methylketone derivatives was the generation of the fully elaborated CMK **12** (Scheme 2). The utility of the CMK moiety to prepare acyloxy- and hydroxy-substituted methylketones is well established. Elaboration of **10** in a sequence of deprotection/1-*bis*(dimethylamino)methylene]-1*H*-1,2,3-triazolo[4,5-*b*]-pyridinium 3-oxid hexafluorophosphate (HATU)-mediated peptide couplings provided CMK derivative **12** in moderate yield with no epimerization observed. Reaction of **12** with various carboxylic acids in the presence of cesium fluoride at 60 °C provided acyloxymethylketones **13**–**28**. Using this synthetic approach with substitution of P₂ and amine capping structural elements provided inhibitors **3** and **29**–**31**.

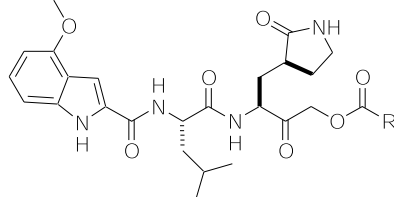
Hydroxymethylketone (HMK) derivatives were accessed by two complementary approaches illustrated in Scheme 3. Elaboration of the P₁'-protected oxymethyl intermediate **9** by sequential amide bond coupling reactions provided benzyl-ether derivatives such as **34** in moderate yields with a low propensity for epimerization at the P₁ center. Hydrogenolytic debenzilation readily afforded the final HMK inhibitors exemplified by **36**. Alternatively, fully elaborated CMK derivatives such as **35** were reacted with benzoylformic acid followed by methanolysis to generate HMK final products such as **36**.³⁶ Alkylation of the terminal hydroxyl was achieved under microwave-assisted conditions in the presence of silver (I) oxide to afford alkoxyethylketone inhibitors, as illustrated by **37**. Using these two synthetic approaches with substitution of P₂ and amine capping structural elements provided inhibitors **4** and **38**–**50**.

Biological Evaluation. Irreversible Inhibitors of SARS CoV-1 3CL^{pro}. The warhead reactivity and binding affinity to P₁' are both important design considerations to ensure specificity of irreversible inhibitors. Krantz has demonstrated that the inherent chemical reactivity of acyloxymethylketones can be tuned to inhibit cysteine proteases through the modulation of substituent effects on the carboxylate leaving group.³⁷ The importance of leaving group "strength" was confirmed by the strong dependence between the p*K*_a of the leaving carboxylate and cathepsin B enzyme inhibition. These otherwise weak electrophiles are elegant "quiescent" inhibitors

that harness the very same interactions with catalytic residues that lead to proteolysis rate acceleration. Molecular modeling of a 2,6-dichlorobenzoate design with SARS CoV-1 3CL^{pro} indicated that a low strain conformation of the ketone carbonyl was aligned in the oxyanion hole and the substituted benzoate is accommodated within the P₁' site. A series of acyloxymethylketone derivatives were prepared, as depicted in Table 1.

As expected, chloromethylketone **12** is a potent irreversible inhibitor of SARS CoV-1 3CL^{pro}. Compounds **22**–**25** possess the most electron-deficient benzoate leaving groups and display kinetics consistent with irreversible inhibition. The remaining entries appear to be reversible inhibitors in the time scale of the assay, with **28** possessing the most potent IC₅₀. A

Table 1. SARS CoV-1 3CL^{pro} Inhibition Data for Acyloxymethylketone Inhibitors



entry	R	SARS CoV-1 3CL ^{pro} FRET ^a	
		<i>k</i> _{obs} / <i>I</i> (M ⁻¹ s ⁻¹)	IC ₅₀ (nM)
12		283,039 ± 22,586	
13	Me		220 ± 0.5
14	cyc-propyl		182 ± 6
15	tert-butyl		230 ± 5
16	Ph		86 ± 3
17	4-OMe-Ph		79 ± 3
18	4-Me-Ph		87 ± 2
19	4-CN-Ph		53 ± 1
20	4-F-Ph		82 ± 3
21	4-Cl-Ph		97 ± 3
22	2,6-(Cl) ₂ -Ph	62,993 ± 2,501	
23	2,6-(F) ₂ -Ph	12,776 ± 594	
24	2-OH-4-Cl-Ph	11,525 ± 40	
25	2-F, 4-CN-Ph	13,321 ± 2,309	
26	2,6-(Me) ₂ -Ph		74 ± 4
27	2,6-(MeO) ₂ -Ph		205 ± 2
28	2-CN-Ph		17 ± 2

^aSee the Experimental Section for details on assay methods; the values were calculated from at least eight data points with at least two independent determinations.

crystal structure (PDB code 6XHN)³⁸ of **28** in complex with SARS CoV-1 3CL^{pro} at 2.25 Å shows a covalent adduct, which demonstrates the bimodal activity of certain acyloxy inhibitors (Figure 4). In this structure, the electron density for the 2-

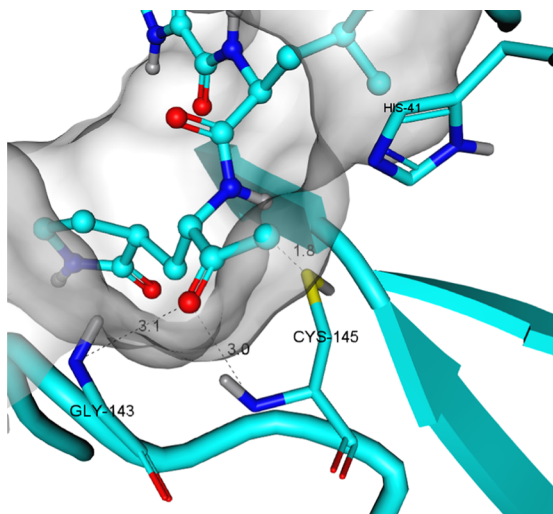


Figure 4. Cocystal structure of the covalent adduct of **28** bound to SARS CoV-1 3CL^{pro} (PDB code 6XHN). The Connolly surface for the inhibitor binding pocket is shown in gray. The bonds are represented as dashed lines, with the bond length between heavy atoms depicted.

cyanobenzoate moiety is absent and the 3CL^{pro} active-site cysteine (Cys145) sulfur forms a covalent bond to the methylene carbon (1.8 Å C–S bond length). The ketone carbonyl is positioned within the oxyanion hole and as such engaging in hydrogen bonds with backbone NH groups of Gly143 and Cys145. A detailed analysis of an extended hydrogen bond network from catalytic His41 reveals that the side-chain imidazole serves as a hydrogen bond donor to the interior of the protease. Specifically, the imidazole hydrogen is directed toward a lone pair electron acceptor from a structural water. We can conclude that this water must be an acceptor to His41 as one of the water hydrogens is engaged with acceptor electrons on the side chain of Asp187, and the second hydrogen engages a terminating acceptor backbone carbonyl on Asp176 through a short network that includes the side chains of an internal, neutral His164 and Thr175.

The 2,6-dichlorobenzoate derivative **22** displays the highest levels of potency in the SARS CoV-1 3CL^{pro} and in antiviral cytopathic effect assays in Vero 76 cells ($EC_{50} = 0.29 \pm 0.19 \mu M$).³⁹ We note here that the assay in Vero 76 cells provided data establishing antiviral activity, but the translation of potency measured in Vero cells, which have high efflux potential, to the potency achievable in human lung cells was unknown (vide infra). As expected, **22** possesses low levels of reactivity toward endogenous nucleophiles such as glutathione ($t_{1/2} > 60$ min)⁴⁰ and exhibits high levels of stability in human plasma ($t_{1/2} > 240$ min).⁴¹ Although **22** displays a promising activity profile, it possesses very poor solubility in clinically relevant IV vehicle formulations, thus limiting its development as an IV clinical agent.

To improve the solubility characteristics of inhibitors incorporating the lipophilic 2,6-dichlorobenzoate, a limited set of inhibitors containing smaller or more polar amine capping fragments were prepared (Table 2). Replacement of

Table 2. SARS CoV-1 3CL^{pro} Inhibition Data for P₃-Modified Acyloxymethylketone Inhibitors

SARS CoV-1 3CL ^{pro} FRET ^a				
Entry	R ₁	R ₂	k_{obs}/I (M ⁻¹ s ⁻¹)	IC ₅₀ (nM)
22			62,993 ± 2,501	
29	O- <i>tert</i> -butyl			24% inhibition @ 1 μM
30	Me			1,028 ± 32
31			30,287 ± 1,686	
3			5,834 ± 151	

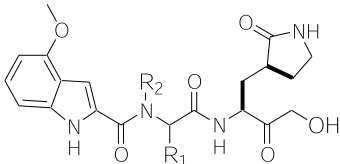
^aSee the Experimental Section for details on assay methods; the values were calculated from at least eight data points with at least two independent determinations.




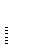
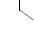
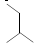
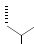
the 4-methoxy indole cap present in **22** with a benzimidazole provided **31**. This inhibitor displayed potent irreversible inhibition kinetics but did not improve solubility compared to **22**. Reduction in the size of the P₂ capping element as represented by **29** and **30** provided derivatives that possessed weak reversible SARS CoV-1 3CL^{pro} inhibition.

Another design to replace the 4-methoxy indole was the (2*R*)-tetrahydrofuran-2-carboxylate, which molecular modeling suggested could make additional favorable protein interactions with a Gln189 side chain and led to the preparation of **3**. Initially, this derivative appeared to display reversible binding kinetics. However, further kinetic studies of compound **3** with the SARS CoV-1 3CL^{pro} protein demonstrated irreversible time-dependent inactivation of this enzyme ($k_{obs}/I = 5834 \pm 151$ M⁻¹ s⁻¹). Additionally, **3** possessed potent antiviral activity in Vero cells ($EC_{50} = 2.4 \mu M$) and solubility in vehicle formulations almost 20-fold higher than **22**. Evaluation of the pharmacokinetic profile of **3** in rat suggested that this inhibitor possessed properties potentially sufficient for an IV continuous infusion dosing paradigm.⁴²

Although irreversible inhibition can provide an extended pharmacodynamic effect when protein resynthesis rate is slow compared to drug clearance, such extended effects for 3CL^{pro} inhibition were not necessarily expected. The 3CL^{pro}-mediated proteolysis of newly expressed viral polypeptides is essential to virus replication; however, this activity only occurs during a single step in the virus life cycle that closely follows each cell infection. Viral particles themselves are not reliant on 3CL^{pro} activity nor are the remaining coronavirus life cycle steps. Each event of cell infection initiates newly synthesized 3CL^{pro}. Because detailed kinetics of this process are not understood, reversible and irreversible inhibitors were investigated equally.

Reversible Inhibitors of SARS CoV-1 3CL^{pro}. Peptidyl HMK inhibitors and their corresponding ethers have been designed as potent reversible cysteine protease inhibitors of cathepsin

Table 3. SARS 3CL^{pro} Inhibition Data for P₂-Modified HMK Inhibitors


Entry	R ₁	R ₂	SARS CoV-1 3CL ^{pro} FRET ^a IC ₅₀ (nM)	SARS CoV-1 ^b EC ₅₀ (μM)
36		H	7 ± 1	10 ± 1.8
4		H	4 ± 0.3 ^c	5 ± 1.4
38		Me	83 ± 6	19 ^d
39		H	20 ± 1	10 ^d
40		H	34 ± 1	33 ^d
41		H	44 ± 1	14 ± 1.1
42		H	103 ± 4	47 ^d

^a & ^b See the [Experimental Section](#) for details on assay methods; the values were calculated from at least eight data points with at least two independent determinations. ^c This value is a K_i measurement. ^d These values are from a single determination.

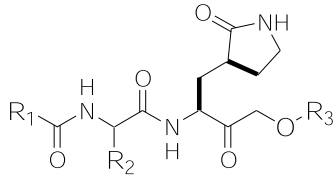
K³⁴ and cruzain.⁴³ High-resolution crystal structures of two such inhibitors complexed with cruzain highlighted the presence of a strong hydrogen bond between the catalytic His and the α -hydroxyl moiety of the inhibitor but interestingly no covalent bond between the active-site Cys and the ketone pharmacophore. Utilizing the crystal structure of **28** in complex with SARS CoV-1 3CL^{pro}, molecular modeling of an HMK-based design indicated the potential for establishing a covalent bond between the sulfur of the active-site cysteine (Cys145) and the HMK carbonyl as well as hydrogen bond interactions between catalytic His41 and the terminal hydroxy moiety. Additionally, the structure of **28** suggested the possibility to increase the lipophilic filling of the deep hydrophobic S₂ pocket as a strategy to increase binding affinity. To evaluate these structure-based observations, a series of reversible HMK inhibitors containing P₂ diversity were prepared as depicted in [Table 3](#).

As suggested by molecular modeling, the S₂ site appears to accommodate a variety of linear, branched, and cyclic alkyl moieties (entries **36** and **39–41**). Interestingly, the P₂ Phe derivative **42** displayed less potent inhibition of the SARS CoV-1 3CL^{pro} than the corresponding saturated analogue **41**. Also noteworthy is the large attenuation in enzyme inhibition seen with P₂-N-methyl-Leu inhibitor **38** (IC₅₀ = 83 nM) as compared to **4** (K_i = 4 nM). This loss of potency is consistent with the inhibitor ligand interactions observed with **2** and **4** that show the P₂ NH involved in a hydrogen bond with the side-chain amide of Gln189. Additionally, the methyl

substitution in **38** would be expected to alter the conformation of the 4-methoxy indole cap and perturb the observed ligand–enzyme hydrogen bond network present in **2** and **4**.

The results for **4** and the other examples in [Table 3](#) reveal a high antiviral EC₅₀/enzyme IC₅₀ ratio, which may arise from poor cell permeability. Indeed, these HMK inhibitors exhibit very low permeability and high levels of efflux beyond the sensitivity of the Caco-2 *in vitro* assay. However, the impact of high efflux on antiviral potencies from Vero 76 cells (derived from monkey kidney) versus disease-relevant human lung epithelial cells is unknown. To better understand the observed high antiviral EC₅₀/enzyme IC₅₀ ratio for **4**, we evaluated the role of efflux in the Vero 76 cell line by the *in vitro* experimental design discussed further below. Concurrently, a strategy to design molecules reducing efflux by active transporters, such as P-glycoprotein, was pursued to decrease high antiviral EC₅₀/enzyme IC₅₀ ratios. An analysis of the physicochemical properties of **4** suggested that increasing logP, reducing polar surface area (PSA), and reducing the number of hydrogen bond donors/acceptors were design strategies with the potential to improve cellular permeability and reduce efflux.

An examination of the crystal structure of **2** in complex with SARS CoV-1 3CL^{pro} suggested a limited functional role for the 4-methoxy substituent contained in the P₃ indole cap. Additionally, the terminal α -hydroxyl moiety located at P₁' appeared to provide a potential opportunity to remove a hydrogen bond donor. Although it was anticipated that the α -

Table 4. SARS CoV-1 3CL^{pro} Inhibition Data for P₃- and P₂-Modified Hydroxymethyl and Alkoxyethylketone Inhibitors


Entry	R ₁	R ₂	R ₃	SARS CoV-1 3CL ^{pro} FRET ^a IC ₅₀ (nM)	SARS CoV-1 ^b EC ₅₀ (μM)
36			H	7 ± 1	10 ± 1.8
37			Me	35 ± 1	32 ^d
43			H	20 ± 1	17 ^d
44			Me	105 ± 4	46 ^d
45			Et	112 ± 4	20 ^d
46			H	91 ± 2	33 ^d
47			Me	1,076 ± 52	>100 ^d
4			H	4 ± 0.3 ^c	5 ± 1.4
48			Me	53 ± 1	31 ± 1.2
49			H	38 ± 1	20 ^d
50			Me	131 ± 3	45 ^d

^a&^b See the [Experimental Section](#) for details on assay methods; the values were calculated from at least eight data points with at least two independent determinations. ^cThis value is a K_i measurement. ^dThese values are from a single determination.

hydroxyl moiety would form a hydrogen bond to the catalytic His41, the directionality of this interaction was uncertain. As noted earlier, His41 presents a hydrogen bond donor to the interior of the protease, leaving an acceptor to participate in the proton transfer cycling from neutral to cationic in the putative catalytic mechanism⁴⁴ of proteolysis. If His41 is protonated in the inhibitor-bound complex, a lone pair from the α -hydroxyl moiety would function as a hydrogen bond acceptor from the proton on the His residue. On the other hand, if His41 is deprotonated, the hydrogen of the α -hydroxyl moiety would act as a hydrogen bond donor to the nitrogen lone pair of the His residue. Consistent with the strategy to decrease PSA and hydrogen bond donors, a series of inhibitors were prepared that contained alterations to the P₃ cap and substitution of the α -hydroxyl group.

Table 4 summarizes this effort where two of the optimal P₂ residues (Leu and β -tert-butyl-Ala) were conserved. Removal of the methoxy group from the indole generally led to slightly weaker potency in both the enzymatic and antiviral assays across pairs (43 vs 36, 44 vs 37, 50 vs 48 and 49 vs 4) and therefore no improvement in the antiviral/protease inhibition ratio. The impact of more significant changes to the P₃ cap is illustrated by tetrahydrofuranyl derivatives 46 and 47. These derivatives lack the lipophilic aryl ring and NH hydrogen bond donor present in the indole P₃ cap and exhibit a pronounced

reduction in enzymatic and antiviral potency. A noteworthy reduction in biochemical and antiviral potency was observed in comparing each hydroxymethylketone derivative with its corresponding ether counterpart. These results suggest that modest structural and physicochemical alterations of 4 fail to significantly decrease the high EC₅₀/IC₅₀ ratios for this class of peptidomimetics. However, *in vitro* analysis of 4 revealed this derivative to possess high levels of metabolic stability in human liver microsomes ($t_{1/2}$ = 107 min).⁴⁵ Further evaluation of this breakthrough derivative in several aqueous-based formulations suitable for IV administration indicated high levels of solubility.⁴⁶

Cocrystal structures of 4 bound to the 3CL^{pro} of both SARS CoV-1 and CoV-2 were solved at 1.47 and 1.26 Å resolutions, respectively (PDB codes 6XHL and 6XHM).⁴⁷ As expected, the ligand binding sites of the main protease from SARS CoV-1 and SARS CoV-2 are conserved in sequence and are nearly identical structurally. The schematic diagram in Figure 5 is representative of the covalent adduct between 4 and the 3CL^{pro} from both CoV-1 and CoV-2. The warhead HMK carbonyl carbon of 4 forms a covalent bond to the 3CL^{pro} active-site cysteine (Cys145) sulfur generating a tetrahedral carbinol complex (1.8 Å C–S bond length). This carbinol hydroxyl forms hydrogen bonds with the backbone NH of Cys145 and with the amide NH of Gly143 via a bridging water molecule.

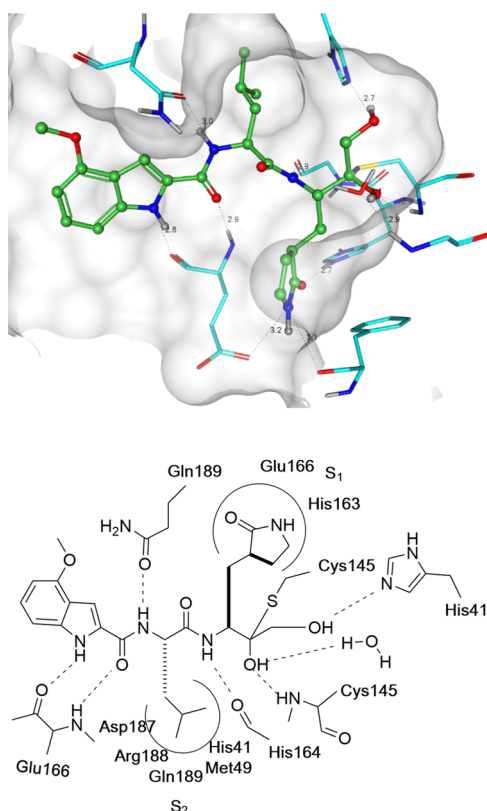


Figure 5. Cocrystal structure of the covalent adduct of **4** bound to SARS CoV-2 3CL^{pro} (6XHM). The Connolly surface for the inhibitor binding pocket is shown in gray. The bonds are represented as dashed lines, with the bond length between heavy atoms depicted. The schematic rendering of the active site with dashed lines represented as hydrogen bonds with key residues and curved lines to show S₁ and S₂ binding pockets is depicted.

Another key active-site interaction is the hydrogen bond between the primary alcohol moiety of **4** and the catalytic His41. Similar interactions between catalytic His residues and the OH moiety of HMK in other protease–inhibitor complexes have been reported.⁴³

In S₁, the lactam carbonyl of **4** forms a strong hydrogen bond with the side chain of His163, while the lactam NH is within the hydrogen-bonding distance but poorly aligned with the side-chain oxygen of Glu166 and the backbone oxygen of Phe140. These three residues partially define the bottom and edge of the S₁ pocket. Additionally, the backbone carbonyl and NH of Glu166 form β -sheet-like hydrogen-bonding interactions with the NH and C2-carbonyl of the indole fragment of **4**. The NH of the P₂ Leu of inhibitor **4** and the side chain of Gln189 form a hydrogen bond, while the carbonyl of P₂ Leu is exposed to the solvent. The inhibitor P₁ NH forms a strong hydrogen bond with the backbone carbonyl of His164. The inhibitor's lipophilic leucine residue is bound to the SARS 3CL^{pro} in the hydrophobic S₂ pocket formed by residues Asp187, Arg188, Gln189, Met49, and His41. The indole portion of **4** does not protrude into the S₃ pocket but rather rests across a partially collapsed S₃, making extended van der Waals interactions across the 189–191 residue backbone atoms. The closed S₃ is the only significant conformational difference compared to a recently reported structure of SARS CoV-2 3CL^{pro} inhibited by α -ketoamides.⁸ The energetics of this extended interaction, the associated protein conformation

stabilities, or warhead difference may contribute to the 3-order-of-magnitude increased SARS CoV-2 3CL^{pro} potency of HMK **4** (see below) compared to that of the referenced ketoamides.

Hydroxymethylketone **4** was evaluated against a panel of other viral and human proteases (Table 5). In general, **4** is

Table 5. Protease Inhibition by **4**

protease	source	% inhibition @ 10 μ M ^a	IC ₅₀ (μ M) ^a
3CL ^{pro}	SARS CoV-1		0.004 \pm 0.0003 ^b
3CL ^{pro}	SARS CoV-2		0.00027 \pm 0.0001 ^b
cathepsin B	human	93	1.3 \pm 0.1
cathepsin D	human	3	>10
leukocyte elastase	human	–31	>10
chymotrypsin	human	8	>10
thrombin	human	–28	>10
pepsin	human	–2	>10
caspase 2	human	–20	>10
HIV-1	HIV-1	0	>10
HCV	HCV	16	>10
HRV	HRV		1.7 \pm 1
hCoV 229E	human		0.004 \pm 0.0004

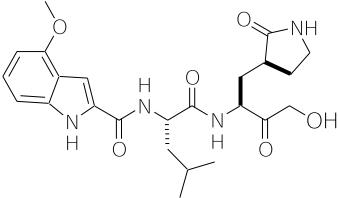
^aSee the Experimental Section for details on assay methods; the values were calculated from at least eight data points with at least two independent determinations. ^bFor SARS CoV-1 and CoV-2 3CL^{pro}, K_i values are reported here.

highly selective for 3CL^{pro} inhibition, displaying IC₅₀ values of >10 μ M against many of the other proteases and possessing modest levels of inhibition of cathepsin B (IC₅₀ = 1.3 μ M) and rhinovirus 3C^{pro} (IC₅₀ = 1.7 μ M). High levels of similarity between the catalytic sites of 3CL^{pro} proteases suggest the potential of **4** as a pan-coronavirus inhibitor. Testing revealed that **4** demonstrates potent inhibition of the related hCoV 229E protease (IC₅₀ = 0.004 μ M) but more importantly, given the current global pandemic, potently inhibits SARS CoV-2 3CL^{pro} with a K_i of 0.27 nM.

The antiviral specificity of **4** was evaluated against a panel of viruses (Table 6). No antiviral activity was observed when **4** was tested against two human rhinovirus strains (HRV-14 and HRV-16), human immunodeficiency virus-1 (HIV-1), or human cytomegalovirus (HCMV) in cell culture. This compound also does not inhibit the HCV replicon. As anticipated by the potent hCoV 229E protease activity, **4** is a potent inhibitor of the human coronavirus hCoV 229E in MRC-5 cells (human lung-derived) with an EC₅₀ of 0.090 μ M.

The hCoV 229E antiviral potency is more than 50-fold greater than that for SARS CoV-1 in the Vero 76 line, even though **4** possesses nearly equivalent 3CL^{pro} biochemical potency for the hCoV 229E and CoV-1 viruses. While undefined differences between hCoV 229E and SARS CoV-1 could account for these large differences in antiviral EC₅₀/enzyme IC₅₀ ratios, different active transporter expression

Table 6. Viral Inhibition by 4



virus	EC ₅₀ (μM) ^a	CC ₅₀ (μM) ^a
SARS CoV-1	4.8 ± 2.2	452
hCoV 229E	0.09 ± 0.04	>40
HRV-14	>100	>1,260
HRV-16	>100	>1,260
HIV-1 RF	>32	>32
HCV replicon	>320	>320
HCMV RC256	>100	>100

^aSee the Experimental Section for details on assay methods; the values were calculated from at least eight data points with at least two independent determinations.

levels between MRC-5 and Vero 76 cell lines may also be a contributing factor. Consistent with the previously stated goal to characterize the impact of efflux on potency measured in the SARS CoV-1 antiviral assay, we co-dosed a known P-glycoprotein transport inhibitor at a fixed concentration (0.5 μM CP-100356)⁴⁸ in a full dose–response of inhibitor 4. This resulted in a pronounced potency shift of SARS CoV-1 antiviral activity (EC₅₀ = 0.11 μM) that now more closely matched the antiviral potency seen for hCoV 229E. As a control, the same co-dosing of efflux inhibitor led to no such shift in the hCoV 229E antiviral potency of 4, demonstrating that the human lung-derived MRC-5 cells show less P-glycoprotein-based transporter under similar assay conditions. These results suggest that the high antiviral EC₅₀/enzyme IC₅₀ ratio observed in Vero 76 cells is an artifact of the high efflux potential of that assay cell line and may underestimate the antiviral potency in human lung cells, the relevant tissue for SARS and COVID-19. Assays to directly measure the antiviral potency of 4 against SARS CoV-2 in clinically relevant human lung cells are currently under investigation.

CONCLUSIONS

This report details the efforts to identify irreversible and reversible peptidomimetic inhibitors of the SARS CoV-1 3CL^{pro} as potential IV agents for the treatment of SARS and other coronavirus diseases. Two classes, acloxymethylketones and hydroxymethylketones, were discovered as potent inhibitors of the SARS 3CL^{pro}. The hydroxymethylketone derivative 4 demonstrated potent SARS CoV-1 inhibition in 3CL^{pro} and antiviral assays. Additionally, 4 possesses acceptable solubility, stability in plasma, and low *in vitro* and *in vivo* clearances suitable for further development as a coronavirus treatment.⁴⁹ Importantly, the potent inhibition of SARS CoV-2 3CL^{pro} has prompted further preclinical investigations of 4 as a potential therapeutic treatment for patients with COVID-19.

EXPERIMENTAL SECTION

General Procedures. Unless otherwise noted, materials were obtained from commercial suppliers and used without further purification. The removal of solvent under reduced pressure or concentration refers to distillation using a Büchi rotary evaporator attached to a vacuum pump (3 mmHg). Products obtained as solids

or high-boiling oils were dried under vacuum (1 mmHg). Silica gel chromatography was performed on either a CombiFlash (Teledyne ISCO), SP4, or Isolera (Biotage) purification system. All reactions were performed under a positive pressure of nitrogen or argon or with a drying tube at an ambient temperature (unless otherwise stated) in anhydrous solvents, unless otherwise indicated. Analytical thin-layer chromatography (TLC) was performed on glass-backed silica gel 60 F254 plates (Analtech, 0.25 mm), eluting with the appropriate solvent ratio (v/v). The reactions were assayed by high-performance liquid chromatography–mass spectrometry (LCMS) or TLC and terminated as judged by the consumption of the starting material. LCMS utilized wavelengths of 254 and 220 nm and either electrospray ionization (ESI) in positive mode or atmospheric-pressure chemical ionization (APCI) in positive mode. The TLC plates were visualized using UV light, *p*-anisaldehyde, phosphomolybdic acid, or iodine staining. Microwave-assisted reactions were run in a Biotage Initiator. ¹H NMR spectra were recorded on a Bruker XWIN-NMR (400 MHz) spectrometer. Proton chemical shifts are reported in parts per million downfield from tetramethylsilane (TMS). ¹H NMR data are reported as chemical shift (multiplicity, coupling constant, integration). Multiplicities are denoted as follows: s, singlet; d, doublet; t, triplet; q, quartet; dd, doublet of doublets; dt, doublet of triplets; and brs, broad singlet. For spectra obtained in CDCl₃, DMSO-*d*₆, and CD₃OD, the residual protons (7.27, 2.50, and 3.31 ppm, respectively) were used as the internal references. The purity of the final products is >95% as determined by HPLC and/or ¹H NMR analyses.

***N*-(*tert*-Butoxycarbonyl)-3-[(3*S*)-2-oxopyrrolidin-3-yl]-L-alanine (6).** A 3 L multineck flask equipped with an overhead stirrer and internal thermometer was charged with methyl *N*-(*tert*-butoxycarbonyl)-3-[(3*S*)-2-oxopyrrolidin-3-yl]-L-alaninate (compound 5)³³ (205 g, 716 mmol) followed by methanol (1 L), and the solution was cooled to 0 °C using ice/NaCl bath. NaOH (115 g in 950 mL water, 2.9 mol) solution was precooled to 0 °C and then added to the flask *via* a pressure-equalizing dropping funnel at such a rate to maintain the internal temperature below 5 °C. The resulting solution was stirred at 0 °C for 1 h before neutralizing with conc. hydrochloric acid (keeping the internal temperature below 10 °C) and then removing the methanol *in vacuo*. The residue was diluted with ethyl acetate (400 mL), acidified to pH 3 with conc. hydrochloric acid, and then the mixture was transferred to a sep funnel, and the organics were removed. The aqueous was extracted with ethyl acetate (2 × 400 mL), and the combined organics were washed with brine, dried over MgSO₄, filtered, and concentrated to yield the title compound as a white foam, 95%. ¹H NMR (400 MHz, MeOD) δ 3.98–4.28 (m, 1H), 3.25–3.41 (m, 2H), 2.44–2.57 (m, 1H), 2.29–2.41 (m, 1H), 2.03–2.14 (m, 1H), 1.73–1.90 (m, 2H), 1.44 (s, 9H); MS (APCI–) for C₁₂H₂₀N₂O₅ *m/z* 272.3 (M – H)[–].

***tert*-Butyl ((1*S*)-3-Diazo-2-oxo-1-[(3*S*)-2-oxopyrrolidin-3-yl]-methyl)propyl)carbamate (7).** A solution of *N*-(*tert*-butoxycarbonyl)-3-[(3*S*)-2-oxopyrrolidin-3-yl]-L-alanine (2.72 g, 10.0 mmol) in THF (100 mL) was placed under an atmosphere of N₂ and cooled to –23 °C. The resulting clear colorless solution was successively treated with triethylamine (2.1 mL, 15.0 mmol) followed by isobutylchloroformate (1.6 mL, 12.0 mmol). The reaction mixture gradually became opaque with a fine white precipitate and after 1 h was filtered. The colorless filtrate was transferred to a nonground joint flask, cooled to 0 °C, and slowly treated with a solution of diazomethane (~35 mL, ~16.6 mmol) in diethyl ether. Note: The diazomethane was generated employing a Diazald kit according to the procedure described in the Aldrich Technical Bulletin AL-180. The resulting yellow clear solution was gradually warmed to room temperature (RT) over 16 h. At this time, N₂ was bubbled through the reaction to remove excess diazomethane followed by *in vacuo* concentration. The resulting residue was diluted with ethyl acetate (100 mL), washed once with sat. NaHCO₃ (50 mL), once with brine (50 mL), dried over MgSO₄, filtered, and concentrated to give a crude yellow foam. This material was purified by LC (150 g 230–400 SiO₂, 3–4% methanol/chloroform) to afford 2.72 g (92%) of the title compound as a light yellow foam. ¹H NMR (DMSO-*d*₆) δ 7.63 (bs, 1H), 7.42 (d, *J* = 8 Hz, 1H), 6.06 (bs, 1H), 3.96 (m, 1H), 3.13 (m, 2H), 2.21 (m,

1H), 2.01 (m, 1H), 1.86 (m, 1H), 1.63–1.52 (m, 2H), 1.38 (s, 9H); MS (ESI+) for $C_{13}H_{26}N_4O_4$ m/z 319.0 (M + Na)⁺.

tert-Butyl ((1S)-3-Chloro-2-oxo-1-[(3S)-2-oxopyrrolidin-3-yl]-methyl)propyl)carbamate (8). A three-neck flame-dried flask equipped with a nitrogen inlet and internal thermometer was charged with methyl *N*-(*tert*-butoxycarbonyl)-3-[(3S)-2-oxopyrrolidin-3-yl]-L-alaninate (10 g, 35 mmol), THF (200 mL), and chloriodomethane (10.2 mL, 140 mmol), and the solution was cooled to -77°C . LDA (140 mL, 210 mmol, 1.5 M mono-THF complex in cyclohexane) was added via a pressure-equalizing dropping funnel at such a rate to keep the internal temperature below -70°C . After complete addition, the reaction was stirred for an additional hour and quenched with a mixture of AcOH (33 mL) and THF (200 mL) with a rate of addition regulated to maintain the internal temperature below -65°C . After complete addition, the dark suspension was stirred for 10 min and then warmed to an ambient temperature. The reaction was diluted with ethyl acetate (500 mL), and the organics were washed with water (250 mL), satd. NaHCO_3 (250 mL), and brine (250 mL), dried over MgSO_4 , filtered, and the solvents were removed *in vacuo* to yield the crude product as a dark oil, which was purified by flash chromatography eluting with ethyl acetate. The resulting solid was triturated with diethyl ether to afford the title compound as a pale yellow solid, 5.7 g, 54%. ¹H NMR (400 MHz, $\text{DMSO}-d_6$) δ 7.88 (s, 1H), 7.75 (d, $J = 7.6$ Hz, 1H), 4.73–4.94 (m, 2H), 4.37 (m, 1H), 3.28–3.43 (m, 2H), 2.46 (m, 1H), 2.30–2.40 (m, 1H), 2.02–2.14 (m, 1H), 1.77–1.95 (m, 2H), 1.60 (s, 9H); MS (API-ES+) for $C_{13}H_{21}N_2O_4Cl$ m/z 327.1 (M + Na)⁺; anal. calcd for $C_{13}H_{21}N_2O_4$: C, 51.23; H, 6.95; N, 9.19. Found: C, 51.03; H, 6.93; N, 9.03.

tert-Butyl((1S)-3-(benzyloxy)-2-oxo-1-[(3S)-2-oxopyrrolidin-3-yl]methyl)propyl)carbamate (9). To a 3 L multinecked flask equipped with an overhead stirrer, nitrogen inlet, and internal thermometer was charged *N*-(*tert*-butoxycarbonyl)-3-[(3S)-2-oxopyrrolidin-3-yl]-L-alanine (190 g, 698 mmol) followed by dichloromethane (1100 mL) and the solution was cooled to 0°C employing an ice/NaCl bath. *N,O*-Dimethylhydroxylamine hydrochloric acid salt (68 g, 698 mmol) was added followed by *N*-methylmorpholine (230 mL, 2.09 mol), HOBT hydrate (106 g, 698 mmol), and EDCI (147 g, 768 mmol), and the mixture was stirred at 0°C under nitrogen for 6 h before quenching with water (500 mL). The biphasic mixture was transferred to a sep funnel, and the organics were isolated, washed with 1 M hydrochloric acid (2×500 mL), water (400 mL), satd. NaHCO_3 (2×700 mL), and brine (300 mL) and then dried over MgSO_4 , filtered, and the solvents were evaporated *in vacuo* to yield *tert*-butyl ((1S)-2-[methoxy(methyl)amino]-2-oxo-1-[(3S)-2-oxopyrrolidin-3-yl]methyl)ethyl)carbamate as a pale yellow solid, 173 g, 79%. ¹H NMR (400 MHz, CDCl_3) δ 5.92 (s, 1H), 5.39 (d, $J = 8.8$ Hz, 1H), 4.66 (td, $J = 9.6, 2.8$ Hz, 1H), 3.77 (s, 3H), 3.33 (dd, $J = 9.3, 4.0$ Hz, 2H), 3.19 (s, 2H), 2.41–2.62 (m, 2H), 2.05–2.16 (m, 1H), 1.75–1.95 (m, 1H), 1.67 (m, 1H), 1.41 (s, 9H).

To a 100 mL multinecked flask equipped with a stirrer bar, nitrogen inlet, and internal thermometer were charged magnesium turnings (dried in oven at 100°C overnight, 1.04 g, 43 mmol) and HgCl_2 (774 mg, 2.85 mmol), and the flask was purged with nitrogen for 10 min. THF (50 mL) was added, and the suspension was cooled to -45°C before adding BOM-Cl (5.94 mL, 43 mmol), and the resulting suspension was stirred for 5 h, the temperature returning to 5°C . The suspension was recooled to -50°C , and *tert*-butyl ((1S)-2-[methoxy(methyl)amino]-2-oxo-1-[(3S)-2-oxopyrrolidin-3-yl]methyl)ethyl)carbamate (1.5 g, 4.76 mmol) was added, and the thick suspension was stirred for 48 h under nitrogen and was allowed to come to an ambient temperature. The reaction was quenched by the careful addition of satd. NH_4Cl solution (25 mL), and the mixture was stirred until effervescence ceased and then extracted with ethyl acetate (3×120 mL). The combined organics were dried over MgSO_4 , filtered, and the solvents were evaporated *in vacuo* to yield a crude orange gum, which was purified by flash chromatography, eluting with 1–3% methanol/dichloromethane to afford the title compound as a clear glass, 900 mg, 50%. ¹H NMR (400 MHz, CDCl_3) δ 7.21–7.33 (m, 5H), 5.63–5.73 (m, 2H), 4.52 (m, 3H), 4.19 (q, $J = 17.4$ Hz, 2H), 3.19–3.25 (m, 2H), 2.29–2.42 (m, 2H),

1.68–1.93 (m, 3H), 1.35 (s, 9H); MS (APCI+) for $C_{20}H_{28}N_2O_5$ m/z 378.1 (M + H)⁺.

(3S)-3-[(2S)-2-Amino-4-chloro-3-oxobutyl]pyrrolidin-2-one, Hydrochloride Salt (10). A solution of *tert*-butyl ((1S)-3-diazo-2-oxo-1-[(3S)-2-oxopyrrolidin-3-yl]methyl)propyl) carbamate (592 mg, 2.0 mmol) in 1,4-dioxane (7 mL) was placed under an atmosphere of N_2 and cooled to 0°C . This clear pale yellow solution was dropwise treated with a solution of 4 M hydrochloric acid in 1,4-dioxane (5 mL, 20 mmol) with copious gas evolution observed. Upon complete addition, the reaction was warmed to RT over 1 h with the formation of a white precipitate. The solid was collected by filtration, washed with diethyl ether, and dried to give 401 mg (83%) of the title compound as a white powder. ¹H NMR ($\text{DMSO}-d_6$) δ 8.76 (bs, 3H), 7.96 (s, 1H), 4.93 (d, $J = 16$ Hz, 1H), 4.80 (d, $J = 16$ Hz, 1H), 4.28 (m, 1H), 3.18 (m, 2H), 2.61 (m, 1H), 2.30 (m, 1H), 1.93 (m, 2H), 1.70 (m, 1H); MS (ESI+) for $C_8H_{13}ClN_2O_2$ m/z 205.0 (M + H)⁺.

tert-Butyl ((1S)-3-Bromo-2-oxo-1-[(3S)-2-oxopyrrolidin-3-yl]methyl)propyl)carbamate (11). A solution of *tert*-butyl ((1S)-3-chloro-2-oxo-1-[(3S)-2-oxopyrrolidin-3-yl]methyl)propyl)carbamate (1.26 g, 4.3 mmol) in dichloromethane (107 mL) at 0°C under nitrogen was treated with 48% hydrobromic acid (0.48 mL, 4.3 mmol) with effervescence observed. The reaction was stirred at 0°C for 1 h, washed once with water (30 mL), dried over MgSO_4 , filtered, and concentrated to afford 1.23 g (83%) of the title compound as a white solid. ¹H NMR (400 MHz, $\text{DMSO}-d_6$) δ 7.64 (s, 1H), 7.51 (d, $J = 8$ Hz, 1H), 4.46 (d, $J = 16$ Hz, 1H), 4.41 (d, $J = 16$ Hz, 1H), 4.19 (m, 1H), 3.13 (m, 2H), 2.26 (m, 1H), 2.13 (m, 1H), 1.87 (m, 1H), 1.63 (m, 2H), 1.38 (s, 9H); MS (ESI+) for $C_{13}H_{21}BrN_2O_4$ m/z 371.0 (M + H)⁺.

***N*-((1S)-1-[(1S)-3-Chloro-2-oxo-1-[(3S)-2-oxopyrrolidin-3-yl]methyl)propyl]amino)carbonyl-3-methylbutyl)-4-methoxy-1H-indole-2-carboxamide (12).** A solution of **29**, *N*²-(*tert*-butoxycarbonyl)-*N*¹-((1S)-3-chloro-2-oxo-1-[(3S)-2-oxopyrrolidin-3-yl]methyl)propyl)-L-leucinamide (244 mg, 0.59 mmol) in 1,4-dioxane (1.0 mL) was placed under an atmosphere of N_2 . This clear colorless solution was treated with a solution of 4 M hydrochloric acid in 1,4-dioxane with no observable change. The reaction gradually became opaque with the formation of a gummy precipitate. After 2 h, the volatiles were removed *in vacuo*, diluted with 1:1 ethanol/1,4-dioxane, concentrated, and high-vacuum-dried to give *N*¹-((1S)-3-chloro-2-oxo-1-[(3S)-2-oxopyrrolidin-3-yl]methyl)propyl)-L-leucinamide hydrochloride as an off-white solid. ¹H NMR ($\text{DMSO}-d_6$) δ 9.18 (d, $J = 8$ Hz, 1H), 8.40 (bs, 3H), 7.69 (s, 1H), 4.68 (s, 2H), 4.49 (m, 1H), 3.81 (m, 1H), 3.15 (m, 2H), 2.37 (m, 1H), 2.17 (m, 1H), 1.92 (m, 1H), 1.67 (m, 3H), 1.55 (m, 2H), 0.92 (d, $J = 4$ Hz, 3H), 0.88 (d, $J = 4$ Hz, 3H); MS (ESI+) for $C_{14}H_{24}ClN_3O_3$ m/z 318.1 (M + H)⁺.

A solution of the crude hydrochloride salt and 4-methoxy-1H-indole-2-carboxylic acid (123 mg, 0.64 mmol) in DMF (2.5 mL) was placed under an atmosphere of N_2 and cooled to 0°C . This pale yellow solution was successively treated with HATU (245 mg, 0.64 mmol) and *N*-methylmorpholine (0.14 mL, 1.29 mmol) turning a brighter color. After 30 min, the reaction was quenched with 1:1 ice/sat NaHCO_3 (25 mL) and extracted three times with ethyl acetate (20 mL). The combined organics were washed once with brine (30 mL), dried over MgSO_4 , filtered, and concentrated to give a yellow syrup. This material was purified by LC (30 g 230–400 SiO_2 , 4% methanol/chloroform) to afford 167 mg (58%) of the title compound as an off-white solid. ¹H NMR ($\text{DMSO}-d_6$) δ 11.59 (s, 1H), 8.62 (d, $J = 8$ Hz, 1H), 8.44 (d, $J = 4$ Hz, 1H), 7.65 (s, 1H), 7.38 (s, 1H), 7.10 (t, $J = 8$ Hz, 1H), 7.02 (d, $J = 8$ Hz, 1H), 6.51 (d, $J = 8$ Hz, 1H), 4.60 (d, $J = 16$ Hz, 1H), 4.58 (d, $J = 16$ Hz, 1H), 4.46 (m, 2H), 3.89 (s, 3H), 3.11 (m, 2H), 2.29 (m, 1H), 2.11 (m, 1H), 1.99 (m, 1H), 1.76–1.54 (m, 5H), 0.95 (d, $J = 8$ Hz, 3H), 0.9 (d, $J = 8$ Hz, 3H); MS (ESI+) for $C_{24}H_{31}ClN_4O_5$ m/z 491.1 (M + H)⁺; HRMS (ESI+) calcd for $C_{24}H_{31}ClN_4O_5 + \text{H}^+$ 491.2056, found 491.2058.

(3S)-3-[(*N*)-[4-Methoxy-1H-indol-2-yl]carbonyl]-L-leucyl]amino]-2-oxo-4-[(3S)-2-oxopyrrolidin-3-yl]butyl Acetate (13). An oven-dried 40 mL scintillation vial with a spinbar was charged with acetic acid (27 mg, 0.46 mmol) followed by a solution of *N*-((1S)-1-[(1S)-3-chloro-2-oxo-1-[(3S)-2-oxopyrrolidin-3-yl]methyl]-

propyl)amino]carbonyl]-3-methylbutyl)-4-methoxy-1H-indole-2-carboxamide (172 mg, 0.35 mmol) in DMF (3.5 mL) and purged with N₂. This pale yellow solution was then treated with CsF (122 mg, 0.81 mmol), sealed with a Teflon-lined screwcap, and heated at 65 °C on a reaction block with vigorous stirring. After 3 h, the reaction was cooled to RT, diluted with water (30 mL), and extracted with dichloromethane (4 × 7 mL). The combined organic layers were washed with water (2 × 20 mL), brine (20 mL), and concentrated *in vacuo*. This material was purified by Biotage MPLC (25 M, 2.5–4.5% methanol/dichloromethane) to afford 78 mg (45%) of the title compound as a white solid. ¹H NMR (400 MHz, DMSO-*d*₆) δ 11.57 (s, 1H), 8.57 (d, *J* = 7.8 Hz, 1H), 8.43 (d, *J* = 7.6 Hz, 1H), 7.64 (s, 1H), 7.36 (d, *J* = 1.8 Hz, 1H), 7.08 (t, *J* = 8.0 Hz, 1H), 6.99 (d, *J* = 8.1 Hz, 1H), 6.49 (d, *J* = 7.6 Hz, 1H), 4.83 (d, *J* = 3.0 Hz, 1H), 4.76–4.95 (m, 1H), 4.35–4.50 (m, 2H), 3.87 (s, 3H), 3.03–3.17 (m, 2H), 2.22–2.35 (m, 1H), 2.09–2.22 (m, 1H), 2.07 (s, 3H), 1.90–2.04 (m, 1H), 1.65–1.77 (m, 2H), 1.48–1.65 (m, 3H), 0.94 (d, *J* = 6.3 Hz, 3H), 0.89 (d, *J* = 6.3 Hz, 3H); MS (ESI+) for C₂₆H₃₄N₄O₇ *m/z* 515.2 (M + H)⁺. Anal. calcd for C₂₆H₃₄N₄O₇·0.65 H₂O: C, 59.34; H, 6.76; N, 10.65. Found: C, 59.41; H, 6.63; N, 10.68.

(3S)-3-((N-[(4-Methoxy-1H-indol-2-yl)carbonyl]-L-leucyl)amino)-2-oxo-4-[(3S)-2-oxopyrrolidin-3-yl]butyl Cyclopropanecarboxylate (14). Following the procedure described for the preparation of (3S)-3-((N-[(4-methoxy-1H-indol-2-yl)carbonyl]-L-leucyl)amino)-2-oxo-4-[(3S)-2-oxopyrrolidin-3-yl]butyl acetate but substituting cyclopropanecarboxylic acid and making noncritical variations provided a crude product. This material was purified by Biotage MPLC (25 M, 2.5–4.5% methanol/dichloromethane) to afford 82 mg (43%) of the title compound. ¹H NMR (400 MHz, DMSO-*d*₆) δ 11.57 (d, *J* = 2.0 Hz, 1H), 8.56 (d, *J* = 7.8 Hz, 1H), 8.43 (d, *J* = 7.6 Hz, 1H), 7.63 (s, 1H), 7.36 (d, *J* = 1.5 Hz, 1H), 7.08 (t, *J* = 8.0 Hz, 1H), 6.97–7.02 (m, 1H), 6.49 (d, *J* = 7.6 Hz, 1H), 4.85 (d, 1H), 4.78–4.96 (m, 1H), 4.33–4.51 (m, 2H), 3.87 (s, 3H), 3.02–3.16 (m, 2H), 2.22–2.35 (m, 1H), 2.01–2.11 (m, 1H), 1.89–2.00 (m, 1H), 1.65–1.77 (m, 3H), 1.46–1.65 (m, 3H), 0.81–0.98 (m, 10 H); MS (ESI+) for C₂₈H₃₆N₄O₇ *m/z* 541.2 (M + H)⁺. Anal. calcd for C₂₈H₃₆N₄O₇·0.59 H₂O: C, 61.01; H, 6.80; N, 10.16. Found: C, 61.04; H, 6.72; N, 10.00.

(3S)-3-((N-[(4-Methoxy-1H-indol-2-yl)carbonyl]-L-leucyl)amino)-2-oxo-4-[(3S)-2-oxopyrrolidin-3-yl]butyl Pivalate (15). Following the procedure described for the preparation of (3S)-3-((N-[(4-methoxy-1H-indol-2-yl)carbonyl]-L-leucyl)amino)-2-oxo-4-[(3S)-2-oxopyrrolidin-3-yl]butyl acetate but substituting pivalic acid and making noncritical variations provided a crude product. This material was purified by Biotage MPLC (25 M, 2.5–4.5% methanol/dichloromethane) to afford 152 mg (78%) of the title compound. ¹H NMR (400 MHz, DMSO-*d*₆) δ 11.58 (s, 1H), 8.56 (d, *J* = 7.8 Hz, 1H), 8.44 (d, *J* = 7.8 Hz, 1H), 7.64 (s, 1H), 7.36 (s, 1H), 7.08 (t, *J* = 8.0 Hz, 1H), 6.99 (d, 1H), 6.49 (d, *J* = 7.6 Hz, 1H), 4.84 (s, 1H), 4.77–4.94 (m, 1H), 4.34–4.51 (m, 2H), 3.87 (s, 3H), 3.02–3.16 (m, 2H), 1.91–2.36 (m, 3H), 1.48–1.78 (m, 5H), 1.16 (s, 9H), 0.94 (d, *J* = 6.3 Hz, 3H), 0.89 (d, *J* = 6.3 Hz, 3H); MS (ESI+) for C₂₉H₄₀N₄O₇ *m/z* 557.2 (M + H)⁺. Anal. calcd for C₂₉H₄₀N₄O₇·0.76 H₂O: C, 61.07; H, 7.34; N, 9.82. Found: C, 61.14; H, 7.63; N, 9.59.

(3S)-3-((N-[(4-Methoxy-1H-indol-2-yl)carbonyl]-L-leucyl)amino)-2-oxo-4-[(3S)-2-oxopyrrolidin-3-yl]butyl Benzoate (16). Following the procedure described for the preparation of (3S)-3-((N-[(4-methoxy-1H-indol-2-yl)carbonyl]-L-leucyl)amino)-2-oxo-4-[(3S)-2-oxopyrrolidin-3-yl]butyl acetate but substituting benzoic acid and making noncritical variations provided a crude product. This material was purified by Biotage MPLC (25 M, 2.5–4.5% methanol/dichloromethane) to afford 183 mg (91%) of the title compound. ¹H NMR (400 MHz, DMSO-*d*₆) δ 11.59 (s, 1H), 8.64 (d, *J* = 8.1 Hz, 1H), 8.46 (d, *J* = 7.6 Hz, 1H), 7.98 (d, *J* = 8.1 Hz, 2H), 7.91–7.95 (m, 1H), 7.66–7.71 (m, 1H), 7.66 (s, 1H), 7.52–7.57 (m, 1H), 7.37 (d, *J* = 1.8 Hz, 1H), 7.08 (t, *J* = 8.0 Hz, 1H), 6.96–7.02 (m, 1H), 6.49 (d, *J* = 7.6 Hz, 1H), 5.13 (s, 1H), 5.06–5.24 (m, 1H), 4.44–4.53 (m, 2H), 3.87 (s, 3H), 3.04–3.15 (m, 2H), 2.34 (m, 1H), 2.07–2.27 (m, 1H), 1.98–2.07 (m, 1H), 1.52–1.79 (m, 5H), 0.94 (d, *J* = 6.3 Hz, 3H), 0.89 (d, *J* = 6.3 Hz, 3H); MS (ESI+) for C₃₁H₃₆N₄O₇ *m/z* 577.2

(M + H)⁺. Anal. calcd for C₃₁H₃₆N₄O₇·1.04 H₂O: C, 62.54; H, 6.45; N, 9.41. Found: C, 62.49; H, 6.54; N, 9.31.

(3S)-3-((N-[(4-Methoxy-1H-indol-2-yl)carbonyl]-L-leucyl)amino)-2-oxo-4-[(3S)-2-oxopyrrolidin-3-yl]butyl 4-Methoxybenzoate (17). Following the procedure described for the preparation of (3S)-3-((N-[(4-methoxy-1H-indol-2-yl)carbonyl]-L-leucyl)amino)-2-oxo-4-[(3S)-2-oxopyrrolidin-3-yl]butyl acetate but substituting 4-methoxybenzoic acid and making noncritical variations provided a crude product. This material was purified by Biotage MPLC (25 M, 2.5–4.5% methanol/dichloromethane) to afford 145 mg (68%) of the title compound. ¹H NMR (400 MHz, DMSO-*d*₆) δ 11.59 (d, *J* = 1.8 Hz, 1H), 8.62 (d, *J* = 7.8 Hz, 1H), 8.46 (d, *J* = 7.6 Hz, 1H), 7.93 (d, *J* = 9.1 Hz, 2H), 7.65 (s, 1H), 7.37 (d, *J* = 2.0 Hz, 1H), 7.04–7.11 (m, 2H), 7.00 (dd, *J* = 8.6, 3.0 Hz, 2H), 6.50 (d, *J* = 7.6 Hz, 1H), 5.07 (s, 1H), 5.01–5.18 (m, 1H), 4.44–4.51 (m, 2H), 3.87 (s, 3H), 3.83 (s, 3H), 3.04–3.17 (m, 2H), 2.28–2.38 (m, 1H), 2.07–2.25 (m, 1H), 1.97–2.06 (m, 1H), 1.50–1.79 (m, 5H), 0.94 (d, *J* = 6.3 Hz, 3H), 0.89 (d, *J* = 6.3 Hz, 3H); MS (ESI+) for C₃₂H₃₈N₄O₈ *m/z* 607.2 (M + H)⁺. Anal. calcd for C₃₂H₃₈N₄O₈·0.80 H₂O·0.05 DCM: C, 61.56; H, 6.40; N, 8.96. Found: C, 61.84; H, 6.36; N, 8.58.

(3S)-3-((N-[(4-Methoxy-1H-indol-2-yl)carbonyl]-L-leucyl)amino)-2-oxo-4-[(3S)-2-oxopyrrolidin-3-yl]butyl 4-Methylbenzoate (18). Following the procedure described for the preparation of (3S)-3-((N-[(4-methoxy-1H-indol-2-yl)carbonyl]-L-leucyl)amino)-2-oxo-4-[(3S)-2-oxopyrrolidin-3-yl]butyl acetate but substituting 4-methylbenzoic acid and making noncritical variations provided a crude product. This material was purified by Biotage MPLC (25 M, 2.5–4.5% methanol/dichloromethane) to afford 92 mg (44%) of the title compound. ¹H NMR (400 MHz, DMSO-*d*₆) δ 11.59 (d, *J* = 1.8 Hz, 1H), 8.63 (d, *J* = 8.1 Hz, 1H), 8.46 (d, *J* = 7.6 Hz, 1H), 7.87 (d, *J* = 8.1 Hz, 2H), 7.65 (s, 1H), 7.37 (d, *J* = 1.8 Hz, 1H), 7.34 (d, *J* = 8.3 Hz, 2H), 7.08 (t, *J* = 8.0 Hz, 1H), 6.97–7.01 (m, 1H), 6.50 (d, *J* = 7.8 Hz, 1H), 5.09 (s, 1H), 5.03–5.20 (m, 1H), 4.43–4.52 (m, 2H), 3.87 (s, 3H), 3.04–3.17 (m, 2H), 2.38 (s, 3H), 2.28–2.34 (m, 1H), 2.06–2.14 (m, 1H), 1.96–2.06 (m, 1H), 1.51–1.78 (m, 5H), 0.94 (d, *J* = 6.3 Hz, 3H), 0.89 (d, *J* = 6.3 Hz, 3H); MS (ESI+) for C₃₂H₃₈N₄O₇ *m/z* 591.2 (M + H)⁺. Anal. calcd for C₃₂H₃₈N₄O₇·0.10 H₂O·0.11 DCM: C, 64.08; H, 6.43; N, 9.31. Found: C, 64.36; H, 6.41; N, 8.92.

(3S)-3-((N-[(4-Methoxy-1H-indol-2-yl)carbonyl]-L-leucyl)amino)-2-oxo-4-[(3S)-2-oxopyrrolidin-3-yl]butyl 4-Cyanobenzoate (19). Following the procedure described for the preparation of (3S)-3-((N-[(4-methoxy-1H-indol-2-yl)carbonyl]-L-leucyl)amino)-2-oxo-4-[(3S)-2-oxopyrrolidin-3-yl]butyl acetate but substituting 4-cyanobenzoic acid and making noncritical variations provided a crude product. This material was purified by Biotage MPLC (25 M, 2.5–4.5% methanol/dichloromethane) to afford 159 mg (75%) of the title compound. ¹H NMR (400 MHz, DMSO-*d*₆) δ 11.58 (d, *J* = 2.0 Hz, 1H), 8.64 (d, *J* = 8.1 Hz, 1H), 8.46 (d, *J* = 7.6 Hz, 1H), 8.09–8.14 (m, 2H), 7.99–8.05 (m, 2H), 7.66 (s, 1H), 7.37 (d, *J* = 1.5 Hz, 1H), 7.08 (t, *J* = 8.0 Hz, 1H), 6.99 (d, *J* = 8.3 Hz, 1H), 6.50 (d, *J* = 7.6 Hz, 1H), 5.17 (d, *J* = 2.8 Hz, 1H), 5.11–5.27 (m, 1H), 4.44–4.53 (m, 2H), 3.87 (s, 3H), 3.04–3.17 (m, 2H), 2.28–2.38 (m, 1H), 2.07–2.26 (m, 1H), 1.97–2.06 (m, 1H), 1.51–1.78 (m, 5H), 0.94 (d, *J* = 6.3 Hz, 3H), 0.89 (d, *J* = 6.3 Hz, 3H); MS (ESI+) for C₃₂H₃₅N₅O₇ *m/z* 602.2 (M + H)⁺. Anal. calcd for C₃₂H₃₅N₅O₇·0.90 H₂O: C, 62.21; H, 6.00; N, 11.33. Found: C, 62.23; H, 6.06; N, 11.58.

(3S)-3-((N-[(4-Methoxy-1H-indol-2-yl)carbonyl]-L-leucyl)amino)-2-oxo-4-[(3S)-2-oxopyrrolidin-3-yl]butyl 4-Fluorobenzoate (20). Following the procedure described for the preparation of (3S)-3-((N-[(4-methoxy-1H-indol-2-yl)carbonyl]-L-leucyl)amino)-2-oxo-4-[(3S)-2-oxopyrrolidin-3-yl]butyl acetate but substituting 4-fluorobenzoic acid and making noncritical variations provided a crude product. This material was purified by Biotage MPLC (25 M, 2.5–4.5% methanol/dichloromethane) to afford 136 mg (65%) of the title compound. ¹H NMR (400 MHz, DMSO-*d*₆) δ 11.58 (d, *J* = 2.0 Hz, 1H), 8.63 (d, *J* = 7.8 Hz, 1H), 8.46 (d, *J* = 7.6 Hz, 1H), 8.04 (dd, *J* = 8.6, 5.6 Hz, 2H), 7.65 (s, 1H), 7.35–7.41 (m, 3H), 7.08 (t, *J* = 8.0 Hz, 1H), 6.99 (d, *J* = 8.1 Hz, 1H), 6.50 (d, *J* = 7.6 Hz, 1H), 5.12 (d, *J* = 1.3 Hz, 1H), 5.06–5.23 (m, 1H), 4.44–4.52 (m, 2H), 3.87 (s, 3H), 3.04–3.17 (m, 2H), 2.28–2.38 (m, 1H), 2.07–2.26 (m, 1H), 1.98–

2.06 (m, 1H), 1.52–1.79 (m, 5H), 0.94 (d, J = 6.3 Hz, 3H), 0.89 (d, J = 6.3 Hz, 3H); MS (ESI+) for $C_{31}H_{35}FN_4O_7$ m/z 595.2 ($M + H$)⁺. Anal. calcd for $C_{31}H_{35}FN_4O_7 \cdot 0.59 H_2O \cdot 0.06 DCM$: C, 61.28; H, 5.98; N, 9.20. Found: C, 61.27; H, 5.98; N, 9.11.

(3S)-3-((N-[(4-Methoxy-1H-indol-2-yl)carbonyl]-L-leucyl)amino)-2-oxo-4-[(3S)-2-oxopyrrolidin-3-yl]butyl 4-Chlorobenzoate (21). Following the procedure described for the preparation of (3S)-3-((N-[(4-methoxy-1H-indol-2-yl)carbonyl]-L-leucyl)amino)-2-oxo-4-[(3S)-2-oxopyrrolidin-3-yl]butyl acetate but substituting 4-chlorobenzoic acid and making noncritical variations provided a crude product. This material was purified by Biotage MPLC (25 M, 2.5–4.5% methanol/dichloromethane) to afford 172 mg (80%) of the title compound. ¹H NMR (400 MHz, DMSO- d_6) δ 11.58 (d, J = 1.8 Hz, 1H), 8.63 (d, J = 7.8 Hz, 1H), 8.46 (d, J = 7.6 Hz, 1H), 7.98 (d, J = 8.6 Hz, 2H), 7.65 (s, 1H), 7.62 (d, J = 8.6 Hz, 2H), 7.37 (d, J = 1.8 Hz, 1H), 7.08 (t, J = 8.0 Hz, 1H), 6.99 (d, J = 8.3 Hz, 1H), 6.50 (d, J = 7.6 Hz, 1H), 5.13 (d, J = 1.5 Hz, 1H), 5.07–5.23 (m, 1H), 4.44–4.52 (m, 2H), 3.87 (s, 3H), 3.04–3.14 (m, 2H), 2.28–2.38 (m, 1H), 2.06–2.26 (m, 1H), 1.97–2.06 (m, 1H), 1.51–1.78 (m, 5H), 0.94 (d, J = 6.3 Hz, 3H), 0.89 (d, J = 6.3 Hz, 3H); MS (ESI+) for $C_{31}H_{35}ClN_4O_7$ m/z 611.1 ($M + H$)⁺. Anal. calcd for $C_{31}H_{35}ClN_4O_7 \cdot 0.72 H_2O \cdot 0.05 DCM$: C, 59.36; H, 5.86; N, 8.92. Found: C, 59.31; H, 5.99; N, 9.23.

(3S)-3-((N-[(4-Methoxy-1H-indol-2-yl)carbonyl]-L-leucyl)amino)-2-oxo-4-[(3S)-2-oxopyrrolidin-3-yl]butyl 2,6-Dichlorobenzoate (22). Following the procedure described for the preparation of (3S)-3-((N-[(4-methoxy-1H-indol-2-yl)carbonyl]-L-leucyl)amino)-2-oxo-4-[(3S)-2-oxopyrrolidin-3-yl]butyl acetate but substituting 2,6-dichlorobenzoic acid and making noncritical variations provided a crude product. This material was purified by LC (20 g 230–400 SiO₂, 3% methanol/chloroform) to afford 114 mg (65%) of the title compound as a white solid. ¹H NMR (DMSO- d_6) δ 11.57 (d, J = 2 Hz, 1H), 8.62 (d, J = 8 Hz, 1H), 8.46 (d, J = 4 Hz, 1H), 7.65–7.53 (m, 4H), 7.36 (s, 1H), 7.08 (t, J = 8 Hz, 1H), 6.99 (d, J = 8 Hz, 1H), 6.49 (d, J = 8 Hz, 1H), 5.19 (d, J = 20 Hz, 1H), 5.15 (d, J = 20 Hz, 1H), 4.51 (m, 2H), 3.87 (s, 3H), 3.11 (m, 2H), 2.30 (m, 1H), 2.06 (m, 2H), 1.76–1.51 (m, 5H), 0.94 (d, J = 8 Hz, 3H), 0.89 (d, J = 8 Hz, 3H); MS (ESI+) for $C_{31}H_{34}Cl_2N_4O_7$ m/z 645.1 ($M + H$)⁺; Anal. Calcd for $C_{31}H_{34}Cl_2N_4O_7 \cdot 0.2 H_2O$: C, 57.36; H, 5.34; N, 8.63. Found: C, 57.23; H, 5.55; N, 8.46. HRMS (ESI+) calcd for $C_{31}H_{34}Cl_2N_4O_7 + H^+$ 645.1877, found 645.1871.

(3S)-3-((N-[(4-Methoxy-1H-indol-2-yl)carbonyl]-L-leucyl)amino)-2-oxo-4-[(3S)-2-oxopyrrolidin-3-yl]butyl 2,6-Difluorobenzoate (23). Following the procedure described for the preparation of (3S)-3-((N-[(4-methoxy-1H-indol-2-yl)carbonyl]-L-leucyl)amino)-2-oxo-4-[(3S)-2-oxopyrrolidin-3-yl]butyl acetate but substituting 2,6-difluorobenzoic acid and making noncritical variations provided a crude brown oily solid. This material was triturated with chloroform/ethyl acetate to afford 180 mg (75%) of the title compound as a white solid. ¹H NMR (DMSO- d_6) δ 11.65 (d, J = 2 Hz, 1H), 8.68 (d, J = 8 Hz, 1H), 8.54 (d, J = 8 Hz, 1H), 7.73–7.65 (m, 2H), 7.36 (s, 1H), 7.27 (t, J = 8 Hz, 1H), 7.08 (t, J = 8 Hz, 1H), 6.99 (d, J = 8 Hz, 1H), 6.49 (d, J = 8 Hz, 1H), 5.19 (d, J = 16 Hz, 1H), 5.14 (d, J = 16 Hz, 1H), 4.48 (m, 2H), 3.87 (s, 3H), 3.11 (m, 2H), 2.32 (m, 1H), 2.11–1.91 (m, 2H), 1.81–1.56 (m, 5H), 0.94 (d, J = 4 Hz, 3H), 0.89 (d, J = 4 Hz, 3H); MS (ESI+) for $C_{31}H_{34}F_2N_4O_7$ m/z 613.2 ($M + H$)⁺; HRMS (ESI+) calcd for $C_{31}H_{34}F_2N_4O_7 + H^+$ 613.2469, found 613.2476.

(3S)-3-((N-[(4-Methoxy-1H-indol-2-yl)carbonyl]-L-leucyl)amino)-2-oxo-4-[(3S)-2-oxopyrrolidin-3-yl]butyl 4-Chloro-2-hydroxybenzoate (24). Following the procedure described for the preparation of (3S)-3-((N-[(4-methoxy-1H-indol-2-yl)carbonyl]-L-leucyl)amino)-2-oxo-4-[(3S)-2-oxopyrrolidin-3-yl]butyl acetate but substituting 4-chlorosalicylic acid and making noncritical variations provided a crude brown syrup. This material was purified by Biotage MPLC (25 M, 2–3% methanol/dichloromethane) to afford 64 mg (25%) of the title compound as a tan solid. ¹H NMR (DMSO- d_6) δ 11.58 (s, 1H), 10.50 (bs, 1H), 8.65 (d, J = 8 Hz, 1H), 8.46 (d, J = 8 Hz, 1H), 7.81 (d, J = 8 Hz, 1H), 7.63 (m, 1H), 7.37 (s, 1H), 7.08 (m, 2H), 7.00 (m, 2H), 6.50 (d, J = 8 Hz, 1H), 5.16 (d, J = 16 Hz, 2H), 5.11 (d, J = 16 Hz, 2H), 4.49 (m, 2H), 3.87 (s, 3H), 3.13 (m, 2H), 2.32 (m, 1H),

2.11–1.98 (m, 2H), 1.76–1.55 (m, 5H), 0.94 (d, J = 6 Hz, 3H), 0.89 (d, J = 6 Hz, 3H); MS (ESI-) for $C_{31}H_{35}ClN_4O_8$ m/z 625.1 ($M - H$)⁻; anal. calcd for $C_{31}H_{35}ClN_4O_8 \cdot 0.1 H_2O \cdot 0.14 CHCl_3$: C, 57.93; H, 5.52; N, 8.68. Found: C, 58.04; H, 5.78; N, 8.74; HRMS (ESI+) calcd for $C_{31}H_{35}ClN_4O_8 + H^+$ 627.2216, found 627.2219.

(3S)-3-((N-[(4-Methoxy-1H-indol-2-yl)carbonyl]-L-leucyl)amino)-2-oxo-4-[(3S)-2-oxopyrrolidin-3-yl]butyl 4-Cyano-2-fluorobenzoate (25). Following the procedure described for the preparation of (3S)-3-((N-[(4-methoxy-1H-indol-2-yl)carbonyl]-L-leucyl)amino)-2-oxo-4-[(3S)-2-oxopyrrolidin-3-yl]butyl acetate but substituting 4-cyano-2-fluorobenzoic acid and making noncritical variations provided a crude oily brown solid. This material was purified by Biotage MPLC (25 M, 2.5–3.5% methanol/dichloromethane) to afford 119 mg (48%) of the title compound as an off-white powder. ¹H NMR (DMSO- d_6) δ 11.58 (d, J = 2 Hz, 1H), 8.63 (d, J = 8 Hz, 1H), 8.46 (d, J = 8 Hz, 1H), 8.06 (m, 2H), 7.83 (d, J = 8 Hz, 1H), 7.65 (s, 1H), 7.36 (d, J = 2 Hz, 1H), 7.08 (t, J = 8 Hz, 1H), 6.99 (d, J = 8 Hz, 1H), 6.50 (d, J = 8 Hz, 1H), 5.16 (d, J = 16 Hz, 1H), 5.11 (d, J = 16 Hz, 1H), 4.49 (m, 2H), 3.87 (s, 3H), 3.11 (m, 2H), 2.32 (m, 1H), 2.10–1.98 (m, 2H), 1.77–1.53 (m, 5H), 0.94 (d, J = 6 Hz, 3H), 0.89 (d, J = 6 Hz, 3H); MS (ESI+) for $C_{32}H_{34}FN_4O_7$ m/z 620.1 ($M + H$)⁺; anal. calcd for $C_{32}H_{34}FN_4O_7 \cdot 0.3 H_2O$: C, 61.49; H, 5.58; N, 11.20. Found: C, 61.47; H, 5.61; N, 10.98; HRMS (ESI+) calcd for $C_{32}H_{34}FN_4O_7 + H^+$ 620.2515, found 620.2532.

(3S)-3-((N-[(4-Methoxy-1H-indol-2-yl)carbonyl]-L-leucyl)amino)-2-oxo-4-[(3S)-2-oxopyrrolidin-3-yl]butyl 2,6-Dimethylbenzoate (26). Following the procedure described for the preparation of (3S)-3-((N-[(4-methoxy-1H-indol-2-yl)carbonyl]-L-leucyl)amino)-2-oxo-4-[(3S)-2-oxopyrrolidin-3-yl]butyl acetate but substituting 2,6-dimethylbenzoic acid and making noncritical variations provided a crude brown foam. This material was purified by Biotage MPLC (25 M, 3–4% methanol/dichloromethane) to afford 177 mg (73%) of the title compound as an off-white glass. ¹H NMR (DMSO- d_6) δ 11.58 (d, J = 2 Hz, 1H), 8.63 (d, J = 8 Hz, 1H), 8.46 (d, J = 8 Hz, 1H), 7.65 (s, 1H), 7.36 (s, 1H), 7.25 (t, J = 8 Hz, 1H), 7.08 (m, 3H), 7.00 (d, J = 8 Hz, 1H), 6.49 (d, J = 8 Hz, 1H), 5.11 (s, 2H), 4.51 (m, 2H), 3.87 (s, 3H), 3.10 (m, 2H), 2.32–2.21 (m, 7H), 2.07 (m, 2H), 1.78–1.53 (m, 5H), 0.94 (d, J = 8 Hz, 3H), 0.89 (d, J = 8 Hz, 3H); MS (ESI+) for $C_{33}H_{40}N_4O_7$ m/z 605.2 ($M + H$)⁺; anal. calcd for $C_{33}H_{40}N_4O_7 \cdot 0.3 H_2O \cdot 0.2 CHCl_3$: C, 62.90; H, 6.49; N, 8.84. Found: C, 62.95; H, 6.42; N, 8.72. HRMS (ESI+) calcd for $C_{33}H_{40}N_4O_7 + H^+$ 605.2970, found 605.2985.

(3S)-3-((N-[(4-Methoxy-1H-indol-2-yl)carbonyl]-L-leucyl)amino)-2-oxo-4-[(3S)-2-oxopyrrolidin-3-yl]butyl 2,6-Dimethoxybenzoate (27). Following the procedure described for the preparation of (3S)-3-((N-[(4-methoxy-1H-indol-2-yl)carbonyl]-L-leucyl)amino)-2-oxo-4-[(3S)-2-oxopyrrolidin-3-yl]butyl acetate but substituting 2,6-dimethoxybenzoic acid and making noncritical variations provided a crude brown foam. This material was purified by Biotage MPLC (25 M, 3–4% methanol/dichloromethane) to afford 169 mg (66%) of the title compound as an off-white solid. ¹H NMR (DMSO- d_6) δ 11.58 (d, J = 2 Hz, 1H), 8.55 (d, J = 8 Hz, 1H), 8.45 (d, J = 8 Hz, 1H), 7.64 (s, 1H), 7.40–7.35 (m, 2H), 7.08 (t, J = 8 Hz, 1H), 7.00 (d, J = 8 Hz, 1H), 6.71 (d, J = 8 Hz, 1H), 6.50 (d, J = 8 Hz, 1H), 5.01 (d, J = 16 Hz, 1H), 4.95 (d, J = 16 Hz, 1H), 4.53–4.48 (m, 2H), 3.87 (s, 3H), 3.75 (s, 6H), 3.08 (m, 2H), 2.31 (m, 1H), 2.11–1.90 (m, 2H), 1.75–1.55 (m, 5H), 0.94 (d, J = 8 Hz, 3H), 0.89 (d, J = 8 Hz, 3H); MS (ESI+) for $C_{33}H_{40}N_4O_9$ m/z 637.2 ($M + H$)⁺; anal. calcd for $C_{33}H_{40}N_4O_9 \cdot 0.25 H_2O \cdot 0.25 CHCl_3$: C, 59.51; H, 6.12; N, 8.35. Found: C, 59.49; H, 6.08; N, 8.42.

(3S)-3-((N-[(4-Methoxy-1H-indol-2-yl)carbonyl]-L-leucyl)amino)-2-oxo-4-[(3S)-2-oxopyrrolidin-3-yl]butyl 2-Cyanobenzoate (28). Following the procedure described for the preparation of (3S)-3-((N-[(4-methoxy-1H-indol-2-yl)carbonyl]-L-leucyl)amino)-2-oxo-4-[(3S)-2-oxopyrrolidin-3-yl]butyl acetate but substituting 2-cyanobenzoic acid and making noncritical variations provided a crude brown oily solid. This material was triturated with chloroform/ethyl acetate to afford 91 mg (38%) of the title compound as a white solid. ¹H NMR (DMSO- d_6) δ 11.58 (s, 1H), 8.65 (d, J = 8 Hz, 1H), 8.46 (d, J = 8 Hz, 1H), 8.17 (m, 1H), 8.04 (m, 1H), 7.88 (m, 1H), 7.65 (s, 1H),

7.37 (s, 1H), 7.08 (t, $J = 8$ Hz, 1H), 6.99 (d, $J = 8$ Hz, 1H), 6.49 (d, $J = 8$ Hz, 1H), 5.19 (m, 2H), 4.50 (m, 2H), 3.87 (s, 3H), 3.11 (m, 2H), 2.32 (m, 1H), 2.07–1.97 (m, 2H), 1.76–1.56 (m, 5H), 0.94 (d, $J = 6$ Hz, 3H), 0.89 (d, $J = 6$ Hz, 3H); MS (ESI+) for $C_{32}H_{35}N_5O_7$ m/z 602.2 ($M + H$)⁺; anal. calcd for $C_{32}H_{35}N_5O_7 \cdot 0.4 H_2O$: C, 63.12; H, 5.93; N, 11.50. Found: C, 63.16; H, 5.96; N, 11.43; HRMS (ESI+) calcd for $C_{32}H_{35}N_5O_7 + H$ 602.2609, found 602.2610.

(3S)-3-[(*tert*-Butoxycarbonyl)amino]-2-oxo-4-[(3S)-2-oxopyrrolidin-3-yl]butyl 2,6-Dichlorobenzoate. A solution of *tert*-butyl ((1S)-3-bromo-2-oxo-1-[[[(3S)-2-oxopyrrolidin-3-yl]methyl]propyl]-carbamate (1.17 g, 3.2 mmol) in DMF (16 mL) was treated with 2,6-dichlorobenzoic acid (794 mg, 4.2 mmol) followed by cesium fluoride (1.18 g, 7.4 mmol). The resulting suspension was placed in a preheated oil bath at 65 °C for 2 h. The reaction was cooled to an ambient temperature, diluted with ethyl acetate (100 mL), washed once with water (40 mL) and with brine (40 mL), dried over $MgSO_4$, filtered, and concentrated to give a crude yellow syrup. This material was purified by Biotage MPLC (25 M, 4.5% methanol/dichloromethane) to afford 1.19 mg (80%) of the title compound as an off-white glass. ¹H NMR (400 MHz, DMSO- d_6) δ 7.60 (m, 5H), 5.35 (s, 2H), 4.32 (m, 1H), 3.23 (m, 2H), 2.24 (m, 1H), 2.11 (m, 1H), 1.86 (m, 1H), 1.67 (m, 2H), 1.35 (s, 9H); MS (ESI+) for $C_{20}H_{24}Cl_2N_2O_6$ m/z 481.0 ($M + Na$)⁺; HRMS (ESI+) calcd for $C_{20}H_{24}Cl_2N_2O_6 + H$ 481.0903, found 481.0890.

N^2 -(*tert*-Butoxycarbonyl)- N^1 -[(1S)-3-chloro-2-oxo-1-[(3S)-2-oxopyrrolidin-3-yl]methyl]propyl]-*L*-leucinamide. A solution of (3S)-3-[(2S)-2-amino-4-chloro-3-oxobutyl]pyrrolidin-2-one hydrochloride (391 mg, 1.6 mmol) and Boc-Leu-OH (412 mg, 1.8 mmol) in DMF (9 mL) was placed under an atmosphere of N_2 and cooled to 0 °C. This clear pale yellow solution was successively treated with HATU (678 mg, 1.8 mmol) followed by *N*-methylmorpholine (0.41 mL, 3.7 mmol). The reaction mixture gradually became opaque and after 1 h was quenched with 1:1 ice/sat aqueous $NaHCO_3$ (40 mL) and extracted three times with ethyl acetate (40 mL). The combined organics were washed once with brine (30 mL), dried over $MgSO_4$, filtered, and concentrated to give a yellow syrup. This material was purified by LC (50 g 230–400 SiO_2 , 3–5% methanol/chloroform) to afford 636 mg (40%) of N^2 -(*tert*-butoxycarbonyl)- N^1 -[(1S)-3-chloro-2-oxo-1-[(3S)-2-oxopyrrolidin-3-yl]methyl]propyl]-*L*-leucinamide as a white foam. ¹H NMR (DMSO- d_6) δ 8.47 (d, $J = 8$ Hz, 1H), 7.64 (s, 1H), 7.04 (d, $J = 8$ Hz, 1H), 4.60 (d, $J = 16$ Hz, 1H), 4.53 (d, $J = 16$ Hz, 1H), 4.40 (m, 1H), 3.90 (m, 1H), 3.16 (m, 1H), 3.08 (m, 1H), 2.24 (m, 1H), 2.10 (m, 1H), 1.98 (m, 1H), 1.63 (m, 2H), 1.45–1.37 (m, 11 H), 0.89 (d, $J = 4$ Hz, 3H), 0.85 (d, $J = 4$ Hz, 3H); MS (ESI+) for $C_{19}H_{32}ClN_3O_5$ m/z 418.1 ($M + H$)⁺. Anal. calcd for $C_{19}H_{32}ClN_3O_5 \cdot 0.6 H_2O$: C, 53.22; H, 7.81; N, 9.80. Found: C, 53.00; H, 7.65; N, 9.54. HRMS (ESI+) calcd for $C_{19}H_{32}ClN_3O_5 + H$ 418.2103, found 418.2091.

(3S)-3-[(*N*-(*tert*-Butoxycarbonyl)-*L*-leucyl)amino]-2-oxo-4-[(3S)-2-oxopyrrolidin-3-yl]butyl 2,6-Dichlorobenzoate (29). Following the procedure described for the preparation of N^2 -(*tert*-butoxycarbonyl)- N^1 -[(1S)-3-chloro-2-oxo-1-[(3S)-2-oxopyrrolidin-3-yl]methyl]propyl]-*L*-leucinamide but substituting (3S)-3-[(*tert*-butoxycarbonyl)amino]-2-oxo-4-[(3S)-2-oxopyrrolidin-3-yl]butyl 2,6-dichlorobenzoate and making noncritical variations provided a brown foam. This material was purified by LC (50 g 230–400 SiO_2 , 2.5–3.5% methanol/chloroform) to afford 413 mg (61%) of the title compound as a light yellow foam. ¹H NMR (DMSO- d_6) δ 8.47 (d, $J = 8$ Hz, 1H), 7.60 (m, 4H), 7.05 (d, $J = 8$ Hz, 1H), 5.19 (d, $J = 16$ Hz, 1H), 5.13 (d, $J = 16$ Hz, 1H), 4.47 (m, 1H), 3.95 (m, 1H), 3.16 (m, 1H), 3.08 (m, 1H), 2.27 (m, 1H), 2.10 (m, 1H), 2.03 (m, 1H), 1.65 (m, 2H), 1.47–1.37 (m, 11 H), 0.89 (d, $J = 4$ Hz, 3H), 0.85 (d, $J = 4$ Hz, 3H); MS (ESI+) for $C_{26}H_{35}Cl_2N_3O_7$ m/z 572.1 ($M + H$)⁺. Anal. calcd for $C_{26}H_{35}Cl_2N_3O_7 \cdot 0.5 H_2O$: C, 53.70; H, 6.24; N, 7.23. Found: C, 53.74; H, 6.31; N, 7.31; HRMS (ESI+) calcd for $C_{26}H_{35}Cl_2N_3O_7 + Na$ 594.1744, found 594.1729.

(3S)-3-[(*N*-Acetyl-*L*-leucyl)amino]-2-oxo-4-[(3S)-2-oxopyrrolidin-3-yl]butyl 2,6-Dichlorobenzoate (30). Following the procedure described for the preparation of N^2 -acetyl- N^1 -[(1S)-1-(chloroacetyl)-4-(dimethylamino)-4-oxobutyl]- N^2 -methyl-*L*-leucinamide but

substituting (3S)-3-[(*N*-(*tert*-butoxycarbonyl)-*L*-leucyl)amino]-2-oxo-4-[(3S)-2-oxopyrrolidin-3-yl]butyl 2,6-dichlorobenzoate and making noncritical variations provided a pale yellow oil. This material was purified by Biotage MPLC (25 M, 3.5–4.5% methanol/dichloromethane) to afford 161 mg (78%) of the title compound as a white foam. ¹H NMR (DMSO- d_6) δ 8.56 (d, $J = 8$ Hz, 1H), 8.06 (d, $J = 8$ Hz, 1H), 7.65–7.53 (m, 4H), 5.17 (d, $J = 16$ Hz, 1H), 5.10 (d, $J = 16$ Hz, 1H), 4.44 (m, 1H), 4.25 (m, 1H), 3.12 (m, 2H), 2.25 (m, 1H), 2.06 (m, 1H), 1.97 (m, 1H), 1.84 (s, 3H), 1.63 (m, 3H), 1.45 (m, 2H), 0.90 (d, $J = 8$ Hz, 3H), 0.85 (d, $J = 8$ Hz, 3H); MS (ESI+) for $C_{23}H_{29}Cl_2N_3O_6$ m/z 514.0 ($M + H$)⁺; anal. calcd for $C_{23}H_{29}Cl_2N_3O_6 \cdot 0.25 H_2O \cdot 0.1 EtOAc$: C, 53.26; H, 5.79; N, 7.96. Found: C, 53.27; H, 5.82; N, 7.84. HRMS (ESI+) calcd for $C_{23}H_{29}Cl_2N_3O_6 + H$ 514.1506, found 514.1508.

(3S)-3-[(*N*-(1H-Benzimidazol-2-ylcarbonyl)-*L*-leucyl)amino]-2-oxo-4-[(3S)-2-oxopyrrolidin-3-yl]butyl 2,6-Dichlorobenzoate (31). Following the procedure described for the preparation of N -((1S)-1-[[[(1S)-3-chloro-2-oxo-1-[[[(3S)-2-oxopyrrolidin-3-yl]methyl]propyl]amino]carbonyl]-3-methylbutyl]-4-methoxy-1H-indole-2-carboxamide but substituting (3S)-3-[(*N*-(*tert*-butoxycarbonyl)-*L*-leucyl)amino]-2-oxo-4-[(3S)-2-oxopyrrolidin-3-yl]butyl 2,6-dichlorobenzoate and 1H-benzimidazole-2-carboxylic acid and making noncritical variations provided a crude yellow oil. This material was purified by Biotage MPLC (25 M, 3–4% methanol/dichloromethane) to afford 95 mg (72%) of the title compound as an off-white foam. ¹H NMR (DMSO- d_6) δ 13.32 (s, 1H), 8.89 (d, $J = 8$ Hz, 1H), 8.60 (d, $J = 8$ Hz, 1H), 7.74 (d, $J = 8$ Hz, 1H), 7.59 (m, 5H), 7.29 (m, 2H), 5.20 (d, $J = 20$ Hz, 1H), 5.15 (d, $J = 20$ Hz, 1H), 4.56 (m, 2H), 3.12 (m, 2H), 2.30 (m, 1H), 2.01 (m, 2H), 1.83 (m, 1H), 1.65 (m, 4H), 0.92 (d, $J = 8$ Hz, 3H), 0.89 (d, $J = 8$ Hz, 3H); MS (ESI+) for $C_{29}H_{31}Cl_2N_5O_6$ m/z 616.0 ($M + H$)⁺. Anal. calcd for $C_{29}H_{31}Cl_2N_5O_6$: C, 56.50; H, 5.07; N, 11.36. Found: C, 57.28; H, 5.32; N, 11.35. HRMS (ESI+) calcd for $C_{29}H_{31}Cl_2N_5O_6 + H$ 616.1724, found 616.1729.

(3S)-3-[(4-Methyl-*N*-[(2R)-tetrahydrofuran-2-ylcarbonyl]-*L*-leucyl)amino]-2-oxo-4-[(3S)-2-oxopyrrolidin-3-yl]butyl 2,6-Dichlorobenzoate (3). Following the procedure described for the preparation of (3S)-3-[(*N*-[(4-methoxy-1H-indol-2-yl)carbonyl]-*L*-leucyl)amino]-2-oxo-4-[(3S)-2-oxopyrrolidin-3-yl]butyl acetate but substituting N^1 -[(1S)-3-chloro-2-oxo-1-[[[(3S)-2-oxopyrrolidin-3-yl]methyl]propyl]-4-methyl- N^2 -[(2R)-tetrahydrofuran-2-ylcarbonyl]-*L*-leucinamide and 2,6-dichlorobenzoic acid and making noncritical variations provided a light amber residue. The residue was purified by preparative HPLC (Luna 10 μ C18) eluting with a gradient of MeCN containing 0.1% AcOH in water containing 0.1% AcOH to give 0.155 g (54%) of the title compound as a cream colored solid. ¹H NMR (300 MHz, DMSO- d_6) δ 8.52 (d, $J = 8$ Hz, 1H), 7.79 (d, $J = 8$ Hz, 1H), 7.71 (s, 1H), 7.66–7.55 (m, 3H), 5.18 (s, 2H), 4.54–4.40 (m, 1H), 4.37–4.35 (m, 1H), 4.25 (m, 1H), 3.98–3.91 (m, 1H), 3.84–3.72 (m, 1H), 3.23–3.07 (m, 2H), 2.33–2.23 (m, 1H), 2.16–2.05 (m, 2H), 1.86–1.74 (m, 3H), 1.72–1.62 (m, 5H), 0.89 (s, 9H); MS (ESI+) for $C_{27}H_{35}Cl_2N_3O_7$ m/z 584 ($M + H$)⁺. Anal. calcd for $C_{27}H_{35}Cl_2N_3O_7 \cdot 0.5 H_2O$: C, 54.64; H, 6.11; N, 7.08. Found: C, 54.26; H, 6.00; N, 6.87. HRMS (ESI+) calcd for $C_{27}H_{35}Cl_2N_3O_7 + H$ 584.1925, found 584.1921.

N^2 -(*tert*-Butoxycarbonyl)- N^1 -[(1S)-3-chloro-2-oxo-1-[(3S)-2-oxopyrrolidin-3-yl]methyl]propyl]-4-methyl-*L*-leucinamide (32). Following the procedure described for the preparation of N^2 -(*tert*-butoxycarbonyl)- N^1 -[(1S)-3-chloro-2-oxo-1-[[[(3S)-2-oxopyrrolidin-3-yl]methyl]propyl]-*L*-leucinamide but substituting Boc-(β -*t*-butyl)-Ala-OH and making noncritical variations provided a golden syrup. This material was purified by Biotage MPLC (65i column, 2.5–3.5% methanol/chloroform) to afford 3.41 g (40%) of the title compound as a white foam. ¹H NMR (DMSO- d_6) δ 8.39 (d, $J = 8$ Hz, 1H), 7.64 (s, 1H), 7.00 (d, $J = 8$ Hz, 1H), 4.58 (d, $J = 16$ Hz, 1H), 4.52 (d, $J = 16$ Hz, 1H), 4.38 (m, 1H), 3.92 (m, 1H), 3.15 (t, $J = 8$ Hz, 1H), 3.07 (q, $J = 8$ Hz, 1H), 2.22 (m, 1H), 2.09 (m, 1H), 1.97 (m, 1H), 1.62 (m, 2H), 1.50 (m, 2H), 1.36 (s, 9H), 0.88 (s, 9H); MS (ESI+) for $C_{20}H_{34}ClN_3O_6$ m/z 432.1 ($M + H$)⁺.

*N*¹-((1*S*)-3-(Benzyloxy)-2-oxo-1-(((3*S*)-2-oxopyrrolidin-3-yl)methyl)propyl)-*N*²-(*tert*-butoxycarbonyl)-4-methyl-*L*-leucinamide (**33**). Following the procedure described for the preparation of *tert*-butyl [(1*S*)-2-(((1*S*)-3-(benzyloxy)-2-oxo-1-(((3*S*)-2-oxopyrrolidin-3-yl)methyl)propyl)amino]-1-(cyclohexylmethyl)-2-oxoethyl]-carbamate but substituting Boc-(β *t*-butyl)-Ala-OH and making noncritical variations provided a brown syrup. This material was purified by LC (33 g 230–400 SiO₂, 1–2.5% methanol/chloroform) to afford 258 mg (55%) of the title compound as a light yellow foam. ¹H NMR (DMSO-*d*₆) δ 8.23 (d, *J* = 8 Hz, 1H), 7.62 (s, 1H), 7.32 (m, 5H), 6.96 (d, *J* = 8 Hz, 1H), 4.46 (s, 2H), 4.35–4.33 (m, 2H), 4.21 (d, *J* = 16 Hz, 1H), 3.95 (m, 1H), 3.09 (m, 2H), 2.24 (m, 1H), 2.07 (m, 1H), 1.92 (m, 1H), 1.58 (m, 2H), 1.46 (m, 2H), 1.35 (s, 9H), 0.87 (m, 9H); MS (ESI+) for C₂₇H₄₁N₃O₆ *m/z* 504.2 (M + H)⁺.

N-((1*S*)-1-(((1*S*)-3-(Benzyloxy)-2-oxo-1-(((3*S*)-2-oxopyrrolidin-3-yl)methyl)propyl)amino)carbonyl]-3,3-dimethylbutyl)-4-methoxy-1*H*-indole-2-carboxamide (**34**). Following the procedure described for the preparation of *N*-[(1*S*)-2-(((1*S*)-3-(benzyloxy)-2-oxo-1-(((3*S*)-2-oxopyrrolidin-3-yl)methyl)propyl)amino]-1-(cyclohexylmethyl)-2-oxoethyl]-4-methoxy-1*H*-indole-2-carboxamide but substituting *N*¹-((1*S*)-3-(benzyloxy)-2-oxo-1-(((3*S*)-2-oxopyrrolidin-3-yl)methyl)propyl)-*N*²-(*tert*-butoxycarbonyl)-4-methyl-*L*-leucinamide and making noncritical variations provided a golden syrup. This material was purified by Biotage MPLC (25 M column, 3% methanol/chloroform) to afford 173 mg (60%) of the title compound as an off-white foam. ¹H NMR (400 MHz, DMSO-*d*₆) δ 11.58 (s, 1H), 8.43 (app t, *J* = 8 Hz, 2H), 7.62 (s, 1H), 7.32 (m, 6H), 7.08 (t, *J* = 8 Hz, 1H), 7.00 (d, *J* = 8 Hz, 1H), 6.49 (d, *J* = 8 Hz, 1H), 4.52 (m, 1H), 4.47–4.35 (m, 4H), 4.22 (d, *J* = 16 Hz, 1H), 3.87 (s, 3H), 3.05 (m, 2H), 2.28 (m, 1H), 2.06 (m, 1H), 1.93 (m, 1H), 1.64–1.57 (m, 3H), 0.92 (s, 9H); MS (ESI+) for C₃₂H₄₀N₄O₆ *m/z* 577.2 (M + H)⁺; anal. calcd for C₃₂H₄₀N₄O₆·0.33 methanol·0.25 H₂O: C, 65.62; H, 7.13; N, 9.47. Found: C, 65.65; H, 6.90; N, 9.58; HRMS (ESI+) calcd for C₃₂H₄₀N₄O₆ 577.3021, found 577.3001.

N-((1*S*)-1-(((1*S*)-3-Chloro-2-oxo-1-(((3*S*)-2-oxopyrrolidin-3-yl)methyl)propyl)amino)carbonyl]-3,3-dimethylbutyl)-4-methoxy-1*H*-indole-2-carboxamide (**35**). Following the procedure described for the preparation of *N*-((1*S*)-1-(((1*S*)-3-chloro-2-oxo-1-(((3*S*)-2-oxopyrrolidin-3-yl)methyl)propyl)amino)carbonyl]-3-methylbutyl)-4-methoxy-1*H*-indole-2-carboxamide but substituting *N*²-(*tert*-butoxycarbonyl)-*N*¹-((1*S*)-3-chloro-2-oxo-1-(((3*S*)-2-oxopyrrolidin-3-yl)methyl)propyl)-4-methyl-*L*-leucinamide and making noncritical variations provided a pale yellow solid. This material was purified by Biotage MPLC (40 M column, 2–4.5% methanol/chloroform) to afford 920 g (60%) of the title compound as an off-white solid. ¹H NMR (400 MHz, DMSO-*d*₆) δ 11.59 (d, *J* = 1.8 Hz, 1H), 8.54 (d, *J* = 7.8 Hz, 1H), 8.45 (d, *J* = 8.1 Hz, 1H), 7.64 (s, 1H), 7.32 (d, *J* = 1.8 Hz, 1H), 7.08 (t, *J* = 8.0 Hz, 1H), 7.00 (d, *J* = 8.3 Hz, 1H), 6.49 (d, *J* = 7.6 Hz, 1H), 4.52–4.62 (m, 1H), 4.40–4.51 (m, 2H), 3.87 (s, 3H), 3.01–3.16 (m, 2H), 2.19–2.31 (m, 1H), 2.03–2.12 (m, 1H), 1.91–2.01 (m, 1H), 1.81 (dd, *J* = 14.1, 9.9 Hz, 1H), 1.54–1.72 (m, 3H), 0.93 (s, 9H); MS (ESI+) for C₂₅H₃₃ClN₄O₅ *m/z* 505.1 (M + H)⁺; HRMS (ESI+) calcd for (M + H)⁺ 505.2212, found 505.2204.

N-((1*S*)-1-(((1*S*)-3-Hydroxy-2-oxo-1-(((3*S*)-2-oxopyrrolidin-3-yl)methyl)propyl)amino)carbonyl]-3,3-dimethylbutyl)-4-methoxy-1*H*-indole-2-carboxamide (**36**). Following the procedure described for the preparation of *N*-((1*S*)-1-(((1*S*)-3-hydroxy-2-oxo-1-(((3*S*)-2-oxopyrrolidin-3-yl)methyl)propyl)amino)carbonyl]-3-methylbutyl)-4-methoxy-1*H*-indole-2-carboxamide but substituting *N*-((1*S*)-1-(((1*S*)-3-chloro-2-oxo-1-(((3*S*)-2-oxopyrrolidin-3-yl)methyl)propyl)amino)carbonyl]-3,3-dimethylbutyl)-4-methoxy-1*H*-indole-2-carboxamide and making noncritical variations provided a crude brown glass. This material was purified by Biotage MPLC (40 M column, 2–10% methanol/chloroform) to afford 415 mg (53%) of the title compound as a white solid. MS (ESI+) for C₂₅H₃₄N₄O₆ *m/z* 487.2 (M + H)⁺. Alternatively, following the procedure described for the preparation of *N*-((1*S*)-1-(cyclohexylmethyl)-2-(((1*S*)-3-hydroxy-2-oxo-1-(((3*S*)-2-oxopyrrolidin-3-yl)methyl)propyl)amino)-2-oxoethyl]-4-methoxy-1*H*-indole-2-carboxamide but substituting *N*-((1*S*)-1-(((1*S*)-3-(benzyloxy)-2-oxo-1-(((3*S*)-2-oxopyrrolidin-3-yl)methyl)propyl)amino)carbonyl]-3,3-dimethylbutyl)-4-methoxy-1*H*-indole-2-

carboxamide and making noncritical variations provided a tan solid. This material was purified by Biotage MPLC (25 M column, 6–7% methanol/chloroform) to afford 100 mg (77%) of the title compound as a white solid. ¹H NMR (DMSO-*d*₆) δ 11.58 (s, 1H), 8.42 (d, *J* = 8 Hz, 1H), 8.37 (d, *J* = 8 Hz, 1H), 7.62 (s, 1H), 7.32 (s, 1H), 7.08 (t, *J* = 8 Hz, 1H), 6.99 (d, *J* = 8 Hz, 1H), 6.49 (d, *J* = 8 Hz, 1H), 5.04 (t, *J* = 8 Hz, 1H), 4.52 (m, 1H), 4.42 (m, 1H), 4.24 (dd, *J* = 8, 20 Hz, 1H), 4.12 (dd, *J* = 8, 20 Hz, 1H), 3.87 (s, 3H), 3.09 (m, 2H), 2.25 (m, 1H), 2.06 (m, 1H), 1.93 (m, 1H), 1.80 (dd, *J* = 8, 16 Hz, 1H), 0.93 (s, 9H); MS (ESI+) for C₂₅H₃₄N₄O₆ *m/z* 487.2 (M + H)⁺; anal. calcd for C₂₅H₃₄N₄O₆·0.3 H₂O: C, 61.03; H, 7.09; N, 11.39. Found: C, 61.07; H, 7.09; N, 11.22; HRMS (ESI+) calcd for C₂₅H₃₄N₄O₆ 487.2551, found 487.2541.

4-Methoxy-*N*-((1*S*)-1-(((1*S*)-3-methoxy-2-oxo-1-(((3*S*)-2-oxopyrrolidin-3-yl)methyl)propyl)amino)carbonyl]-3,3-dimethylbutyl)-1*H*-indole-2-carboxamide (**37**). Following the procedure described for the preparation of 4-methoxy-*N*-((1*S*)-1-(((1*S*)-3-methoxy-2-oxo-1-(((3*S*)-2-oxopyrrolidin-3-yl)methyl)propyl)amino)carbonyl]-4-methylpentyl)-1*H*-indole-2-carboxamide but substituting *N*-((1*S*)-1-(((1*S*)-3-hydroxy-2-oxo-1-(((3*S*)-2-oxopyrrolidin-3-yl)methyl)propyl)amino)carbonyl]-3,3-dimethylbutyl)-4-methoxy-1*H*-indole-2-carboxamide and making noncritical variations provided a crude product. This material was purified by Biotage MPLC (40S column, 2–5% methanol/chloroform) to afford 21 mg (9%) of the title compound as a pale tan solid. ¹H NMR (400 MHz, DMSO-*d*₆) δ 11.58 (s, 1H), 8.42 (d, *J* = 6.8 Hz, 1H), 7.62 (s, 1H), 7.32 (s, 1H), 7.08 (t, *J* = 7.7 Hz, 1H), 7.00 (d, *J* = 7.8 Hz, 1H), 6.49 (d, *J* = 7.3 Hz, 1H), 4.49–4.55 (m, 1H), 4.32–4.41 (m, 1H), 4.21–4.30 (m, 1H), 4.12 (t, *J* = 16.9 Hz, 1H), 3.87 (s, 3H), 3.23 (s, 3H), 3.01–3.16 (m, 2H), 2.20–2.32 (m, 1H), 2.03–2.15 (m, 1H), 1.87–1.98 (m, 1H), 1.73–1.85 (m, 1H), 1.54–1.70 (m, 3H), 0.93 (s, 9H); MS (ESI+) for C₂₆H₃₆N₄O₆ *m/z* 501.2 (M + H)⁺; HRMS (ESI+) calcd for (M + H)⁺ 501.2708, found 501.2701.

N-((1*S*)-1-(((1*S*)-3-Hydroxy-2-oxo-1-(((3*S*)-2-oxopyrrolidin-3-yl)methyl)propyl)amino)carbonyl]-3-methylbutyl)-4-methoxy-1*H*-indole-2-carboxamide (**4**). A solution of *N*-((1*S*)-1-(((1*S*)-3-chloro-2-oxo-1-(((3*S*)-2-oxopyrrolidin-3-yl)methyl)propyl)amino)carbonyl]-3-methylbutyl)-4-methoxy-1*H*-indole-2-carboxamide (488 mg, 0.99 mmol) and benzoylformic acid (195 mg, 1.3 mmol) in DMF (6.5 mL) was placed under an atmosphere of N₂. This clear pale yellow solution was treated with cesium fluoride (350 mg, 2.3 mmol) followed by heating to 65 °C. After 4 h, the now yellow suspension was cooled to RT, diluted with ethyl acetate (60 mL), washed three times with water (30 mL) and once with brine (30 mL), dried over MgSO₄, filtered, and concentrated to give (3*S*)-3-((*N*-[(4-methoxy-1*H*-indol-2-yl)carbonyl]-*L*-leucyl)amino)-2-oxo-4-[(3*S*)-2-oxopyrrolidin-3-yl]butyl oxo(phenyl)acetate as a crude yellow foam. MS (ESI+) for C₃₂H₃₆N₄O₈ *m/z* 605.2 (M + H)⁺. A solution of the crude (3*S*)-3-((*N*-[(4-methoxy-1*H*-indol-2-yl)carbonyl]-*L*-leucyl)amino)-2-oxo-4-[(3*S*)-2-oxopyrrolidin-3-yl]butyl oxo(phenyl)acetate in methanol (40 mL) was placed under an atmosphere of N₂ and treated with potassium carbonate (7 mg, 0.05 mmol) with vigorous stirring. After 1 h, the volatiles were removed *in vacuo* (bath < 30 °C) to give a crude yellow glass. This material was purified by Biotage MPLC (25 M column, 6% methanol/chloroform) to afford 346 mg (73%) of the title compound as an off-white solid. ¹H NMR (DMSO-*d*₆) δ 11.56 (s, 1H), 8.44 (d, *J* = 8 Hz, 1H), 8.39 (d, *J* = 8 Hz, 1H), 7.61 (s, 1H), 7.35 (s, 1H), 7.08 (t, *J* = 8 Hz, 1H), 6.99 (d, *J* = 8 Hz, 1H), 6.49 (d, *J* = 8 Hz, 1H), 5.04 (t, *J* = 8 Hz, 1H), 4.46 (m, 2H), 4.25 (dd, *J* = 8, 20 Hz, 1H), 4.13 (dd, *J* = 8, 20 Hz, 1H), 3.87 (s, 3H), 3.10 (m, 2H), 2.28 (m, 1H), 2.08 (m, 1H), 1.92 (m, 1H), 1.70–1.53 (m, 5H), 0.93 (d, *J* = 8 Hz, 3H), 0.89 (d, *J* = 8 Hz, 3H); MS (ESI+) for C₂₄H₃₂N₄O₆ *m/z* 473.2 (M + H)⁺.

*N*¹-((1*S*)-3-(Benzyloxy)-2-oxo-1-(((3*S*)-2-oxopyrrolidin-3-yl)methyl)propyl)-*N*²-(*tert*-butoxycarbonyl)-*N*²-methyl-*L*-leucinamide. Following the procedure described for the preparation of *tert*-butyl [(1*S*)-2-(((1*S*)-3-(benzyloxy)-2-oxo-1-(((3*S*)-2-oxopyrrolidin-3-yl)methyl)propyl)amino]-1-(cyclohexylmethyl)-2-oxoethyl]-carbamate but substituting Boc-*N*-methyl-Leu and making noncritical variations provided a crude brown oil. This material was purified by Biotage

flash chromatography, eluting with methanol/dichloromethane to afford the title compound (123 mg, 47%) as a yellow gum. ^1H NMR (400 MHz, CDCl_3) δ 7.22–7.33 (m, 5H), 5.76 (bd, 1H), 4.73 (s, 1H), 4.46–4.59 (m, 2H), 4.08–4.27 (m, 2H), 3.14–3.28 (m, 2H), 2.68 (s, 3H), 2.16–2.38 (m, 2H), 1.88–2.00 (m, 1H), 1.56–1.86 (m, 5H), 1.41 (s, 9H), 0.94 (d, J = 8 Hz, 3H), 0.89 (d, J = 8 Hz, 3H).

N-((1*S*)-1-(((1*S*)-3-(Benzyloxy)-2-oxo-1-((3*S*)-2-oxopyrrolidin-3-yl)methyl)propyl)amino]carbonyl]-3-methylbutyl)-4-methoxy-*N*-methyl-1*H*-indole-2-carboxamide. Following the procedure described for the preparation of *N*-((1*S*)-2-(((1*S*)-3-(benzyloxy)-2-oxo-1-((3*S*)-2-oxopyrrolidin-3-yl)methyl)propyl)amino]-1-(cyclohexylmethyl)-2-oxoethyl)-4-methoxy-1*H*-indole-2-carboxamide but substituting N^1 -((1*S*)-3-(benzyloxy)-2-oxo-1-((3*S*)-2-oxopyrrolidin-3-yl)methyl)propyl)- N^2 -(*tert*-butoxycarbonyl)- N^2 -methyl-*L*-leucineamide and making noncritical variations provided a crude brown oil. This material was purified by Biotage flash chromatography, eluting with methanol/dichloromethane to afford the title compound as a clear oil, 67 mg, 48%. ^1H NMR (400 MHz, CDCl_3) δ 9.83 (s, 1H), 7.95 (s, 1H), 7.26–7.36 (m, 5H), 7.18 (t, J = 8.0 Hz, 1H), 7.04 (d, J = 8.3 Hz, 1H), 7.00 (s, 1H), 6.48 (d, J = 7.8 Hz, 1H), 5.87 (s, 1H), 5.18–5.27 (m, 1H), 4.70 (s, 1H), 4.50–4.63 (m, 2H), 4.16–4.36 (m, 2H), 3.93 (s, 3H), 3.32 (s, 3H), 3.03–3.18 (m, 2H), 2.22 (s, 2H), 1.91–2.02 (m, 1H), 1.81 (t, J = 7.3 Hz, 3H), 1.66–1.72 (m, 1H), 1.55 (s, 1H), 0.87–1.01 (m, 6H); MS (API-ES $^-$) for $\text{C}_{32}\text{H}_{40}\text{N}_4\text{O}_6$ m/z 576.7 ($\text{M} - \text{H}$) $^-$.

N-((1*S*)-1-(((1*S*)-3-Hydroxy-2-oxo-1-((3*S*)-2-oxopyrrolidin-3-yl)methyl)propyl)amino]carbonyl]-3-methylbutyl)-4-methoxy-*N*-methyl-1*H*-indole-2-carboxamide (**38**). Following the procedure described for the preparation of *N*-((1*S*)-1-(cyclohexylmethyl)-2-(((1*S*)-3-hydroxy-2-oxo-1-((3*S*)-2-oxopyrrolidin-3-yl)methyl)propyl)amino]-2-oxoethyl)-4-methoxy-1*H*-indole-2-carboxamide but substituting *N*-((1*S*)-1-(((1*S*)-3-(benzyloxy)-2-oxo-1-((3*S*)-2-oxopyrrolidin-3-yl)methyl)propyl)amino]carbonyl]-3-methylbutyl)-4-methoxy-*N*-methyl-1*H*-indole-2-carboxamide and making noncritical variations provided a crude clear glass. This material was purified by Biotage flash chromatography, eluting with methanol/dichloromethane to afford the title compound as a white foam, 42 mg, 82%. ^1H NMR (400 MHz, CDCl_3) δ 10.16 (s, 1H), 8.26 (s, 1H), 7.18 (t, J = 8.0 Hz, 1H), 7.05 (d, J = 8.1 Hz, 1H), 6.99 (d, J = 2.3 Hz, 1H), 6.48 (d, J = 7.6 Hz, 1H), 6.09 (s, 1H), 5.14–5.27 (m, 1H), 4.51–4.65 (m, 1H), 4.25–4.50 (m, 2H), 3.94 (s, 3H), 3.26–3.46 (m, 3H), 3.11–3.24 (m, 1H), 3.01–3.11 (m, 1H), 1.48–2.39 (m, 9H), 0.88–1.02 (m, 6H); MS (API-ES $^-$) for $\text{C}_{25}\text{H}_{34}\text{N}_4\text{O}_6$ m/z 485.3 ($\text{M} - \text{H}$) $^-$.

N^2 -(*tert*-Butoxycarbonyl)- N^1 -((1*S*)-3-chloro-2-oxo-1-((3*S*)-2-oxopyrrolidin-3-yl)methyl)propyl)-*L*-norleucineamide. Following the procedure described for the preparation of N^2 -(*tert*-butoxycarbonyl)- N^1 -((1*S*)-3-chloro-2-oxo-1-((3*S*)-2-oxopyrrolidin-3-yl)methyl)propyl)-*L*-leucineamide but substituting Boc-NorLeu-OH and making noncritical variations provided a golden syrup. This material was purified by LC (100 g 230–400 SiO_2 , 2.5–3.5% methanol/chloroform) to afford 727 mg (42%) of the title compound as a light yellow foam. ^1H NMR ($\text{DMSO}-d_6$) δ 8.45 (d, J = 8 Hz, 1H), 7.62 (s, 1H), 7.00 (d, J = 8 Hz, 1H), 4.59 (d, J = 16 Hz, 1H), 4.53 (d, J = 16 Hz, 1H) in a 42% isolated yield. ^1H NMR (400 MHz, CDCl_3) δ 4.38 (m, 1H), 3.80 (m, 1H), 3.15 (m, 1H), 3.06 (m, 1H), 2.22 (m, 1H), 2.07 (m, 1H), 1.98 (m, 1H), 1.63–1.51 (m, 4H), 1.36 (m, 9H), 1.24 (m, 4H), 0.83 (t, J = 8 Hz, 3H); MS (ESI $^+$) for $\text{C}_{19}\text{H}_{32}\text{ClN}_4\text{O}_5$ m/z 418.1 ($\text{M} + \text{H}$) $^+$.

N-((1*S*)-1-(((1*S*)-3-Chloro-2-oxo-1-((3*S*)-2-oxopyrrolidin-3-yl)methyl)propyl)amino]carbonyl]-3-methylbutyl)-4-methoxy-1*H*-indole-2-carboxamide. Following the procedure described for the preparation of *N*-((1*S*)-1-(((1*S*)-3-chloro-2-oxo-1-((3*S*)-2-oxopyrrolidin-3-yl)methyl)propyl)amino]carbonyl]-3-methylbutyl)-4-methoxy-1*H*-indole-2-carboxamide but substituting N^2 -(*tert*-butoxycarbonyl)- N^1 -((1*S*)-3-chloro-2-oxo-1-((3*S*)-2-oxopyrrolidin-3-yl)methyl)propyl)-*L*-norleucineamide and making no other critical variations provided a crude yellow foam. This material was purified by Biotage MPLC (25 M column, 3% methanol/chloroform) to afford 254 mg (63%) of the title compound as an off-white solid. ^1H NMR ($\text{DMSO}-d_6$) δ 11.56 (s, 1H), 8.57 (d, J = 8 Hz, 1H), 8.39 (d, J = 4 Hz, 1H), 7.62 (s, 1H), 7.36 (s, 1H), 7.08 (t, J = 8 Hz, 1H), 6.99 (d, J = 8 Hz, 1H), 6.49 (d, J

= 8 Hz, 1H), 4.58 (d, J = 16 Hz, 1H), 4.56 (d, J = 16 Hz, 1H), 4.43 (m, 1H), 4.35 (m, 1H), 3.87 (s, 3H), 3.09 (m, 2H), 2.27 (m, 1H), 2.08 (m, 1H), 1.97 (m, 1H), 1.74–1.54 (m, 4H), 1.30 (m, 4H), 0.86 (t, J = 8 Hz, 3H); MS (ESI $^+$) for $\text{C}_{24}\text{H}_{31}\text{N}_4\text{O}_5\text{Cl}$ m/z 491.1 ($\text{M} + \text{H}$) $^+$; anal. calcd for $\text{C}_{24}\text{H}_{31}\text{ClN}_4\text{O}_5$: C, 58.71; H, 6.36; N, 11.41. Found: C, 58.66; H, 6.45; N, 11.22.

N-((1*S*)-1-(((1*S*)-3-Hydroxy-2-oxo-1-((3*S*)-2-oxopyrrolidin-3-yl)methyl)propyl)amino]carbonyl]pentyl)-4-methoxy-1*H*-indole-2-carboxamide (**39**). Following the procedure described for the preparation of *N*-((1*S*)-1-(((1*S*)-3-hydroxy-2-oxo-1-((3*S*)-2-oxopyrrolidin-3-yl)methyl)propyl)amino]carbonyl]-3-methylbutyl)-4-methoxy-1*H*-indole-2-carboxamide but substituting *N*-((1*S*)-1-(((1*S*)-3-chloro-2-oxo-1-((3*S*)-2-oxopyrrolidin-3-yl)methyl)propyl)amino]carbonyl]pentyl)-4-methoxy-1*H*-indole-2-carboxamide and making noncritical variations provided a crude yellow foam. This material was purified by Biotage MPLC (25 M column, 5–6% methanol/chloroform) to afford 82 mg (35%) of the title compound as a white foam. ^1H NMR ($\text{DMSO}-d_6$) δ 11.57 (s, 1H), 8.42 (d, J = 8 Hz, 1H), 8.38 (d, J = 8 Hz, 1H), 7.62 (s, 1H), 7.35 (s, 1H), 7.09 (t, J = 8 Hz, 1H), 6.99 (d, J = 8 Hz, 1H), 6.49 (d, J = 8 Hz, 1H), 5.06 (t, J = 8 Hz, 1H), 4.44 (m, 2H), 4.25 (dd, J = 8, 20 Hz, 1H), 4.14 (dd, J = 8, 20 Hz, 1H), 3.87 (s, 3H), 3.08 (m, 2H), 2.28 (m, 1H), 2.10 (m, 1H), 1.91 (m, 1H), 1.74–1.54 (m, 4H), 1.32 (m, 4H), 0.87 (t, J = 8 Hz, 3H); MS (ESI $^+$) for $\text{C}_{24}\text{H}_{32}\text{N}_4\text{O}_6$ m/z 473.2 ($\text{M} + \text{H}$) $^+$; anal. calcd for $\text{C}_{24}\text{H}_{32}\text{N}_4\text{O}_6 \cdot 0.6 \text{H}_2\text{O} \cdot 0.2 \text{ethyl acetate}$: C, 59.46; H, 7.01; N, 11.18. Found: C, 53.37; H, 6.94; N, 11.23; HRMS (ESI $^+$) calcd for $\text{C}_{24}\text{H}_{32}\text{N}_4\text{O}_6 + \text{H}^+$ 473.2395, found 473.2382.

Methyl N-[(9*H*-Fluoren-9-ylmethoxy)carbonyl]-5-methyl-*L*-norleucinate. To a solution of *N*-[(9*H*-fluoren-9-ylmethoxy)carbonyl]-5-methyl-*L*-norleucine (2.14 g, 5.8 mmol) in methanol (15 mL) is added toluene (30 mL) followed by the dropwise addition of TMS-diazomethane (2.9 mL, 2 M in hexane, 5.8 mmol). TLC analysis indicated incomplete reaction, and TMS-diazomethane was added dropwise until a yellow color persisted. At this time, the reaction was quenched by the addition of AcOH (1 mL) followed by concentration *in vacuo*. The residue was purified by Biotage flash chromatography, eluting with ethyl acetate/hexane to afford the title compound as a white solid, 2.18 g, 98%. ^1H NMR (400 MHz, CDCl_3) δ 7.76 (d, J = 7.6 Hz, 2H), 7.60 (dd, J = 7.2, 3.9 Hz, 2H), 7.40 (t, J = 7.2 Hz, 2H), 7.31 (t, J = 7.5 Hz, 2H), 5.26 (d, J = 8.6 Hz, 1H), 4.31–4.51 (m, 3H), 4.23 (t, J = 7.1 Hz, 1H), 3.75 (s, 3H), 1.78–1.93 (m, 1H), 1.60–1.76 (m, 1H), 1.45–1.60 (m, 1H), 1.05–1.34 (m, 2H), 0.88 (d, J = 4 Hz, 3H), 0.86 (d, J = 4 Hz, 3H); MS (APCI $^+$) for $\text{C}_{23}\text{H}_{27}\text{NO}_4$ m/z 160.1 ($\text{M-Fmoc} + \text{H}$) $^+$.

Methyl N-(*tert*-Butoxycarbonyl)-5-methyl-*L*-norleucinate. To a solution of methyl *N*-[(9*H*-fluoren-9-ylmethoxy)carbonyl]-5-methyl-*L*-norleucinate (2.18 g, 5.72 mmol) in DMF (50 mL) was added KF (2.33 g, 40.04 mmol) followed by triethylamine (1.70 mL, 12.24 mmol) and di-*tert*-butyl dicarbonate (7.39 mmol), and the mixture was stirred at an ambient temperature. After 4 h, TLC analysis indicated incomplete reaction and the reaction mixture was treated with a second portion of KF (2.7 g, 46.55 mmol) and BOC_2O (800 mg, 3.67 mmol). After 16 h, the mixture was diluted with diethyl ether (300 mL), washed with satd. NaHCO_3 (2 \times 50 mL), 1 M hydrochloric acid (2 \times 50 mL), NaHCO_3 (50 mL), and brine (50 mL), dried over MgSO_4 , filtered, and the solvents were evaporated *in vacuo* to yield the crude product, which was purified by Biotage flash chromatography eluting with dichloromethane/hexane to afford the title compound as a clear oil, 980 mg, 66%. ^1H NMR (400 MHz, CDCl_3) δ 4.96 (d, J = 6.8 Hz, 1H), 4.21–4.32 (m, 1H), 3.72 (s, 3H), 1.72–1.85 (m, 1H), 1.46–1.66 (m, 2H), 1.43 (s, 9H), 1.11–1.29 (m, 2H), 0.88 (d, J = 4 Hz, 3H), 0.86 (d, J = 4 Hz, 3H); MS (API-ES $^+$) for $\text{C}_{13}\text{H}_{25}\text{NO}_4$ m/z 282.2 ($\text{M} + \text{Na}$) $^+$.

N-(*tert*-Butoxycarbonyl)-5-methyl-*L*-norleucine. To a solution of methyl *N*-(*tert*-butoxycarbonyl)-5-methyl-*L*-norleucinate (980 mg, 3.78 mmol) in THF (30 mL) at 0 $^\circ\text{C}$ was added a solution (precooled to 5 $^\circ\text{C}$) of LiOH (1 M, 11.3 mL, 11.33 mmol), and the resulting mixture was stirred at 0 $^\circ\text{C}$ for 1 h and then allowed to warm to an ambient temperature. The reaction was acidified to pH 2 with 1 M hydrochloric acid and extracted with ethyl acetate (3 \times 60 mL).

The combined organics were washed with brine (100 mL), dried over MgSO_4 , filtered, and the solvent was removed *in vacuo* to yield the title compound as a clear oil, 990 mg, 99%. ^1H NMR (400 MHz, CDCl_3) δ 4.96 (d, J = 7.8 Hz, 1H), 4.23–4.34 (m, 1H), 1.75–1.93 (m, 2H), 1.60–1.72 (m, 1H), 1.50–1.59 (m, 1H), 1.44 (s, 9H), 1.19–1.30 (m, 1H), 0.88 (d, J = 4 Hz, 3H), 0.86 (d, J = 4 Hz, 3H); MS (API-ES+) for $\text{C}_{12}\text{H}_{23}\text{NO}_4$ m/z 268.1 ($\text{M} + \text{Na}$) $^+$.

N^2 -(*tert*-butoxycarbonyl)- N^1 -((1*S*)-3-chloro-2-oxo-1-[[[(3*S*)-2-oxopyrrolidin-3-yl]methyl]propyl]-5-methyl-L-norleucinamide. Following the procedure described for the preparation of N^2 -(*tert*-butoxycarbonyl)- N^1 -((1*S*)-3-chloro-2-oxo-1-[[[(3*S*)-2-oxopyrrolidin-3-yl]methyl]propyl]-L-leucinamide but substituting *N*-(*tert*-butoxycarbonyl)-5-methyl-L-norleucine and making noncritical variations provided a crude golden oil. This material was purified by Biotage flash chromatography, eluting with methanol/dichloromethane to afford the title compound as an off-white solid, 360 mg, 41%. ^1H NMR (400 MHz, $\text{DMSO}-d_6$) δ 8.45 (d, J = 8.1 Hz, 1H), 7.62 (s, 1H), 7.02 (d, J = 7.1 Hz, 1H), 4.49–4.62 (m, 2H), 4.33–4.44 (m, 1H), 3.78 (m, 1H), 3.15 (t, J = 8.7 Hz, 1H), 3.00–3.10 (m, 1H), 2.18–2.30 (m, 1H), 2.04–2.14 (m, 1H), 1.92–2.02 (m, 1H), 1.40–1.68 (m, 5H), 1.36 (s, 9H), 1.05–1.25 (m, J = 7.3 Hz, 2H), 0.83 (d, J = 1.52 Hz, 3H), 0.82 (d, J = 1.52 Hz, 3H); MS (API-ES+) for $\text{C}_{20}\text{H}_{34}\text{N}_3\text{O}_5\text{Cl}$ m/z 454.2 ($\text{M} + \text{Na}$) $^+$.

N -((1*S*)-1-[[[(1*S*)-3-chloro-2-oxo-1-[[[(3*S*)-2-oxopyrrolidin-3-yl]methyl]propyl]amino]carbonyl]-4-methoxy-1*H*-indole-2-carboxamide. Following the procedure described for the preparation of N -((1*S*)-1-[[[(1*S*)-3-chloro-2-oxo-1-[[[(3*S*)-2-oxopyrrolidin-3-yl]methyl]propyl]amino]carbonyl]-3-methylbutyl)-4-methoxy-1*H*-indole-2-carboxamide but substituting N^2 -(*tert*-butoxycarbonyl)- N^1 -((1*S*)-3-chloro-2-oxo-1-[[[(3*S*)-2-oxopyrrolidin-3-yl]methyl]propyl]-5-methyl-L-norleucinamide and making no other critical variations provided a crude yellow foam. This material was purified by Biotage MPLC (25 M column, 2.5–3.5% methanol/chloroform) to afford 307 mg (73%) of the title compound as a white solid. ^1H NMR ($\text{DMSO}-d_6$) δ 11.57 (s, 1H), 8.59 (d, J = 8 Hz, 1H), 8.41 (d, J = 4 Hz, 1H), 7.64 (s, 1H), 7.37 (s, 1H), 7.09 (t, J = 8 Hz, 1H), 7.00 (d, J = 8 Hz, 1H), 6.49 (d, J = 8 Hz, 1H), 4.59 (s, 2H), 4.44 (m, 1H), 4.35 (m, 1H), 3.87 (s, 3H), 3.08 (m, 2H), 2.26 (m, 1H), 2.07 (m, 1H), 1.98 (m, 1H), 1.70–1.51 (m, 5H), 1.25 (m, 2H), 0.88 (d, J = 4 Hz, 3H), 0.86 (d, J = 4 Hz, 3H); MS (ESI+) for $\text{C}_{25}\text{H}_{33}\text{ClN}_4\text{O}_5$ m/z 505.2 ($\text{M} + \text{H}$) $^+$; HRMS (ESI+) calcd for $\text{C}_{25}\text{H}_{33}\text{ClN}_4\text{O}_5 + \text{H}^+$ 505.2212, found 505.2204.

N -((1*S*)-1-[[[(1*S*)-3-hydroxy-2-oxo-1-[[[(3*S*)-2-oxopyrrolidin-3-yl]methyl]propyl]amino]carbonyl]-4-methylpentyl)-4-methoxy-1*H*-indole-2-carboxamide (40). Following the procedure described for the preparation of N -((1*S*)-1-[[[(1*S*)-3-chloro-2-oxo-1-[[[(3*S*)-2-oxopyrrolidin-3-yl]methyl]propyl]amino]carbonyl]-3-methylbutyl)-4-methoxy-1*H*-indole-2-carboxamide but substituting N -((1*S*)-1-[[[(1*S*)-3-chloro-2-oxo-1-[[[(3*S*)-2-oxopyrrolidin-3-yl]methyl]propyl]amino]carbonyl]-4-methylpentyl)-4-methoxy-1*H*-indole-2-carboxamide and making noncritical variations provided a crude yellow foam. This material was purified by Biotage MPLC (25 M column, 5–5.5% methanol/chloroform) to afford 135 mg (50%) of the title compound as a white foam. ^1H NMR ($\text{DMSO}-d_6$) δ 11.57 (s, 1H), 8.42 (d, J = 8 Hz, 1H), 8.38 (d, J = 8 Hz, 1H), 7.62 (s, 1H), 7.35 (s, 1H), 7.09 (t, J = 8 Hz, 1H), 6.99 (d, J = 8 Hz, 1H), 6.49 (d, J = 8 Hz, 1H), 5.06 (t, J = 8 Hz, 1H), 4.47–4.30 (m, 2H), 4.25 (dd, J = 8, 20 Hz, 1H), 4.14 (dd, J = 8, 20 Hz, 1H), 3.87 (s, 3H), 3.09 (m, 2H), 2.30 (m, 1H), 2.08 (m, 1H), 1.92 (m, 1H), 1.72–1.51 (m, 5H), 1.25 (m, 2H), 0.87 (d, J = 4 Hz, 3H), 0.86 (d, J = 4 Hz, 3H); MS (ESI+) for $\text{C}_{25}\text{H}_{34}\text{N}_4\text{O}_6$ m/z 487.1 ($\text{M} + \text{H}$) $^+$; HRMS (ESI+) calcd for $\text{C}_{25}\text{H}_{34}\text{N}_4\text{O}_6$ 487.2551, found 487.2541.

tert-Butyl [(1*S*)-2-[[[(1*S*)-3-(benzyloxy)-2-oxo-1-[[[(3*S*)-2-oxopyrrolidin-3-yl]methyl]propyl]amino]-1-(cyclohexylmethyl)-2-oxoethyl]carbamate. To a solution of *tert*-butyl [(1*S*)-3-(benzyloxy)-2-oxo-1-[[[(3*S*)-2-oxopyrrolidin-3-yl]methyl]propyl]carbamate (200 mg, 0.53 mmol) in dioxane (5 mL) was added 4 M hydrochloric acid/dioxane (5 mL), and the solution was stirred at an ambient temperature for 4 h before removing the solvents *in vacuo*, azeotroping the residue with toluene (2 \times 10 mL), and drying *in vacuo* for 1 h. The crude

hydrochloride salt was taken into DMF (3 mL), and the solution was cooled to 0 $^\circ\text{C}$ before adding *N*-Boc-cyclohexylalanine-OH (139 mg, 0.53 mmol), collidine (156 μL , 1.22 mmol), and HATU (194 mg, 0.53 mmol) in order, and the resulting suspension was stirred at 0 $^\circ\text{C}$ for 5 h. The reaction was quenched by the addition of water (30 mL), and the mixture was extracted with diethyl ether (3 \times 75 mL). The combined organics were dried over MgSO_4 , filtered, and the solvents were removed *in vacuo* to yield the crude product, which was purified by flash chromatography, eluting with 1–3% methanol/dichloromethane to afford the title compound as a pale brown gum, 205 mg, 76%. The product was contaminated with \sim 20% of another diastereoisomer. ^1H NMR (400 MHz, CDCl_3) δ 7.69 (d, J = 5.6 Hz, 1H), 7.26–7.42 (m, 5H), 5.93 (s, 1H), 4.94 (d, J = 7.6 Hz, 1H), 4.72 (m, 1H), 4.60 (d, J = 11.6 Hz, 1H), 4.55 (d, J = 11.6 Hz, 1H), 4.14–4.34 (m, 3H), 3.27 (m, 2H), 2.23–2.51 (m, 3H), 1.56–2.05 (m, 9H), 1.33–1.48 (m, 9H), 1.05–1.29 (m, 4H), 0.80–1.03 (m, 2H).

N -[[[(1*S*)-2-[[[(1*S*)-3-(benzyloxy)-2-oxo-1-[[[(3*S*)-2-oxopyrrolidin-3-yl]methyl]propyl]amino]-1-(cyclohexylmethyl)-2-oxoethyl]-4-methoxy-1*H*-indole-2-carboxamide. To a solution of *tert*-butyl [(1*S*)-2-[[[(1*S*)-3-(benzyloxy)-2-oxo-1-[[[(3*S*)-2-oxopyrrolidin-3-yl]methyl]propyl]amino]-1-(cyclohexylmethyl)-2-oxoethyl]carbamate (200 mg, 0.38 mmol) in dioxane (4 mL) was added 4 M hydrochloric acid/dioxane (4 mL), and the solution was stirred at an ambient temperature for 2 h before removing the solvents *in vacuo*, azeotroping the residue with toluene (2 \times 10 mL), and drying *in vacuo* for 1 h. The crude hydrochloride salt was taken into DMF (3 mL), and the solution was cooled to 0 $^\circ\text{C}$ before adding 4-methoxyindole-2-carboxylic acid (73 mg, 0.38 mmol), collidine (125 μL , 0.95 mmol), and HATU (144 mg, 0.38 mmol) in order, and the resulting suspension was stirred at 0 $^\circ\text{C}$ for 6 h. The reaction was quenched by the addition of water (20 mL), and the mixture was extracted with diethyl ether (3 \times 50 mL). The combined organics were washed with water (20 mL) and brine (20 mL), dried over MgSO_4 , filtered, and the solvents were removed *in vacuo* to yield the crude product, which was purified by Biotage flash chromatography, eluting with 1–3% methanol/dichloromethane to afford the title compound as a pale brown gum, 90 mg, 39%. The product was contaminated with \sim 20% of another diastereomer from the previous step. ^1H NMR (400 MHz, CDCl_3) δ 9.59 (s, 1H), 8.13 (d, J = 6.6 Hz, 1H), 7.21–7.32 (m, 5H), 7.11 (t, J = 8.0 Hz, 1H), 7.02 (d, J = 1.5 Hz, 1H), 6.94 (d, J = 8.3 Hz, 1H), 6.72–6.78 (m, 1H), 6.42 (d, J = 7.8 Hz, 1H), 5.97 (s, 1H), 4.73 (m, 1H), 4.64 (m, 1H), 4.53 (d, J = 11.6 Hz, 1H), 4.46 (d, J = 11.6 Hz, 1H), 4.26 (d, J = 17.2 Hz, 1H), 4.15 (d, J = 17.4 Hz, 1H), 3.87 (s, 3H), 3.08–3.16 (m, 2H), 2.27–2.38 (m, 1H), 1.92 (m, 1H), 1.49–1.84 (m, 9H), 1.26–1.42 (m, 1H), 0.98–1.23 (m, 4H), 0.78–0.98 (m, 2H); MS (APCI+) for $\text{C}_{34}\text{H}_{42}\text{N}_4\text{O}_6$ m/z 603.2 ($\text{M} + \text{H}$) $^+$.

N -[(1*S*)-1-(cyclohexylmethyl)-2-[[[(1*S*)-3-hydroxy-2-oxo-1-[[[(3*S*)-2-oxopyrrolidin-3-yl]methyl]propyl]amino]-2-oxoethyl]-4-methoxy-1*H*-indole-2-carboxamide (41). To a solution of N -[(1*S*)-2-[[[(1*S*)-3-(benzyloxy)-2-oxo-1-[[[(3*S*)-2-oxopyrrolidin-3-yl]methyl]propyl]amino]-1-(cyclohexylmethyl)-2-oxoethyl]-4-methoxy-1*H*-indole-2-carboxamide (80 mg, 0.13 mmol) in EtOH (3 mL) was added 10% Pd/C (50 mg), and the suspension was hydrogenated at an ambient temperature under H_2 (1 atm balloon) for 5 h. The catalyst was removed by filtration, and the solvents were evaporated *in vacuo* to yield the crude product, which was purified by Biotage flash chromatography, eluting with 2–10% methanol/dichloromethane to afford the title compound, 37 mg, 55% as a white solid. ^1H NMR (400 MHz, MeOD) δ 7.19 (s, 1H), 7.05 (t, J = 8.0 Hz, 1H), 6.93 (d, J = 8.1 Hz, 1H), 6.41 (d, J = 7.8 Hz, 1H), 4.52–4.59 (m, 2H), 4.27 (m, 2H), 3.83 (s, 3H), 3.08–3.21 (m, 2H), 2.47 (m, 1H), 2.13–2.24 (m, 1H), 1.92–2.03 (m, 1H), 1.53–1.79 (m, 9H), 1.31–1.45 (m, 1H), 1.04–1.29 (m, 3H), 0.81–1.02 (m, 2H); MS (APCI+) for $\text{C}_{27}\text{H}_{36}\text{N}_4\text{O}_6$ m/z 513.2 ($\text{M} + \text{H}$) $^+$; anal. calcd for $\text{C}_{27}\text{H}_{36}\text{N}_4\text{O}_6 \cdot 0.8 \text{ H}_2\text{O}$: C, 61.53; H, 7.19; N, 10.63. Found: C, 61.83; H, 7.12; N, 10.27.

N-(*tert*-butoxycarbonyl)- N -((1*S*)-3-chloro-2-oxo-1-[[[(3*S*)-2-oxopyrrolidin-3-yl]methyl]propyl)-L-phenylalaninamide. Following the procedure described for the preparation of N^2 -(*tert*-butoxycarbonyl)- N^1 -((1*S*)-3-chloro-2-oxo-1-[[[(3*S*)-2-oxopyrrolidin-3-yl]methyl]-

propyl)-L-leucinamide but substituting Boc-Phe-OH and making noncritical variations provided a crude brown oil. This material was purified by Biotage flash chromatography, eluting with methanol/dichloromethane to afford the title compound as a white solid, 351 mg, 36%. ¹H NMR (400 MHz, CDCl₃) δ 8.02 (s, 1H), 7.19–7.31 (m, 5H), 5.77 (s, 1H), 5.10 (d, *J* = 6.1 Hz, 1H), 4.52–4.57 (m, 1H), 4.44 (m, 1H), 4.01–4.12 (m, 2H), 3.26–3.37 (m, 2H), 3.01–3.08 (m, 2H), 2.29–2.37 (m, 1H), 2.15–2.25 (m, 1H), 1.98–2.06 (m, 1H), 1.75–1.91 (m, 2H), 1.40 (s, 9H); MS (API-ES[−]) for C₂₂H₃₀N₃O₅Cl *m/z* 450.2 (M + H)[−].

N-((1*S*)-3-Chloro-2-oxo-1-[[[(3*S*)-2-oxopyrrolidin-3-yl]methyl]propyl)-*N*-[(4-methoxy-1*H*-indol-2-yl)carbonyl]-L-phenylalaninamide. Following the procedure described for the preparation of *N*-((1*S*)-1-[[[(1*S*)-3-chloro-2-oxo-1-[[[(3*S*)-2-oxopyrrolidin-3-yl]methyl]propyl]amino]carbonyl]-3-methylbutyl)-4-methoxy-1*H*-indole-2-carboxamide but substituting *N*-(*tert*-butoxycarbonyl)-*N*-((1*S*)-3-chloro-2-oxo-1-[[[(3*S*)-2-oxopyrrolidin-3-yl]methyl]propyl)-L-phenylalaninamide and making noncritical variations provided a crude green solid. This material was purified by Biotage flash chromatography, eluting with methanol/dichloromethane to afford the title compound as a white solid, 300 mg, 91%. ¹H NMR (400 MHz, DMSO-*d*₆) δ 11.52 (d, *J* = 2.0 Hz, 1H), 8.68 (d, *J* = 7.8 Hz, 1H), 8.61 (d, *J* = 7.8 Hz, 1H), 7.61 (s, 1H), 7.37 (d, *J* = 7.1 Hz, 2H), 7.31 (d, *J* = 1.8 Hz, 1H), 7.26 (t, *J* = 7.6 Hz, 2H), 7.16 (t, *J* = 7.2 Hz, 1H), 7.07 (t, 1H), 6.97 (d, *J* = 8.1 Hz, 1H), 6.49 (d, *J* = 7.6 Hz, 1H), 4.68 (m, 1H), 4.38–4.49 (m, 3H), 3.88 (s, 3H), 2.97–3.17 (m, 4H), 2.20–2.32 (m, 1H), 2.02–2.14 (m, 1H), 1.93–2.02 (m, 1H), 1.52–1.69 (m, 2H); MS (APCI±) for C₂₇H₃₉N₄O₅Cl *m/z* 526.0 (M + H)[−].

N-((1*S*)-3-Hydroxy-2-oxo-1-[[[(3*S*)-2-oxopyrrolidin-3-yl]methyl]propyl)-*N*-[(4-methoxy-1*H*-indol-2-yl)carbonyl]-L-phenylalaninamide (42). Following the procedure described for the preparation of *N*-((1*S*)-1-[[[(1*S*)-3-hydroxy-2-oxo-1-[[[(3*S*)-2-oxopyrrolidin-3-yl]methyl]propyl]amino]carbonyl]-3-methylbutyl)-4-methoxy-1*H*-indole-2-carboxamide but substituting *N*-((1*S*)-3-chloro-2-oxo-1-[[[(3*S*)-2-oxopyrrolidin-3-yl]methyl]propyl)-*N*-[(4-methoxy-1*H*-indol-2-yl)carbonyl]-L-phenylalaninamide and making noncritical variations provided a crude greenish gum. This material was purified by Biotage flash chromatography, eluting with methanol/dichloromethane to afford the title compound as an off-white solid, 123 mg, 44%. ¹H NMR (400 MHz, DMSO-*d*₆) δ 11.50 (d, *J* = 2.0 Hz, 1H), 8.58 (dd, *J* = 8.2, 3.9 Hz, 2H), 7.63 (s, 1H), 7.35–7.43 (m, 2H), 7.31 (d, *J* = 1.8 Hz, 1H), 7.27 (t, *J* = 7.6 Hz, 2H), 7.17 (t, *J* = 7.3 Hz, 1H), 7.08 (t, *J* = 8.0 Hz, 1H), 6.98 (d, *J* = 8.1 Hz, 1H), 6.48 (d, *J* = 7.8 Hz, 1H), 5.06 (t, *J* = 6.1 Hz, 1H), 4.72 (m, 1H), 4.48 (m, 1H), 4.16 (m, 2H), 3.89 (s, 3H), 2.97–3.18 (m, 4H), 2.24–2.36 (m, 1H), 2.04–2.18 (m, 1H), 1.88–2.01 (m, 1H), 1.55–1.76 (m, 2H); MS (APCI+) for C₂₇H₃₀N₄O₆ *m/z* 507.1 (M + H)⁺; anal. calcd for C₂₇H₃₀N₄O₆ · 1.25 H₂O: C, 61.29; H, 6.19; N, 10.59. Found: C, 61.37; H, 6.06; N, 10.49.

N-((1*S*)-1-[[[(1*S*)-3-Chloro-2-oxo-1-[[[(3*S*)-2-oxopyrrolidin-3-yl]methyl]propyl]amino]carbonyl]-3,3-dimethylbutyl)-1*H*-indole-2-carboxamide. Following the procedure described for the preparation of *N*-((1*S*)-1-[[[(1*S*)-3-chloro-2-oxo-1-[[[(3*S*)-2-oxopyrrolidin-3-yl]methyl]propyl]amino]carbonyl]-3-methylbutyl)-4-methoxy-1*H*-indole-2-carboxamide but substituting *N*²-(*tert*-butoxycarbonyl)-*N*¹-((1*S*)-3-chloro-2-oxo-1-[[[(3*S*)-2-oxopyrrolidin-3-yl]methyl]propyl)-4-methyl-L-leucinamide and indole-2-carboxylic acid and making no other critical variations provided a crude yellow foam. This material was purified by Biotage MPLC (40 M column, 2.5–3.5% methanol/chloroform) to afford 1.06 g (62%) of the title compound as a light yellow foam. ¹H NMR (DMSO-*d*₆) δ 11.59 (s, 1H), 8.58 (d, *J* = 8 Hz, 1H), 8.50 (d, *J* = 8 Hz, 1H), 7.64 (s, 1H), 7.61 (d, *J* = 8 Hz, 1H), 7.41 (d, *J* = 8 Hz, 1H), 7.23 (s, 1H), 7.17 (t, *J* = 8 Hz, 1H), 7.02 (t, *J* = 8 Hz, 1H), 4.62–4.50 (m, 3H), 4.45 (m, 1H), 3.10 (m, 2H), 2.25 (m, 1H), 2.08 (m, 1H), 1.96 (m, 1H), 1.80 (m, 1H), 1.72–1.58 (m, 3H), 0.94 (s, 9H); MS (ESI+) for C₂₄H₃₁ClN₄O₄ *m/z* 475.1 (M + H)⁺; anal. calcd for C₂₄H₃₁ClN₄O₄ · 0.35 CHCl₃: C, 56.59; H, 6.12; N, 10.84. Found: C, 56.38; H, 6.18; N, 10.75; HRMS (ESI+) calcd for C₂₄H₃₁ClN₄O₄ 475.2107, found 475.2122.

N-((1*S*)-1-[[[(1*S*)-3-Hydroxy-2-oxo-1-[[[(3*S*)-2-oxopyrrolidin-3-yl]methyl]propyl]amino]carbonyl]-3,3-dimethylbutyl)-1*H*-indole-2-carboxamide (43). Following the procedure described for the preparation of *N*-((1*S*)-1-[[[(1*S*)-3-hydroxy-2-oxo-1-[[[(3*S*)-2-oxopyrrolidin-3-yl]methyl]propyl]amino]carbonyl]-3-methylbutyl)-4-methoxy-1*H*-indole-2-carboxamide but substituting *N*-((1*S*)-1-[[[(1*S*)-3-chloro-2-oxo-1-[[[(3*S*)-2-oxopyrrolidin-3-yl]methyl]propyl]amino]carbonyl]-3,3-dimethylbutyl)-1*H*-indole-2-carboxamide and making noncritical variations provided a crude yellow foam. This material was purified by Biotage MPLC (40 M column, 4.5–5.5% methanol/chloroform) to afford 730 mg (72%) of the title compound as a white solid. ¹H NMR (DMSO-*d*₆) δ 11.59 (s, 1H), 8.49 (d, *J* = 8 Hz, 1H), 8.43 (d, *J* = 8 Hz, 1H), 7.62 (s, 1H), 7.60 (s, 1H), 7.41 (d, *J* = 8 Hz, 1H), 7.23 (s, 1H), 7.17 (t, *J* = 8 Hz, 1H), 7.02 (t, *J* = 8 Hz, 1H), 5.05 (t, *J* = 8 Hz, 1H), 4.56 (m, 1H), 4.43 (m, 1H), 4.25 (dd, *J* = 8, 20 Hz, 1H), 4.13 (dd, *J* = 8, 20 Hz, 1H), 3.10 (m, 2H), 2.25 (m, 1H), 2.07 (m, 1H), 1.93 (m, 1H), 1.80 (m, 1H), 1.64 (m, 3H), 0.94 (s, 9H); MS (ESI+) for C₂₄H₃₂N₄O₅ *m/z* 457.1 (M + H)⁺; anal. calcd for C₂₄H₃₂N₄O₅ · 0.2 CHCl₃ · 0.2 ethyl acetate · 0.25 H₂O: C, 59.75; H, 6.88; N, 11.15. Found: C, 59.67; H, 6.72; N, 11.03; HRMS (ESI+) calcd for C₂₄H₃₂N₄O₅ 457.2446, found 457.2439.

N-((1*S*)-1-[[[(1*S*)-3-Methoxy-2-oxo-1-[[[(3*S*)-2-oxopyrrolidin-3-yl]methyl]propyl]amino]carbonyl]-3,3-dimethylbutyl)-1*H*-indole-2-carboxamide (44). Following the procedure described for the preparation of 4-methoxy-*N*-((1*S*)-1-[[[(1*S*)-3-methoxy-2-oxo-1-[[[(3*S*)-2-oxopyrrolidin-3-yl]methyl]propyl]amino]carbonyl]-4-methylpentyl)-1*H*-indole-2-carboxamide but substituting *N*-((1*S*)-1-[[[(1*S*)-3-hydroxy-2-oxo-1-[[[(3*S*)-2-oxopyrrolidin-3-yl]methyl]propyl]amino]carbonyl]-3,3-dimethylbutyl)-1*H*-indole-2-carboxamide and making noncritical variations provided a crude tan foam. This material was purified by Biotage MPLC (25 M column, 3.5–4.5% methanol/chloroform) to afford 43 mg (15%) of the title compound as a white solid. ¹H NMR (DMSO-*d*₆) δ 11.58 (s, 1H), 8.48 (apar t, *J* = 8 Hz, 2H), 7.61 (apar d, *J* = 8 Hz, 2H), 7.41 (d, *J* = 8 Hz, 1H), 7.23 (s, 1H), 7.17 (t, *J* = 8 Hz, 1H), 7.02 (t, *J* = 8 Hz, 1H), 4.55 (m, 1H), 4.37 (m, 1H), 4.25 (d, *J* = 20 Hz, 1H), 4.10 (d, *J* = 20 Hz, 1H), 3.23 (s, 3H), 3.06 (m, 2H), 2.27 (m, 1H), 2.07 (m, 1H), 1.91 (m, 1H), 1.79 (m, 1H), 1.69 (m, 3H), 0.94 (s, 9H); MS (ESI+) for C₂₅H₃₄N₄O₅ *m/z* 471.2 (M + H)⁺; anal. calcd for C₂₅H₃₄N₄O₅ · 0.2 ethyl acetate · 0.75 H₂O: C, 61.76; H, 7.46; N, 11.17. Found: C, 61.85; H, 7.15; N, 11.02; HRMS (ESI+) calcd for C₂₅H₃₄N₄O₅ 471.2602, found 471.2595.

N-((1*S*)-1-[[[(1*S*)-3-Ethoxy-2-oxo-1-[[[(3*S*)-2-oxopyrrolidin-3-yl]methyl]propyl]amino]carbonyl]-3,3-dimethylbutyl)-1*H*-indole-2-carboxamide (45). Following the procedure described for the preparation of *N*-((1*S*)-1-[[[(1*S*)-3-methoxy-2-oxo-1-[[[(3*S*)-2-oxopyrrolidin-3-yl]methyl]propyl]amino]carbonyl]-3,3-dimethylbutyl)-1*H*-indole-2-carboxamide but substituting iodoethane and making noncritical variations provided a crude tan foam. This material was purified by Biotage MPLC (25 M column, 3–5% methanol/chloroform) to afford 19 mg (6%) of the title compound as an off-white solid. ¹H NMR (DMSO-*d*₆) δ 11.58 (s, 1H), 8.48 (d, *J* = 8 Hz, 1H), 8.45 (d, *J* = 8 Hz, 1H), 7.61 (apar d, *J* = 8 Hz, 2H), 7.41 (d, *J* = 8 Hz, 1H), 7.23 (s, 1H), 7.17 (t, *J* = 8 Hz, 1H), 7.02 (t, *J* = 8 Hz, 1H), 4.56 (m, 1H), 4.40 (m, 1H), 4.28 (d, *J* = 16 Hz, 1H), 4.13 (d, *J* = 16 Hz, 1H), 3.41 (m, 2H), 3.06 (m, 2H), 2.26 (m, 1H), 2.09 (m, 1H), 1.91 (m, 1H), 1.82 (m, 1H), 1.63 (m, 3H), 1.08 (t, *J* = 8 Hz, 3H), 0.94 (s, 9H); MS (ESI+) for C₂₆H₃₆N₄O₅ *m/z* 485.2 (M + H)⁺; HRMS (ESI+) calcd for C₂₆H₃₆N₄O₅ 485.2759, found 485.2756.

*N*¹-((1*S*)-3-Chloro-2-oxo-1-[[[(3*S*)-2-oxopyrrolidin-3-yl]methyl]propyl)-4-methyl-*N*²-[(2*R*)-tetrahydrofuran-2-ylcarbonyl]-L-leucinamide. Following the procedure described for the preparation of *N*-((1*S*)-1-[[[(1*S*)-3-chloro-2-oxo-1-[[[(3*S*)-2-oxopyrrolidin-3-yl]methyl]propyl]amino]carbonyl]-3-methylbutyl)-4-methoxy-1*H*-indole-2-carboxamide but substituting *N*²-(*tert*-butoxycarbonyl)-*N*¹-((1*S*)-3-chloro-2-oxo-1-[[[(3*S*)-2-oxopyrrolidin-3-yl]methyl]propyl)-4-methyl-L-leucinamide and (2*R*)-tetrahydrofuran-2-carboxylic acid and making noncritical variations provided a crude product. This crude material was purified by Biotage MPLC (40 M cartridge, chloroform mobile phase with 2% methanol followed by 3%

methanol, sample loaded in chloroform) resulting in the isolation of 1.13 g (61%) of the title compound as a light yellow foam. $R_f = 0.27$ (95:5 dichloromethane/methanol); ^1H NMR (400 MHz, DMSO- d_6) δ 8.47 (d, $J = 8$ Hz, 1H), 7.72 (d, $J = 8$ Hz, 1H), 7.68 (s, 1H), 4.55 (s, 2H), 4.44–4.36 (m, 1H), 4.35–4.27 (m, 1H), 4.21 (dd, $J = 8, 5$ Hz, 1H), 3.95–3.86 (m, 1H), 3.79–3.71 (m, 1H), 3.18–3.07 (m, 2H), 2.21 (td, $J = 9, 4$ Hz, 1H), 2.13–2.03 (m, 2H), 1.97–1.88 (m, 1H), 1.85–1.74 (m, 3H), 1.68–1.56 (m, 4H), 0.88 (s, 9H); MS (ESI+) for $\text{C}_{20}\text{H}_{32}\text{ClN}_3\text{O}_5$ m/z 430 ($M + \text{H}$).

N^1 -((1S)-3-Hydroxy-2-oxo-1-[[[(3S)-2-oxopyrrolidin-3-yl]methyl]propyl]-4-methyl- N^2 -[(2R)-tetrahydrofuran-2-ylcarbonyl]-L-leucinamide (46). Following the procedure described for the preparation of N -((1S)-1-[[[(1S)-3-hydroxy-2-oxo-1-[[[(3S)-2-oxopyrrolidin-3-yl]methyl]propyl]amino]carbonyl]-3-methylbutyl]-4-methoxy-1H-indole-2-carboxamide but substituting N^1 -((1S)-3-chloro-2-oxo-1-[[[(3S)-2-oxopyrrolidin-3-yl]methyl]propyl]-4-methyl- N^2 -[(2R)-tetrahydrofuran-2-ylcarbonyl]-L-leucinamide and making noncritical variations provided a crude product. This material was purified by a series of two radial chromatographies (first –2 mm plate, 90:10 dichloromethane/methanol to 90:20, sample loaded in 90:10) (second –1 mm plates, 90:10 dichloromethane/methanol to 95:5, sample loaded in dichloromethane) to provide 0.402 g (46%) of the title compound as a light yellow foam. $R_f = 0.44$ (90:10 dichloromethane/methanol); ^1H NMR (400 MHz, DMSO- d_6) δ 8.27 (d, $J = 8$ Hz, 1H), 7.71 (d, $J = 9$ Hz, 1H), 7.65 (s, 1H), 5.11 (t, $J = 6$ Hz, 1H), 4.46–4.38 (m, 1H), 4.37–4.30 (m, 1H), 4.24–4.15 (m, 2H), 4.14–4.08 (m, 1H), 3.96–3.87 (m, 1H), 3.79–3.70 (m, 1H), 3.18–3.06 (m, 2H), 2.25–2.16 (m, 1H), 2.13–2.02 (m, 2H), 1.87–1.75 (m, 4H), 1.66–1.54 (m, 4H), 0.88 (s, 9H); MS (ESI+) for $\text{C}_{20}\text{H}_{33}\text{N}_3\text{O}_6$ m/z 412 ($M + \text{H}$). Anal. calcd for $\text{C}_{20}\text{H}_{33}\text{N}_3\text{O}_6 \cdot 0.5\text{H}_2\text{O}$: C, 57.12; H, 8.16; N, 9.99. Found: C, 57.25; H, 7.93; N, 9.68. HRMS (ESI+) calcd for $\text{C}_{20}\text{H}_{33}\text{N}_3\text{O}_6 + \text{H}$ 412.2442, found 412.2447.

N^1 -((1S)-3-Methoxy-2-oxo-1-[[[(3S)-2-oxopyrrolidin-3-yl]methyl]propyl]-4-methyl- N^2 -[(2R)-tetrahydrofuran-2-ylcarbonyl]-L-leucinamide (47). Following the procedure described for the preparation of 4-methoxy- N -((1S)-1-[[[(1S)-3-methoxy-2-oxo-1-[[[(3S)-2-oxopyrrolidin-3-yl]methyl]propyl]amino]carbonyl]-3-methylbutyl]-1H-indole-2-carboxamide but substituting N^1 -((1S)-3-hydroxy-2-oxo-1-[[[(3S)-2-oxopyrrolidin-3-yl]methyl]propyl]-4-methyl- N^2 -[(2R)-tetrahydrofuran-2-ylcarbonyl]-L-leucinamide and making noncritical variations provided a crude product. This material was purified by radial chromatography (1 mm plate, 95:5 dichloromethane/methanol, sample loaded in dichloromethane) resulting in the isolation of 45.6 mg (22%) of the title compound as a light orange gum and as a mixture of diastereomers. $R_f = 0.30$ (95:5 dichloromethane/methanol); ^1H NMR (400 MHz, DMSO- d_6 , major diastereomer) δ 8.33 (d, $J = 8$ Hz, 1H), 7.70 (d, $J = 9$ Hz, 1H), 7.66 (s, 1H), 4.39–4.28 (m, 2H), 4.24–4.07 (m, 3H), 3.94–3.86 (m, 1H), 3.75 (q, $J = 7$ Hz, 1H), 3.24 (s, 3H), 3.18–3.06 (m, 2H), 2.27–2.15 (m, 1H), 2.14–2.03 (m, 2H), 1.92–1.73 (m, 4H), 1.67–1.53 (m, 4H), 0.88 (s, 9H); MS (ESI+) for $\text{C}_{21}\text{H}_{35}\text{N}_3\text{O}_6$ m/z 426 ($M + \text{H}$). HRMS (ESI+) calcd for $\text{C}_{21}\text{H}_{35}\text{N}_3\text{O}_6 + \text{H}$ 426.2599, found 426.2604.

4-Methoxy- N -((1S)-1-[[[(1S)-3-methoxy-2-oxo-1-[[[(3S)-2-oxopyrrolidin-3-yl]methyl]propyl]amino]carbonyl]-3-methylbutyl]-1H-indole-2-carboxamide (48). A solution of N -((1S)-1-[[[(1S)-3-hydroxy-2-oxo-1-[[[(3S)-2-oxopyrrolidin-3-yl]methyl]propyl]amino]carbonyl]-3-methylbutyl]-4-methoxy-1H-indole-2-carboxamide (185 mg, 0.39 mmol), iodomethane (0.12 mL, 2.0 mmol), and silver(I) oxide (182 mg, 0.79 mmol) in dichloromethane (12 mL) was placed under an atmosphere of N_2 . The resulting black thick suspension was heated to reflux for 18 h, treated with a second portion of iodomethane (0.12 mL, 2.0 mmol), and returned to reflux for an additional 24 h. The reaction was cooled to RT, diluted with dichloromethane (20 mL), washed once with water (20 mL), once with brine (20 mL), dried over MgSO_4 , filtered, and concentrated to give a crude tan solid. This material was purified by Biotage MPLC (25 M column, 3.5–4.5% methanol/chloroform) to afford 19 mg (10%) of the title compound as an off-white solid. ^1H NMR (DMSO- d_6) δ 11.57 (s, 1H), 8.48 (d, $J = 8$ Hz, 1H), 8.40 (d, $J = 8$ Hz, 1H), 7.63 (s, 1H), 7.35 (s, 1H), 7.08 (t, $J = 8$ Hz, 1H), 6.99 (d, $J = 8$ Hz,

1H), 6.49 (d, $J = 8$ Hz, 1H), 4.47 (m, 1H), 4.38 (m, 1H), 4.25 (d, $J = 16$ Hz, 1H), 4.11 (d, $J = 16$ Hz, 1H), 3.87 (s, 3H), 3.23 (s, 3H), 3.08 (m, 2H), 2.31 (m, 1H), 2.08 (m, 1H), 1.92 (m, 1H), 1.72–1.51 (m, 5H), 0.93 (d, $J = 8$ Hz, 3H), 0.88 (d, $J = 8$ Hz, 3H); MS (ESI+) for $\text{C}_{25}\text{H}_{34}\text{N}_4\text{O}_6$ m/z 487.2 ($M + \text{H}$); HRMS (ESI+) calcd for $\text{C}_{25}\text{H}_{34}\text{N}_4\text{O}_6 + \text{H}$ 487.2551, found 487.2563.

N -((1S)-1-[[[(1S)-3-Chloro-2-oxo-1-[[[(3S)-2-oxopyrrolidin-3-yl]methyl]propyl]amino]carbonyl]-3-methylbutyl]-1H-indole-2-carboxamide. Following the procedure described for the preparation of N -((1S)-1-[[[(1S)-3-chloro-2-oxo-1-[[[(3S)-2-oxopyrrolidin-3-yl]methyl]propyl]amino]carbonyl]-3-methylbutyl]-4-methoxy-1H-indole-2-carboxamide but substituting indole-2-carboxylic acid and making noncritical variations provided a crude orange foam. This material was purified by Biotage flash chromatography, eluting with methanol/dichloromethane to afford the title compound as an off-white solid, 1.75 g, 82%. ^1H NMR (400 MHz, DMSO- d_6) δ 11.58 (s, 1H), 8.64 (d, $J = 7.8$ Hz, 1H), 8.50 (d, $J = 7.8$ Hz, 1H), 7.55–7.69 (m, 2H), 7.42 (d, $J = 8.3$ Hz, 1H), 7.26 (d, $J = 1.5$ Hz, 1H), 7.16 (m, 1H), 7.02 (t, $J = 7.5$ Hz, 1H), 4.53–4.66 (m, 2H), 4.39–4.52 (m, 2H), 2.94–3.18 (m, 2H), 2.22–2.35 (m, 1H), 2.03–2.16 (m, 1H), 1.89–2.02 (m, 1H), 1.45–1.82 (m, 5H), 0.93 (d, $J = 6.3$ Hz, 3H), 0.88 (d, $J = 6.3$ Hz, 3H); MS (APCI–) for $\text{C}_{25}\text{H}_{29}\text{N}_4\text{O}_4\text{Cl}$ m/z 459.1 ($M - \text{H}$) $^-$.

N -((1S)-1-[[[(1S)-3-Hydroxy-2-oxo-1-[[[(3S)-2-oxopyrrolidin-3-yl]methyl]propyl]amino]carbonyl]-3-methylbutyl]-1H-indole-2-carboxamide (49). Following the procedure described for the preparation of N -((1S)-1-[[[(1S)-3-hydroxy-2-oxo-1-[[[(3S)-2-oxopyrrolidin-3-yl]methyl]propyl]amino]carbonyl]-3-methylbutyl]-4-methoxy-1H-indole-2-carboxamide but substituting N -((1S)-1-[[[(1S)-3-chloro-2-oxo-1-[[[(3S)-2-oxopyrrolidin-3-yl]methyl]propyl]amino]carbonyl]-3-methylbutyl]-1H-indole-2-carboxamide and making noncritical variations provided a crude black gum. This material was purified by Biotage flash chromatography, eluting with methanol/dichloromethane to afford the title compound as an off-white solid, 218 mg, 18%. ^1H NMR (400 MHz, DMSO- d_6) δ 11.58 (s, 1H), 8.42–8.61 (m, 2H), 7.61 (d, $J = 8.6$ Hz, 2H), 7.41 (d, $J = 8.1$ Hz, 1H), 7.26 (s, 1H), 7.17 (t, $J = 7.6$ Hz, 1H), 7.02 (t, $J = 7.5$ Hz, 1H), 5.02 (t, 1H), 4.38–4.58 (m, 2H), 4.09–4.32 (m, 2H), 3.01–3.17 (m, 2H), 2.24–2.38 (m, 1H), 2.03–2.22 (m, 2H), 1.92 (m, 1H), 1.46–1.77 (m, 4H), 0.85–0.99 (m, 6H); MS (APCI+) for $\text{C}_{23}\text{H}_{30}\text{N}_4\text{O}_5$ m/z 443.1 ($M + \text{H}$) $^+$; anal. calcd for $\text{C}_{23}\text{H}_{30}\text{N}_4\text{O}_5 \cdot 0.55 \text{H}_2\text{O} \cdot 0.05 \text{DCM}$: C, 60.62; H, 6.89; N, 12.27. Found: C, 60.83; H, 6.90; N, 11.93.

N -((1S)-1-[[[(1S)-3-Methoxy-2-oxo-1-[[[(3S)-2-oxopyrrolidin-3-yl]methyl]propyl]amino]carbonyl]-3-methylbutyl]-1H-indole-2-carboxamide (50). Following the procedure described for the preparation of 4-methoxy- N -((1S)-1-[[[(1S)-3-methoxy-2-oxo-1-[[[(3S)-2-oxopyrrolidin-3-yl]methyl]propyl]amino]carbonyl]-4-methylpentyl]-1H-indole-2-carboxamide but substituting N -((1S)-1-[[[(1S)-3-hydroxy-2-oxo-1-[[[(3S)-2-oxopyrrolidin-3-yl]methyl]propyl]amino]carbonyl]-3-methylbutyl]-1H-indole-2-carboxamide and making noncritical variations provided a crude pale brown oil. This material was purified by Biotage flash chromatography, eluting with methanol/dichloromethane to afford the title compound as a white foam, 15 mg, 7%. ^1H NMR (CDCl_3) δ 9.52 (s, 1H), 8.38 (d, $J = 6.1$ Hz, 1H), 7.62 (d, $J = 8.1$ Hz, 1H), 7.40 (dd, $J = 8.1, 3.8$ Hz, 1H), 7.20–7.29 (m, 1H), 7.11 (t, $J = 7.5$ Hz, 1H), 6.98 (dd, $J = 11.4, 1.5$ Hz, 1H), 6.87 (d, $J = 8.3$ Hz, 1H), 5.98 (d, $J = 13.1$ Hz, 1H), 4.71–4.88 (m, 1H), 4.63 (m, 1H), 4.08–4.33 (m, 2H), 3.38–3.44 (s, 3H), 3.08–3.33 (m, 2H), 2.28–2.63 (m, 2H), 2.13–2.25 (m, 1H), 1.55–2.10 (m, 4H), 0.85–1.03 (m, 6H); MS (APCI–) for $\text{C}_{24}\text{H}_{32}\text{N}_4\text{O}_5$ m/z 455.2 ($M - \text{H}$) $^-$.

SARS CoV-1 Protease FRET Assay and Analysis. Proteolytic activity of coronavirus 3CL protease is measured using a continuous fluorescence resonance energy-transfer assay. The SARS 3CL^{pro} FRET assay measures the protease-catalyzed cleavage of TAMRA-SITSAVLQSGFRKMK-(DABCYL)-OH to TAMRA-SITSAVLQ and SGFRKMK(DABCYL)-OH. The fluorescence of the cleaved TAMRA (ex. 558 nm/em. 581 nm) peptide was measured using a TECAN SAFIRE fluorescence plate reader over the course of 10 min.

Typical reaction solutions contained 20 mM HEPES (pH 7.0), 1 mM EDTA, 4.0 FRET substrate, 4% DMSO, and 0.005% Tween-20. Assays were initiated with the addition of 25 nM SARS CoV-1 3CL^{pro} nucleotide sequence 9985–10902 of the Urbani strain of SARS coronavirus complete genome sequence (NCBI accession number AY278741). Percent inhibition was determined in duplicate at a 0.001 mM level of inhibitor. Data was analyzed with the nonlinear regression analysis program KaleidaGraph using the equation

$$FU = \text{offset} + (\text{limit})(1 - e - (k_{\text{obs}})t)$$

where offset equals the fluorescence signal of the uncleaved peptide substrate, and limit equals the fluorescence of the fully cleaved peptide substrate. The k_{obs} is the first-order rate constant for this reaction and, in the absence of any inhibitor, represents the utilization of a substrate. In an enzyme start reaction, which contains an irreversible inhibitor, and where the calculated limit is less than 20% of the theoretical maximum limit, the calculated k_{obs} represents the rate of inactivation of coronavirus 3CL protease. The slope (k_{obs}/I) of a plot of k_{obs} vs $[I]$ is a measure of the avidity of the inhibitor for an enzyme. For very fast irreversible inhibitors, k_{obs}/I is calculated from observations at only one or two $[I]$ rather than as a slope. For the determination of IC_{50} values for reversible inhibitors, the data was analyzed with the nonlinear regression analysis programs Xlfit3.05 (IDBS, Guildford, U.K.) or GraphPad Prism 8.02 (GraphPad Software San Diego, CA).

SARS CoV-2 Protease FRET Assay and Analysis. The proteolytic activity of the main protease, 3CL^{pro}, of SARS CoV-2 was monitored using a continuous fluorescence resonance energy-transfer (FRET) assay. The SARS CoV-2 3CL^{pro} assay measures the activity of full-length SARS CoV-2 3CL protease to cleave a synthetic fluorogenic substrate peptide with the following sequence DABCYL-KTSAVLQ-SGFRKME-EDANS modeled on a consensus peptide.⁵⁰ The fluorescence of the cleaved EDANS peptide (excitation 340 nm/emission 490 nm) is measured using a fluorescence intensity protocol on a Flexstation reader (Molecular Devices). The fluorescent signal is reduced in the presence of PF-00835231, a potent inhibitor of SARS CoV-2 3CL^{pro}. The assay reaction buffer contained 20 mM Tris–HCl (pH 7.3), 100 mM NaCl, 1 mM EDTA, 5 mM TCEP, and 25 μ M peptide substrate. Enzyme reactions were initiated with the addition of 15 nM SARS CoV-2 3CL protease and allowed to proceed for 60 min at 23 °C. Percent inhibition or activity was calculated based on control wells containing no compound (0% inhibition/100% activity) and a control compound (100% inhibition/0% activity). IC_{50} values were generated using a four-parameter fit model using ABASE software (IDBS). K_i values were fit to the Morrison equation with the enzyme concentration parameter fixed to 15 nM, the K_m parameter fixed to 14 μ M, and the substrate concentration parameter fixed to 25 μ M using Activity Base software (IDBS).

SARS CoV-1 Antiviral Assays. All assays were performed in BSL3 containment. Vero 76 cells were plated at 10 000 cells per well using phenol red-free DMEM or IMEM (Gibco). After adhering for 2 h at 37 °C, various concentrations of compound (320, 100, 33, 10, 3.3, 1.0, 0.3, or 0.1 μ M) were added and the cells were infected with 2.6×10^3 PFU/well SARS CoV Toronto-2 (provided as a gift from Dr. Heinz Feldman (NIAID, Hamilton, MT)) or mock-infected with the medium only. After 66 h, cell viability was determined using either the neutral red method or the CellTiter-Glo Luminescent Cell Viability Assay (Promega, Madison, WI). For the neutral red method, the cells were washed twice with PBS, and 100 μ L of DMEM pH 4.5 containing 0.066% neutral red was added to the cells for 2 h at 37 °C. The cells were again washed twice with PBS, 100 μ L of buffer solution (50% EtOH, 1% acetic acid) was added, and the OD was read at 540 nm after a 10 min incubation at 37 °C with shaking. Data are expressed as the percent of neutral red or luminescent signal in wells of compound-treated cells compared to the signal in wells of uninfected, compound-free cells. The 50% effective concentration (EC_{50}) is calculated as the concentration of the compound that increases the percent of the neutral red or luminescent signal in infected, compound-treated cells to 50% of that produced by uninfected, compound-free cells. The 50% cytotoxicity concentration

(CC_{50}) is calculated as the concentration of the compound that decreases the percent of the neutral red or luminescent signal in uninfected, compound-treated cells to 50% of that produced in uninfected, compound-free cells.^{51,52}

hCoV 229E Antiviral assays. MRC-5 cells were plated at 10 000 cells per well using phenol red-free MEM (Gibco). Various concentrations of compound (320, 100, 33, 10, 3.3, 1.0, 0.3, or 0.1 μ M) were added, and the cells were infected with an amount of hCoV 229E, which caused 80% cell death in 4 days or mock-infected with the medium only. After 4 days, cell viability was determined using the XTT dye reduction method.⁵³ Data are expressed as the percent of neutral red or luminescent signal in wells of compound-treated cells compared to the signal in wells of uninfected, compound-free cells. The 50% effective concentration (EC_{50}) is calculated as the concentration of the compound that increases the percent of the neutral red or luminescent signal in infected, compound-treated cells to 50% of that produced by uninfected, compound-free cells. The 50% cytotoxicity concentration (CC_{50}) is calculated as the concentration of the compound that decreases the percent of the neutral red or luminescent signal in uninfected, compound-treated cells to 50% of that produced in uninfected, compound-free cells.

Other Antiviral Assays. The following antiviral assays for HCMV,⁵⁴ HIV-RF,⁵⁵ HRV-14, and HRV-16,⁵⁴ as well as the HCV replicon,^{56,57} were performed as described in the above references.

Expression and Purification of CoV-2 3CL Protease. The expression and purification strategy followed previous studies on SARS CoV-1 3CL^{pro}.⁵⁸ Genes encoding SARS CoV-1 3CL^{pro} and SARS CoV-2 M^{pro} MN908947.3 were synthesized with codon usage optimized for *Escherichia coli* expression (Genscript and IDT). Genes were cloned into a modified pET24a vector to produce a TEV-cleavable N-terminal 6xHis tag under the T7 promoter control. BL21(DE3) cells (LifeTech) were grown in Terrific Broth (Teknova) at 37 °C until an $OD_{600} = 0.6$ – 0.8 and induced with 0.4 M IPTG for 5 h at 30 °C. Cell pellets were stored at -80 °C until purification. Cell pellets were resuspended and lysed by microfluidization in Buffer A (20 mM Tris pH 8.0 + 150 mM NaCl). Lysates were clarified at $25,000 \times g$ for 1 h at 4 °C. The soluble lysate was loaded onto a nickel affinity column (Probond) and washed sequentially with Buffer A + 5 mM and 20 mM imidazole. The proteases were eluted with Buffer A + 300 mM imidazole. The His-tag was removed by TEV protease (1:40) during an overnight dialysis step in Buffer A + 1 mM DTT. The CoV M^{pro} proteins were further purified on a HiTrap Q hp (GE Healthcare), and the Q-flow-through material was concentrated and loaded onto a 26/60 Superdex-75 (GE Healthcare) gel filtration column equilibrated with Buffer B (20 mM Tris pH 7.8 + 150 mM NaCl + 1 mM EDTA + 1 mM DTT). Final proteins were concentrated from 5 to 25 mg/mL and were directly moved to crystallization experiments or snap-frozen in liquid nitrogen for storage.

Crystallization/Soak Protocols for SARS1 with 2. Crystals of compound 2 bound to SARS1/CoV-1 DC2 protease were produced via cocrystallization. SARS1/CoV-1 DC2 protease at 10.00 mg/mL was incubated with a 3-fold molar excess of compound 2 for 18 h at 4 °C. The complex was then passed through a 0.45 μ M cellulose acetate spin filter and set up for crystallization using an NT-8 crystallization robot (Formulatrix). Using MRC-2 crystallization plates, wells containing 40 μ L of 4% w/v PEG 6000, 0.1 M MES pH 6.0, and 2.5 mM DTT were dispensed, and then sitting drops consisting of 0.3 μ L protein were set up against a 0.3 μ L well buffer. Crystallization plates were incubated at 21 °C, and rectangular crystals measuring $0.1 \times 0.25 \times 0.25$ mm³ grew within 24 h. Cocrystals were flash-frozen in liquid nitrogen after being passed through a cryo consisting of a well buffer containing 20% glycerol.

Crystallization/Soak Protocols for SARS1 with 28. Crystals of compound 28 bound to SARS1/CoV-1 DC2 protease were produced via cocrystallization. SARS1/CoV-1 DC2 protease at 10.00 mg/mL was incubated with a 3-fold molar excess of compound 28 for 18 h at 4 °C. The complex was then passed through a 0.45 μ M cellulose acetate spin filter and set up for crystallization using an NT-8 crystallization robot (Formulatrix). Using MRC-2 crystallization

plates, wells containing 40 μL of 10% w/v PEG 8000, 0.2 M sodium chloride, 0.1 M sodium potassium phosphate pH 6.2, and 10 mM TCEP were dispensed, and then sitting drops consisting of 0.3 μL protein were set up against a 0.3 μL well buffer. Crystallization plates were incubated at 21 $^{\circ}\text{C}$, and rectangular crystals measuring $0.1 \times 0.25 \times 0.25 \text{ mm}^3$ grew within 24 h. Cocrystals were flash-frozen in liquid nitrogen after being passed through a cryo consisting of a well buffer containing 20% glycerol.

Crystallization/Soak Protocols for SARS1 and SARS2 with 4 (PF-00835231). *LJEC2520 + PF-00835231.* Crystals of PF-00835231 bound to SARS1/CoV-1 DC2 protease *via* cocrystallization: Freshly prepared SARS1/CoV-1 DC2 protease at 10.00 mg/mL was incubated with a 3-fold molar excess of PF-00835231 for 18 h at 4 $^{\circ}\text{C}$. The complex was then passed through a 0.45 μM cellulose acetate spin filter and set up for crystallization using an NT-8 crystallization robot (Formulatrix). Using MRC-2 crystallization plates, wells containing 40 μL of 10% w/v PEG 6000, 0.1 M MES pH 6.0, and 10% glycerol were dispensed, and then sitting drops consisting of 0.15 μL protein were set up against a 0.15 μL well buffer. Crystallization plates were incubated at 21 $^{\circ}\text{C}$, and rectangular crystals measuring $0.2 \times 0.25 \times 0.15 \text{ mm}^3$ grew overnight. Crystals were flash-frozen in liquid nitrogen after being passed through a cryo consisting of a well buffer containing 20% glycerol.

LJEC2521 + PF-00835231. Crystals of PF-00835231 bound to SARS2/CoV-2 mature protease *via* cocrystallization: Freshly prepared SARS2/CoV-2 mature protease at 11.3 mg/mL was incubated with a 3-fold molar excess of PF-00835231 for 18 h at 4 $^{\circ}\text{C}$. The complex was then passed through a 0.45 μM cellulose acetate spin filter and set up for crystallization using an NT-8 crystallization robot (Formulatrix). Using MRC-2 crystallization plates, wells containing 40 μL of 15% v/v 2-propanol, 0.1 M citric acid pH 5.0, and 10% w/v PEG 10 000 were dispensed, and then sitting drops consisting of 0.3 μL protein and a 0.3 μL well buffer were set up. Crystallization plates were incubated at 13 $^{\circ}\text{C}$, and crystals shaped as rectangular blocks measuring $0.1 \times 0.2 \times 0.2 \text{ mm}^3$ grew overnight. Crystals were flash-frozen in liquid nitrogen after being passed through a cryo consisting of a well buffer containing 20% glycerol.

LJEC2522 + PF-00835231. Crystals of PF-00835231 bound to SARS2/CoV-2 DC2 protease *via* soaking: Freshly prepared SARS2/CoV-2 DC2 protease at 25.8 mg/mL was passed through a 0.45 mM cellulose acetate spin filter and set up for crystallization using an NT-8 crystallization robot (Formulatrix). Using MRC-2 crystallization plates, wells containing 40 mL of 0.2 M potassium sodium tartrate tetrahydrate and 20% w/v PEG 3350 were dispensed, and then sitting drops consisting of 0.3 μL protein were set up in a 1:1 ratio with a well buffer. Crystallization plates were incubated at 13 $^{\circ}\text{C}$, and large crystals shaped as beveled plates measuring $0.35 \times 0.2 \times 0.025 \text{ mm}^3$ grew after 48 h. PF-00835231 (in 100% DMSO solution) was introduced to the drop (in situ), at a final concentration of 1 mM, and then incubated at 13 $^{\circ}\text{C}$ for 24 h. Soaked crystals were flash-frozen in liquid nitrogen after being passed through a cryo consisting of a well buffer containing 20% glycerol. Structure determination.

X-ray diffraction data were collected at the IMCA-CAT 17-ID beamline of Advanced Photon Source at Argonne National Labs and processed using autoPROC. Structure of the SARS CoV main protease in complex with PF-835231 was determined by molecular replacement using the published protein structure (PDBID 1Q2W) as the starting model in program Phaser and refined iteratively using autoBUSTER followed by model building in Coot.

Structure of the SARS CoV-2 main protease in complex with PF-835231 was determined similarly by rigid body refinement using the SARS CoV main protease structure in complex with the same ligand as the starting model.

■ ASSOCIATED CONTENT

Supporting Information

The Supporting Information is available free of charge at <https://pubs.acs.org/doi/10.1021/acs.jmedchem.0c01063>.

Molecular formula strings for all compounds with biological data (CSV)

HPLC purity for compound 4 (PDF)

■ AUTHOR INFORMATION

Corresponding Author

Robert L. Hoffman – Pfizer Worldwide Research and Development, San Diego, California 92121, United States; orcid.org/0000-0002-2030-9094; Phone: +1-858-622-3000; Email: robert.l.hoffman@pfizer.com

Authors

Robert S. Kania – Pfizer Worldwide Research and Development, San Diego, California 92121, United States

Mary A. Brothers – Pfizer Worldwide Research and Development, San Diego, California 92121, United States

Jay F. Davies – Pfizer Worldwide Research and Development, San Diego, California 92121, United States

Rose A. Ferre – Pfizer Worldwide Research and Development, San Diego, California 92121, United States

Ketan S. Gajiwala – Pfizer Worldwide Research and Development, San Diego, California 92121, United States

Mingying He – Pfizer Worldwide Research and Development, San Diego, California 92121, United States

Robert J. Hogan – Southern Research Institute, Birmingham, Alabama 35205, United States

Kirk Kozminski – Pfizer Worldwide Research and Development, San Diego, California 92121, United States

Lilian Y. Li – Pfizer Worldwide Research and Development, San Diego, California 92121, United States

Jonathan W. Lockner – Pfizer Worldwide Research and Development, San Diego, California 92121, United States; orcid.org/0000-0001-6148-0579

Jihong Lou – Pfizer Worldwide Research and Development, San Diego, California 92121, United States

Michelle T. Marra – Pfizer Worldwide Research and Development, San Diego, California 92121, United States

Lennert J. Mitchell, Jr. – Pfizer Worldwide Research and Development, San Diego, California 92121, United States

Brion W. Murray – Pfizer Worldwide Research and Development, San Diego, California 92121, United States

James A. Nieman – Pfizer Worldwide Research and Development, San Diego, California 92121, United States; orcid.org/0000-0002-5087-0819

Stephen Noell – Pfizer Worldwide Research and Development, San Diego, California 92121, United States

Simon P. Planken – Pfizer Worldwide Research and Development, San Diego, California 92121, United States; orcid.org/0000-0001-8901-8992

Thomas Rowe – Southern Research Institute, Birmingham, Alabama 35205, United States

Kevin Ryan – Pfizer Worldwide Research and Development, San Diego, California 92121, United States

George J. Smith, III – Pfizer Worldwide Research and Development, San Diego, California 92121, United States

James E. Solowiej – Pfizer Worldwide Research and Development, San Diego, California 92121, United States

Claire M. Steppan – Pfizer Worldwide Research and Development, San Diego, California 92121, United States

Barbara Taggart – Southern Research Institute, Birmingham, Alabama 35205, United States

Complete contact information is available at:

<https://pubs.acs.org/10.1021/acs.jmedchem.0c01063>

Author Contributions

The manuscript was written through the contributions of all authors. All authors have given approval to the final version of the manuscript.

Funding

Funding for the antiviral testing was provided by NIAID under a cooperative agreement between NIAID and Pfizer.

Notes

The authors declare no competing financial interest.

ACKNOWLEDGMENTS

The authors would like to thank the Pfizer La Jolla Discovery Technology group who were responsible for all HRMS, preparative HPLC, and SFC separations. Antiviral testing was performed at the Southern Research Institute (Birmingham, AL). The authors wish to thank Dr. Heinz Feldman (NIAID, Hamilton, MT) for the kind gift of the SARS CoV Toronto-2 cell line enabling this testing. The authors wish to thank Cathy Laughlin, Christopher Tseng, and Jack Secrist for their roles in this collaboration. The authors would also like to thank Kevin Freeman-Cook, Charlotte Allerton, and Gina M. Yanochko-Hoffman for critically reading the manuscript and offering valued editing suggestions.

REFERENCES

- (1) Wu, F.; Zhao, S.; Yu, B.; Chen, Y.-M.; Wang, W.; Song, Z.-G.; Hu, Y.; Tao, Z.-W.; Tian, J.-H.; Pei, Y.-Y.; Yuan, M.-L.; Zhang, Y.-L.; Dai, F.-H.; Liu, Y.; Wang, Q.-M.; Zheng, J.-J.; Xu, L.; Holmes, E. C.; Zhang, Y.-Z. A new coronavirus associated with human respiratory disease in China. *Nature* **2020**, *579*, 265–269.
- (2) Zhou, P.; Yang, X.-L.; Wang, X.-G.; Hu, B.; Zhang, L.; Zhang, W.; Si, H.-R.; Zhu, Y.; Li, B.; Huang, C.-L.; Chen, H.-D.; Chen, J.; Luo, Y.; Guo, H.; Jiang, R.-D.; Liu, M.-Q.; Chen, Y.; Shen, X.-R.; Wang, X.; Zheng, X.-S.; Zhao, K.; Chen, Q.-J.; Deng, F.; Liu, L.-L.; Yan, B.; Zhan, F.-X.; Wang, Y.-Y.; Xiao, G.-F.; Shi, Z.-L. A pneumonia outbreak associated with a new coronavirus of probable bat origin. *Nature* **2020**, *579*, 270–273.
- (3) Marra, M. A.; Jones, J. M.; Astell, C. R.; Holt, R. A.; Brooks-Wilson, A.; Butterfield, Y. S. N.; Khattra, J.; Asano, J. K.; Barber, S. A.; Chan, S. Y.; Cloutier, A.; Coughlin, S. M.; Freeman, D.; Girn, N.; Griffith, O. L.; Leach, S. R.; Mayo, M.; McDonald, H.; Montgomery, S. B.; Pandoh, P. K.; Petrescu, A. S.; Robertson, A. G.; Schein, J. E.; Siddiqui, A.; Smailus, D. E.; Stott, J. M.; Yang, G. S.; Plummer, F.; Andonov, A.; Artsob, H.; Bastien, N.; Bernard, K.; Booth, T. F.; Bowness, D.; Czub, M.; Drebot, M.; Fernando, L.; Flick, R.; Garbutt, M.; Gray, M.; Grolla, A.; Jones, S.; Feldmann, H.; Meyers, A.; Kabani, A.; Li, Y.; Normand, S.; Stroher, U.; Tipples, G. A.; Tyler, S.; Vogrig, R.; Ward, D.; Watson, B.; Brunham, R. C.; Krajden, M.; Petric, M.; Skowronski, D. M.; Upton, C.; Roper, R. L. The genome sequence of the SARS-associated coronavirus. *Science* **2003**, *300*, 1399–1404.
- (4) Rota, P. A.; Oberste, M. S.; Monroe, S. S.; Nix, W. A.; Campagnoli, R.; Icenogle, J. P.; Penaranda, S.; Bankamp, B.; Maher, K.; Chen, M.-H.; Tong, S.; Tamin, A.; Lowe, L.; Frace, M.; DeRisi, J. L.; Chen, Q.; Wang, D.; Erdman, D. D.; Peret, T. C. T.; Burns, C.; Ksiazek, T. G.; Rollin, P. E.; Sanchez, A.; Liffick, S.; Holloway, B.; Limor, J.; McCaustland, K.; Olsen-Rasmussen, M.; Fouchier, R.; Gunther, S.; Osterhaus, A. D. M. E.; Drosten, C.; Pallansch, M. A.; Anderson, L. J.; Bellini, W. J. The genome sequence of the SARS-associated coronavirus. Characterization of a novel coronavirus associated with severe acute respiratory syndrome. *Science* **2003**, *300*, 1394–1399.
- (5) World Health Organization. Cumulative Number of Reported Probable Cases, http://www.who.int/csr/sars/country/2003_06_17/en/index.html (accessed June 17, 2003).
- (6) John Hopkins University. COVID-19 Dashboard by the Center for Systems Science and Engineering (CSSE) at Johns Hopkins University (JHU), <https://coronavirus.jhu.edu/map.html> (accessed June 16, 2020).
- (7) Thiel, V.; Ivanov, K. A.; Putics, A.; Hertzog, T.; Chelle, B.; Bayer, S.; WeiBbrich, B.; Snijder, E. J.; Rabenau, H.; Doerr, H. W.; Gorbelenya, A. E.; Ziebuhr, J. Mechanisms and enzymes involved in SARS coronavirus genome expression. *J. Gen. Virol.* **2003**, *84*, 2305–2315.
- (8) Zhang, L.; Lin, D.; Sun, X.; Curth, U.; Drosten, C.; Sauerhering, L.; Becker, S.; Rox, K.; Hilgenfeld, R. Crystal structure of SARS-CoV-2 main protease provides a basis for design of improved α -ketoamide inhibitors. *Science* **2020**, *368*, No. eabb3405.
- (9) Dai, W.; Zhang, B.; Jiang, X.-M.; Su, H.; Li, J.; Zhao, Y.; Xie, X.; Jin, Z.; Peng, J.; Liu, F.; Li, C.; Li, Y.; Bai, F.; Wang, H.; Cheng, X.; Cen, X.; Hu, S.; Yang, X.; Wang, J.; Liu, X.; Xiao, G.; Jiang, H.; Rao, Z.; Zhang, L.-K.; Xu, Y.; Yang, H.; Liu, H. Structure-based design of antiviral drug candidates targeting the SARS-CoV-2 main protease. *Science* **2020**, *368*, 1331–1335.
- (10) Webber, S. E.; Okano, K.; Little, T. L.; Reich, S. H.; Xin, Y.; Fuhrman, S. A.; Matthews, D. A.; Love, R. A.; Hendrickson, T. F.; Patrick, A. K.; Meador, J. W., III; Ferre, R. A.; Brown, E. L.; Ford, C. E.; Binford, S. L.; Worland, S. T. Tripeptide aldehyde inhibitors of human rhinovirus 3C protease: design, synthesis, biological evaluation, and cocrystal structure solution of P1 glutamine isosteric replacements. *J. Med. Chem.* **1998**, *41*, 2786–2805.
- (11) Shepherd, T. A.; Cox, G. A.; McKinney, E.; Tang, J.; Wakulchik, M.; Zimmerman, R. E.; Villarreal, E. C. Small peptidic aldehyde inhibitors of human rhinovirus 3C protease. *Biorg. Med. Chem. Lett.* **1996**, *6*, 2893–2896.
- (12) Kaldor, S. W.; Hammond, M.; Dressman, B. A.; Labus, J. M.; Chadwell, F. W.; Kline, A. D.; Heinz, B. A. Glutamine-derived aldehydes for the inhibition of human rhinovirus 3C protease. *Biorg. Med. Chem. Lett.* **1995**, *5*, 2021–2026.
- (13) Malcolm, B. A.; Lowe, C.; Shechosky, S.; McKay, R. T.; Yang, C. C.; Shah, V. J.; Simon, R. J.; Vederas, J. C.; Sant, D. V. Peptide aldehyde inhibitors of hepatitis A virus 3C proteinase. *Biochemistry* **1995**, *34*, 8172–8179.
- (14) Marquis, R. W.; Ru, Y.; Yamashita, D. S.; Oh, H.-J.; Yen, J.; Thompson, S. K.; Carr, T. J.; Levy, M. A.; Tomaszek, T. A.; James, C. F.; Smith, W. W.; Zhao, B.; Janson, C. A.; Abdel-Meguid, S. S.; D'Alessio, K. J.; McQueney, M. S.; Veber, D. F. Potent dipeptidylketone inhibitors of the cysteine protease cathepsin K. *Biorg. Med. Chem.* **1999**, *7*, 581–588.
- (15) Huang, L.; Ellman, J. A. General solid-phase method to prepare novel cyclic ketone inhibitors of the cysteine protease cruzain. *Biorg. Med. Chem. Lett.* **2002**, *12*, 2993.
- (16) Yamashita, D. S.; Smith, W. W.; Zhao, B.; Janson, C. A.; Tomaszek, T. A.; Bossard, C. A.; Levy, M. A.; Oh, H.-J.; Carr, S. A.; McQueney, M.; D'Alessio, K. J.; Amegadzie, B. Y.; Hanning, C. R.; Abdel-Meguid, S.; DesJarlais, R. L.; Gleason, J. G.; Veber, D. F.; et al. Structure and design of potent and selective cathepsin K inhibitors. *J. Am. Chem. Soc.* **1997**, *119*, 11351–11352.
- (17) Moon, J. B.; Coleman, R. S.; Hanzlik, R. P. Reversible covalent inhibition of papain by a peptide nitrile. Carbon-13 NMR evidence for a thioimide ester adduct. *J. Am. Chem. Soc.* **1986**, *108*, 1350–1351.
- (18) Cowen, S. D.; Greenspan, D. P.; McQuire, L. W.; Tommasi, A. R.; Van Duzer, J. H. N-substituted peptidyl nitriles as cysteine cathepsin inhibitors. WO01/87828 A1, publication date Nov 22, 2001.
- (19) Li, Z.; Patil, G. S.; Golubski, Z. E.; Hori, H.; Tehrani, K.; Foreman, J. E.; Eveleth, D. D.; Bartus, R. T.; Powers, J. C. Peptide α -keto ester, α -keto amide, and α -keto acid inhibitors of calpains and other cysteine proteases. *J. Med. Chem.* **1993**, *36*, 3472–3480.
- (20) Chen, S.-H.; Lamar, J.; Victor, F.; Snyder, N.; Johnson, R.; Heinz, B. A.; Wakulchik, M.; Wang, Q. M. Synthesis and evaluation of

tripeptidyl alpha-ketoamides as human rhinovirus 3C protease inhibitors. *Biorg. Med. Chem. Lett.* **2003**, *13*, 3531–3536.

(21) Otto, H.-H.; Schirmeister, T. Cysteine proteases and their inhibitors. *Chem. Rev.* **1997**, *97*, 133–172.

(22) Gamcsik, M. P.; Malthouse, J. P. G.; Primrose, W. U.; Mackenzie, N. E.; Boyd, A. S. F.; Russell, R. A.; Scott, A. I. Structure and stereochemistry of tetrahedral inhibitor complexes of papain by direct NMR observation. *J. Am. Chem. Soc.* **1983**, *105*, 6324–6325.

(23) Zhang, L.; Lin, D.; Kusov, Y.; Nian, Y.; Ma, Q.; Wang, J.; von Brunn, A.; Leyssen, P.; Lanko, K.; Neyts, J.; de Wilde, A.; Snijder, E.; Liu, H.; Hilgenfeld, R. α -Ketoamides as broad-spectrum inhibitors of coronavirus and enterovirus replication: Structure-based design, synthesis, and activity assessment. *J. Med. Chem.* **2020**, *63*, 4562–4578.

(24) Powers, J. C.; Asgian, J. L.; Ekici, O. D.; James, K. E. Irreversible inhibitors of serine, cysteine, and threonine proteases. *Chem. Rev.* **2002**, *102*, 4639–4750.

(25) Smith, R. A.; Copp, L. J.; Coles, P. J.; Pauls, H. W.; Robinson, V. J.; Spencer, R. W.; Heard, S. B.; Krantz, A. New inhibitors of cysteine proteinases. Peptidyl acyloxymethyl ketones and the quiescent nucleofuge strategy. *J. Am. Chem. Soc.* **1988**, *110*, 4429–4431.

(26) Dolle, R. E.; Hoyer, D.; Prasad, C. V. C.; Schmidt, S. J.; Helaszek, C. T.; Miller, R. E.; Ator, M. A. P1 aspartate-based peptide α -(2,6-dichlorobenzoyl)oxy methyl ketones as potent time-dependent inhibitors of interleukin-1 β -converting enzyme. *J. Med. Chem.* **1994**, *37*, 563–564.

(27) Brady, K. D.; Giegel, D. A.; Grinnell, C.; Lunney, E.; Talanian, R. V.; Wong, W.; Walker, N. A catalytic mechanism for caspase-1 and for bimodal inhibition of caspase-1 by activated aspartic ketones. *Bioorg. Med. Chem.* **1999**, *7*, 621–631.

(28) Anand, K.; Ziebuhr, J.; Wadhwani, P.; Mesters, J. R.; Hilgenfeld, R. Coronavirus main proteinase (3CL^{pro}) structure: basis for design of anti-SARS drugs. *Science* **2003**, *300*, 1763–1767.

(29) The X-ray crystallographic coordinates for the SARS CoV-1 3CL^{pro} covalently bound with inhibitor 2 is deposited in the Protein Data Bank (PDB), <http://rcsb.rutgers.edu/pdb/index> (PDB code 6XHO).

(30) Dragovich, P. S.; Prins, T. J.; Zhou, R.; Webber, S. E.; Marakovits, J. T.; Fuhrman, S. A.; Patick, A. K.; Mathews, D. A.; Lee, C. A.; Ford, C. E.; Burke, B. J.; Rejto, P. A.; Hendrickson, T. F.; Tuntland, T.; Brown, E. L.; Meador, J. W., III; Ferre, R. A.; Harr, J. E.; Kosa, M. B.; Worland, S. L. Structure-based design, synthesis, and biological evaluation of irreversible human rhinovirus 3C protease inhibitors. 4. Incorporation of P1 lactam moieties as L-glutamine replacements. *J. Med. Chem.* **1999**, *42*, 1213.

(31) Rich, D. H.; Prasad, J. V. N. V.; Sun, C.-Q.; Green, J.; Mueller, R.; Houseman, K.; MacKenzie, D.; Malkovsky, M. New hydroxyethylamine HIV protease inhibitors that suppress viral replication. *J. Med. Chem.* **1992**, *35*, 3803–3812.

(32) Yamashita, D. S.; Dong, X.; Oh, H.-J.; Brook, C. S.; Tomaszek, T. A.; Szwczuk, L.; Tew, D. G.; Veber, D. F. Solid-phase synthesis of a combinatorial array of 1,3-bis(acylamino)-2-butanones, inhibitors of the cysteine proteases cathepsins K and L. *J. Comb. Chem.* **1999**, *1*, 207–215.

(33) Tian, Q.; Nayyar, N. K.; Babu, S.; Chen, L.; Tao, J.; Lee, S.; Tibbetts, A.; Moran, T.; Liou, J.; Guo, M.; Kennedy, T. P. An efficient synthesis of a key intermediate for the preparation of the rhinovirus protease inhibitor AG7088 via asymmetric dianionic cyanomethylation of N-Boc-L-(+)-glutamic acid dimethyl ester. *Tetrahedron Lett.* **2001**, *42*, 6807–6809.

(34) Generation of diazomethane followed Aldrich technical bulletin AL-180 employing Diazald kit.

(35) Mendonca, R. V.; Venkatraman, S.; Palmer, J. T. Novel route to the synthesis of peptides containing 2-amino-1'-hydroxymethyl ketones and their application as cathepsin K inhibitors. *Biorg. Med. Chem. Lett.* **2002**, *12*, 2887–2891.

(36) These conditions result in detectable levels of epimerization at the P₁ site. The resulting diastereomer has been observed by HPLC,

NMR, and LCMS and is readily removed by fractional recrystallization.

(37) Krantz, A.; Copp, L. J.; Coles, P. J.; Smith, R. A.; Heard, S. B. Peptidyl (acyloxy)methyl ketones and the quiescent affinity label concept: the departing group as a variable structural element in the design of inactivators of cysteine proteinases. *Biochemistry* **1991**, *30*, 4678–4687.

(38) The X-ray crystallographic coordinates for the SARS CoV-1 and SARS CoV-2 3CL^{pro} each covalently bound inhibitor 28 are deposited in the Protein Data Bank (PDB), <http://rcsb.rutgers.edu/pdb/index> (PDB Code 6XHN).

(39) Hoffman, R. L.; Kania, R. S.; Nieman, J. A.; Planken, S. P.; Smith, G. J., III. SARS antiviral data for all described inhibitors are disclosed. Preparation of peptides as anticoronaviral agents. WO2005/113580 A1, Dec 1, 2005.

(40) Compound is incubated at 1 μ M substrate concentration and 5 mM GSH in pH 7.8 0.1 M TRIS buffer at 37 °C. Timepoints are taken over 30 min and terminated with 250 mM iodoacetamide to quench the excess GSH. Samples were then diluted in acetonitrile for LC/MS analysis. Data are reported as half-life.

(41) Compound is spiked at 1 μ M substrate concentration in pH 7.4 adjusted (with HCL or NaOH) plasma and incubated at 37 °C. 50 μ L plasma samples were taken at multiple timepoints during a 60 minute incubation and added to 200 μ L acetonitrile to stop enzymatic degradation. Samples were centrifuged at 3000 rpm and 150 μ L supernatant was transferred to a 96 well block for analysis by LC/MS. Data are reported as half-life.

(42) The solubility of 3 is 0.377 mg/mL (2.5% w/v SBEDC, 5 mM phosphate buffer, pH 7.4, made isotonic with 4.25% dextrose). Rat *in vivo* parameters for 3 were from IV dosing used a 50% PEG 200/10% EtOH/40% saline formulation. For 2 mg/kg dose the following values were obtained: 26.2 mL/min/kg CL; 1.0 L/kg V_{dss}; 0.9 t_{1/2} and 1.3 h- μ g/mL AUC.

(43) Huang, L.; Brinen, L. S.; Ellman, J. A. Crystal structures of reversible ketone-based inhibitors of the cysteine protease cruzain. *Biorg. Med. Chem.* **2003**, *11*, 21–29. Interestingly, this reference reports no covalent bond observed between the active site cysteine and the ketone pharmacophore.

(44) Fuentes-Prior, P.; Salvesen, G. S. The protein structures that shape caspase activity, specificity, activation and inhibition. *Biochem. J.* **2004**, *384*, 201–232.

(45) Obach, R. S. Prediction of human clearance of twenty-nine drugs from hepatic microsomal intrinsic clearance data: an examination of in vitro half-life approach and nonspecific binding to microsomes. *Drug Metab. Dispos.* **1999**, *27*, 1350–1359.

(46) Solubility of 4 in several formulation vehicles: 4.6 mg/mL (2.5% w/v SBEDC, 5 mM phosphate buffer, pH 7.4, made isotonic with 4.25% dextrose); 4.6 mg/mL (2.5% w/v SBEDC, 5 mM citrate buffer, pH 7.4, made isotonic with 4.25% dextrose); 6.6 mg/mL (2.5% w/v HPCD).

(47) The X-ray crystallographic coordinates for the SARS CoV-1 3CL^{pro} (PDB Code 6XHL) and SARS CoV-2 3CL^{pro} (6XHM) each covalently bound inhibitor 4 are deposited in the Protein Data Bank (PDB), <http://rcsb.rutgers.edu/pdb/index>.

(48) Wandel, C.; Kim, R. B.; Kajiji, S.; Guengerich, F. P.; Wilkinson, G. R.; Wood, A. A. J. P-glycoprotein and cytochrome P-450 3A inhibition: dissociation of inhibitory potencies. *Cancer Res.* **1999**, *59*, 3944–3948.

(49) *In vivo* parameters for 4 were from IV dosing using a 50% PEG 200/10% EtOH/40% saline formulation. For rat (2 mg/kg) the following values were obtained: 28.6 mL/min/kg CL; 1.2 L/kg V_{dss}; 1.0 t_{1/2} and 1.2 h- μ g/mL AUC. For dog (2 mg/kg) the following values were obtained: 10.5 mL/min/kg CL; 0.4 L/kg V_{dss}; 1.3 t_{1/2} and 3.8 h- μ g/mL AUC. For monkey (4 mg/kg) the following values were obtained: 20.6 mL/min/kg CL; 0.6 L/kg V_{dss}; 1.6 t_{1/2} and 3.8 h- μ g/mL AUC.

(50) Grum-Tokars, V.; Ratia, K.; Begaye, A.; Baker, S.; Mesecar, A. Evaluating the 3C-like protease activity of SARS-Coronavirus:

recommendations for standardized assays for drug discovery. *Virus Res.* **2008**, *133*, 63–73.

(51) Borenfreund, E.; Puerner, J. Toxicity determined in vitro by morphological alterations and neutral red absorption. *Toxicol. Lett.* **1985**, *24*, 119–124.

(52) Smee, D. F.; Hurst, B.; Evans, W.; Clyde, N.; Wright, S.; Peterson, C.; Jung, K.-H.; Day, C. Evaluation of cell viability dyes in antiviral assays with RNA viruses that exhibit different cytopathogenic properties. *J. Virol. Methods* **2017**, *246*, 51–57.

(53) Scudiero, D. A.; Shoemaker, R. H.; Paull, K. D.; Monks, A.; Tierney, S.; Nofziger, T. H.; Currens, M. J.; Seniff, D.; Boyd, M. R. Evaluation of a soluble tetrazolium/formazan assay for cell growth and drug sensitivity in culture using human and other tumor cell lines. *Cancer Res.* **1988**, *48*, 4827–4833.

(54) Weislow, O. S.; Kiser, R.; Fine, D. L.; Bader, J.; Shoemaker, R. H.; Boyd, M. R. New soluble-formazan assay for HIV-1 cytopathic effects: application to high-flux screening of synthetic and natural products for AIDS-antiviral activity. *J. Natl. Cancer Inst.* **1989**, *81*, 577–586.

(55) Hippenmeyer, P. J.; Dilworth, V. M. A rapid assay for determination of antiviral activity against human cytomegalovirus. *Antiviral Res.* **1996**, *32*, 35–42.

(56) Patick, A. K.; Binford, S. L.; Brothers, M. A.; Jackson, R. L.; Ford, C. E.; Diem, M. D.; Maldonado, F.; Dragovich, P. S.; Zhou, R.; Prins, T. J.; Fuhrman, S. A.; Meador, J. W.; Zalman, L. S.; Matthews, D. A.; Worland, S. T. In vitro antiviral activity of AG7088, a potent inhibitor of human rhinovirus 3C protease. *Antimicrob. Agents Chemother.* **1999**, *43*, 2444–2450.

(57) Blight, K. J.; Kolykhalov, A. A.; Rice, C. M. Efficient initiation of HCV RNA replication in cell culture. *Science* **2000**, *290*, 1972–1974.

(58) Solowiej, J.; Thomson, J.; Ryan, K.; Luo, C.; He, M.; Lou, J.; Murray, B. Steady-state and pre-steady-state kinetic evaluation of severe acute respiratory syndrome coronavirus (SARS-CoV) 3CL^{pro} cysteine protease: development of an ion-pair model for catalysis. *Biochemistry* **2008**, *47*, 2617.